Working Paper Series

Peter McAdam, Anders Warne

Density forecast combinations:
the real-time dimension

Abstract: Density forecast combinations are examined in real-time using the log score to compare five methods: fixed weights, static and dynamic prediction pools, as well as Bayesian and dynamic model averaging. Since real-time data involves one vintage per time period and are subject to revisions, the chosen actuals for such comparisons typically differ from the information that can be used to compute model weights. The terms *observation lag* and *information lag* are introduced to clarify the different time shifts involved for these computations and we discuss how they influence the combination methods. We also introduce upper and lower bounds for the density forecasts, allowing us to benchmark the combination methods. The empirical study employs three DSGE models and two BVARs, where the former are variants of the Smets and Wouters model and the latter are benchmarks. The models are estimated on real-time euro area data and the forecasts cover 2001–2014, focusing on inflation and output growth. We find that some combinations are superior to the individual models for the joint and the output forecasts, mainly due to over-confident forecasts of the BVARs during the Great Recession. Combinations with limited weight variation over time and with positive weights on all models provide better forecasts than those with greater weight variation. For the inflation forecasts, the DSGE models are better overall than the BVARs and the combination methods.

Keywords: Bayesian inference, euro area, forecast comparisons, model averaging, prediction pools, predictive likelihood.

JEL Classification Numbers: C11, C32, C52, C53, E37.

NON-TECHNICAL SUMMARY

The benefits of combining density forecasts from different models or forecasters have long been recognized across many academic fields. Not only does model combination provide a way to guard against model uncertainty, it is also a means to improve forecast accuracy. The improvement in forecast accuracy can, for instance, arise from individual models being over-confident in the sense of delivering predictive densities that are too narrow and thereby not *well-calibrated*.

There is though less empirical agreement on the performance and robustness of different combination schemes. Different methods can generate quite different outcomes and reflect different philosophies. For instance, the well-known method of Bayesian model averaging is predicated on the assumption of a complete model space and, accordingly, there is a tendency for a single model to attract all the weight. Optimal prediction pools, make no such assumption: all models in the pool may be false, but nonetheless useful. Straddling these extremes is the enduring puzzle that naïve schemes, such as equal model weights, often outperform more sophisticated alternatives. Equal weighting schemes, though, preclude the possibility of adaption to particular episodes of model improvements. If the forecast horizon contains some dramatic event or particular constellation of shocks, this may be costly. On the other hand, schemes that yield volatile model weights may undermine the practical case for combination methods.

Against this background, our paper makes the following four principle contributions. First, like forecasting itself, gains from model combinations matter most in real time. Yet, the interaction between *model combination schemes and real time data* has not been emphasized in the literature. Apart from fixed-weight combinations, model weights are computed using information about each model's past predictive performance. Measures of predictive performance, such as the log predictive score, are typically dependent on the recorded predictive likelihood values of the individual models. In a real-time context, model weighting emerges when outcomes are imperfectly known: measured values of the predicted variables for period t are, by construction, not observed until $t + l$, which implies that the predictive likelihoods for models should be lagged at least l periods when computing the incremental weights. The upshot is that an event such as the Great Recession—wherein large forecast errors emerge, model performance may diverge, and data revisions may be substantial—mechanically takes time to influence the model weights. Consequently, a "better" model may be under-utilized depending on these lags, or existing sub-optimal model weights may persist.

To that end we define the following terms: *observation lag* is the time difference between the date of the variable and the vintage its actual value is taken from, while *information lag* is the time difference between the date of the variable and the vintage a measured value is taken from. The former concept concerns the data used for the performance measure of density forecast combinations, while the latter is related to the information used for computing combination weights. It should be kept in mind that the information lag comes on top of the forecast horizon so that the sum of the two make up the delay before historical density forecasts can be used for

model weighting. We demonstrate that the assumed length of the information lag matters for the attainable gains from forecast combinations and the ranking of the methods over time.

A second contribution is that, unlike the bulk of the literature, we consider *multi-step-ahead forecasts* in our density combination comparisons: backcasts, nowcasts and up to eight-quarter-ahead forecasts. This matters because models' predictive performance can be highly horizon specific. Again, the Great Recession episode is telling: all models incur large forecast errors, but some "recover" better than others over different horizons and for different reasons. This has implications for the gains obtainable from model combinations in general as well as the specific performance of different combination schemes. A standard one-step-ahead density forecast would be silent on these issues. Third, we introduce *upper and lower bounds* for the density forecasts, allowing us to benchmark the combination methods not only with respect to the available models but against the best and the worst cases given the models involved. These bounds are easily formed from the density forecasts of the models and to our knowledge they have not been discussed in the literature. Fourth, we contribute to the literature on model combinations in a *euro area context*. Relative to that of the US, evidence of real-time density forecasting on euro area data remains scant, despite its similar economic weight, and corresponding evidence on model combinations is scanter still.

The study employs three DSGE models and two Bayesian vector autoregressions (BVARs), where the former are variants of the Smets and Wouters model and the latter are benchmarks. The models are estimated on real-time euro area data and the forecasts cover 2001–2014, focusing on inflation and output growth. We find that some combinations are superior to the individual models for the joint and the output forecasts, mainly due to over-confident forecasts of the BVARs during the Great Recession. Combinations with limited weight variation over time and with positive weights on all models provide better forecasts than those with greater weight variation. For the inflation forecasts, the DSGE models are better overall than the BVARs and the combination methods.

1. INTRODUCTION

The benefits of combining density forecasts from different models or forecasters have long been recognized across many academic fields, such as management science, meteorology and statistics. Density forecast combinations have also received a growing interest among economists and policy makers. Not only does model combination provide a way to guard against model uncertainty, it is also a means to improve forecast accuracy; see, in particular, a recent survey by Aastveit, Mitchell, Ravazzolo, and van Dijk (2019). The improvement in forecast accuracy can, for instance, arise from individual models being over-confident in the sense of delivering predictive densities that are too narrow and thereby not *well-calibrated*; see, e.g., Dawid (1984) and Diebold, Gunther, and Tay (1998). More intuitively, it strains belief that any single model would strictly outperform all others in every time interval. Instead, model rankings are likely to change over time as different information sets and different modelling aspects come into play.

Notwithstanding this positive consensus on forecast combinations, there is less empirical agreement on the performance and robustness of different combination schemes. Different methods can generate quite different outcomes and reflect different philosophies; see Amisano and Geweke (2017). For instance, the well-known method of Bayesian model averaging is predicated on the assumption of a complete model space and, accordingly, there is a tendency for a single model to attract all the weight. Optimal prediction pools, suggested by Hall and Mitchell (2007), make no such assumption: all models in the pool may be false, but nonetheless useful. Straddling these extremes is the enduring puzzle that naïve schemes, such as equal model weights, often outperform more sophisticated alternatives. Equal weighting schemes, though, preclude the possibility of adaption to particular episodes of model improvements. If the forecast horizon contains some dramatic event or particular constellation of shocks, this may be costly. On the other hand, schemes that yield volatile model weights may undermine the practical case for combination methods, especially so perhaps in real time.

Against this background, our paper makes the following four principle contributions. First, like forecasting itself, gains from model combinations matter most in real time. Yet, the interaction between *model combination schemes and real time data* has not been emphasized in the literature. Apart from fixed-weight combinations, model weights are computed using information about each model's past predictive performance. Measures of predictive performance, such as the log predictive score, are typically dependent on the recorded predictive likelihood values of the individual models. In a real-time context, model weighting emerges when outcomes are imperfectly known: measured values of the predicted variables for period t are, by construction, not observed until $t + l$, which implies that the predictive likelihoods for models should be lagged at least l periods when computing the incremental weights. The upshot is that an event such as the Great Recession—wherein large forecast errors emerge, model performance may diverge, and data revisions may be substantial—mechanically takes time to influence the

model weights. Consequently, a "better" model may be under-utilized depending on these lags, or existing sub-optimal model weights may persist.

To that end we define the following terms: *observation lag* is the time difference between the date of the variable and the vintage its actual value is taken from, while *information lag* is the time difference between the date of the variable and the vintage a measured value is taken from. The former concept concerns the data used for the performance measure of density forecast combinations, while the latter is related to the information used for computing combination weights. It should be kept in mind that the information lag comes on top of the forecast horizon so that the sum of the two make up the delay before historical density forecasts can be used for model weighting. We demonstrate that the assumed length of the information lag matters for the attainable gains from forecast combinations and the ranking of the methods over time.

A second contribution is that, unlike the bulk of the literature, we consider *multi-step-ahead forecasts* in our density combination comparisons: backcasts, nowcasts and up to eight-quarter-ahead forecasts.[1] This matters because models' predictive performance can be highly horizon specific. Again, the Great Recession episode is telling: all models incur large forecast errors, but some "recover" better than others over different horizons and for different reasons. This has implications for the gains obtainable from model combinations in general as well as the specific performance of different combination schemes. A standard one-step-ahead density forecast would suppress these issues. Third, we introduce *upper and lower bounds* for the density forecasts, allowing us to benchmark the combination methods not only with respect to the available models but against the best and the worst cases given the models involved. These bounds are easily formed from the density forecasts of the models and to our knowledge have not been discussed in the literature. Fourth, we contribute to the literature on model combinations in a *euro area context*. Relative to that of the US, evidence of real-time density forecasting on euro area data remains scant, despite its similar economic weight, and corresponding evidence on model combinations is scanter still.

The paper is organized as follows. Section 2 discusses probabilistic forecasting and the particular combination methods that we use, namely fixed weights, static and dynamic prediction pools, as well as Bayesian and dynamic model averaging. In so doing, we clarify the equivalence of some methods under different limiting assumptions, and highlight specific methodological modifications required for our exercises. Section 3 overviews the models used: three DSGE models that are variants of the canonical Smets and Wouters model (McAdam and Warne, 2019), as well as two Bayesian vector autoregressions (BVARs), embodying standard and recently developed priors; see Giannone, Lenza, and Primiceri (2015, 2019).

Section 4 describes the recursive estimation of the BVAR models which, like the three DSGE models, are estimated on vintages taken from the euro area real-time database (RTD); see Giannone, Henry, Lalik, and Modugno (2012). In Section 5, the forecast performance of the

---

[1] One exception is Jore, Mitchell, and Vahey (2010) who also suggest a simple recursive weighting scheme for density forecast combinations based on the log predictive score.

models is presented for the sample 2001–2014. This period constitutes an especially challenging laboratory: not only given the real-time and differing information dimensions, but also because it spans a period of relatively calm macroeconomic conditions, undone by the Great Recession.[2] Section 6 contains the bulk of our key results in terms of forecast combinations. We consider the predictive performance of the individual models as well as that of the different combination schemes, study the combination weights and compare the combination methods to the upper and the lower bounds for the selection of models. The sensitivity of results to the information lag assumption is examined and we experiment with combination schemes that modify the initialization of the weights. Finally, Section 7 summarizes the main findings, while additional material is in the Appendices.

2. Density Forecast Combination Methods

Scoring rules are widely used in econometrics and statistics to compare the quality of probabilistic forecasts by attaching a numerical value based on the predictive distribution and an event or value that materializes; see Gneiting and Raftery (2007) for a survey on scoring rules and Gneiting and Katzfuss (2014) for a review on probabilistic forecasting. A scoring rule is said to be *proper* if a forecaster who maximizes the expected score provides his or her true subjective distribution, and it is said to be *local* if the rule only depends on the predictive density and the realized value of the predicted variables. A well-known scoring rule is the log predictive score and, as shown by Bernardo (1979), it is the only proper local scoring rule.[3]

Suppose there are M models to compare in a density forecast exercise and let $p_{t+h|t}^{(i)} = p(x_{t+h}^{(a)}|\mathcal{I}_t^{(i)}, A_i)$ denote the predictive likelihood conditional on the assumptions of model i, denoted by A_i, and the information set of model i, given by $\mathcal{I}_t^{(i)}$. The predictive likelihood is given by the predictive density evaluated at the actual or observed value of the vector of random variables x, realized at time $t + h$ and denoted by $x_{t+h}^{(a)}$, with the integer h being the forecast horizon. The log predictive score of model i for h-step-ahead density forecasts is given by

$$S_{T:T_h,h}^{(i)} = \sum_{t=T}^{T_h} \log\left(p_{t+h|t}^{(i)}\right), \quad i = 1, \ldots, M. \tag{1}$$

The larger the log predictive score is, the better a model can predict the vector of variables x at the h-step-ahead forecast horizon.

A Kalman-filter-based approach to the estimation of the log predictive likelihood in linear state-space models was suggested in a recent paper by Warne, Coenen, and Christoffel (2017). This method was also utilized in our recent paper, McAdam and Warne (2019), where we compare real-time density forecasts for the euro area based on three estimated DSGE models. In the current section, we discuss four approaches to combining the density forecasts from individual

---

[2] Papadopoulos (2017) examines model combination approaches to develop robust macro-financial models for credit risk stress testing in the wake of the Great Recession.

[3] Specifically, the log predictive score is unique up to a positive coefficient of proportionality and a constant which only depends on the historical data.

models: static optimal and dynamic prediction pools (SOP and DP), and Bayesian and dynamic model averaging (BMA and DMA). It may also be noted that these combination schemes cover the three broad combination methodologies discussed by Aastveit et al. (2019): frequentist based optimized combination weights (SOP); Bayesian model averaging weights (BMA and DMA); and flexible Bayesian forecast combination structures (DP). In addition to these four combination schemes, the empirical part of the paper utilizes fixed-weight-based approaches, such as equal weights on all or on a subset of the models.

Notice that the predictive likelihood, $p(x_{t+h}^{(a)}|\mathcal{I}_t^{(i)}, A_i)$, does not include the parameters of the model as these have already been integrated out by accounting for the posterior distribution. Waggoner and Zha (2012) allow the combination weights to follow a hidden Markov process and emphasize the joint estimation of the weights and the parameters of all models. In the empirical exercise we recycle the predictive likelihoods estimates of three DSGE models from McAdam and Warne (2019), while the predictive likelihoods of the VAR models are also estimated separately. This decision is based not only on computational constraints but also on the arguments and justification presented in Del Negro, Hasegawa, and Schorfheide (2016).

Several other density forecast combination methods have recently been introduced to the literature, such as the dynamic Bayesian predictive synthesis in McAlinn and West (2019); the so called generalized density forecast combinations of Kapetanios, Mitchell, Price, and Fawcett (2015); and the state-space approach of Billio, Casarin, Ravazzolo, and van Dijk (2013); see also Aastveit et al. (2019) for additional approaches. We have opted to omit these methods from the current study.

2.1. STATIC OPTIMAL PREDICTION POOLS

Static optimal predictions pools were introduced by Hall and Mitchell (2007) as a means to improve the density forecasts of individual forecasters or models by computing the optimal linear combination of these forecasts. The basic idea is to maximize the log predictive score of a linear combination of the predictive likelihoods of the models in the pool. This linear combination is constrained such that the model weights are constant, non-negative and sum to unity. As a result, the combination of the predictive likelihoods is also a predictive likelihood and the log predictive score is formed by accumulating the log of the pooled predictive likelihoods.

This forecast combination is referred to as static since the weights are treated as constant over time. A recursive approach to the estimation of these weights is more realistic when viewing the problem of comparing models in real time. In that case, the weights of the models can change due to re-optimization with more recent information. Hall and Mitchell (2007) motivate the use of static optimal pools on the grounds that the weights are chosen to minimize the "distance" between the forecasted and the unknown true predictive density in the sense of the Kullback-Leibler information criterion; see Kullback and Leibler (1951). In contrast with combination approaches such as BMA, discussed in Section 2.4, Geweke and Amisano (2011, 2012) point out that static optimal prediction pools do not rely on the assumption that one of the models in

the pool is true, i.e., the approach allows for incomplete models with the effect that all of the models in the pool may be false; see Geweke (2010).[4]

Let $w_{i,h}$ be the weight on model i for h-step-ahead forecasts, satisfying $w_{i,h} \geq 0$ and $\sum_{i=1}^{M} w_{i,h} = 1$. The log predictive score of the static optimal pool is therefore given by

$$S_{T:T_h,h}^{(\text{SOP})} = \sum_{t=T}^{T_h} \log \left(\sum_{i=1}^{M} w_{i,h} p_{t+h|t}^{(i)} \right), \tag{2}$$

where the predictive likelihood of the pool is given by the term being logged on the right hand side of this equation. Estimates of the weights are obtained by maximizing the log score in (2) with respect to the weights and subject to their restrictions.

2.2. Observation and Information Lags

From a recursive perspective, the weights in (2) can only be estimated based on the predictive likelihoods that have been observed at the time. The standard assumption for discrete time data is that variables are observed in the same period that they measure, i.e., x_t is both realized and observed in period t. From a real-time perspective, however, a first release or first estimate of x_t is often not available in period t but is published at a later date. Moreover, most macroeconomic variables are subject to revisions, due to more accurate information appearing with some delay and/or due to changes in measurement methodology. When comparing or evaluating forecasts, a decision must be made regarding which vintage to use for the actuals; see, e.g., Croushore and Stark (2001) and Croushore (2011). In principle, any vintage can be used for the actual value and common choices in the real-time literature are the first release, the annual revision and the latest vintage. Although the latest vintage may reflect actuals that for many periods have not been subject to large revisions, it suffers from possible methodological changes to the measurements that were not known in real time.[5] Similarly, first release data is typically subject to larger revisions in comparison to, for instance, annual revisions data.

The choice of actuals is important since it represents the "true value" of the forecasted variables and therefore affects the outcome of the comparison exercise. To distinguish the data used for comparing forecasts from the data used for computing model weights for *combination methods*, the time difference between the date of the variable and the date of the vintage the actual value is taken from is henceforth called the *observation lag* and in the empirical exercise we use annual revisions data. This means that $x_t^{(a)}$ is taken from vintage $t+4$ such that $x_t^{(a)} = x_t^{(t+4)}$, with the consequence that the observation lag $k = 4$. At the same time, the vintages $t+1$, $t+2$ and $t+3$ typically include measures of x_t, denoted by $x_t^{(m)}$, and these values may be useful when computing the optimal weights recursively. To account for this we also define the term *information lag*, denoted by l, to be the time difference between the date of the variable and

---

[4] See also Pauwels and Vasnev (2016) for further analysis of optimal prediction pool weights and the underlying optimization problem, and Opschoor, van Dijk, and van der Wel (2017) for extensions to alternative scoring rules.

[5] This is certainly true for the euro area RTD, which also reflects a time-varying country composition, where seven EU member countries have been admitted since 2007.

the vintage a measured value is taken from. The minimum information lag is determined by the time delay before to the first publication of x_t, while the maximum may be set equal to the observation lag. These real-time lag concepts are illustrated in Figure 1 and it may be noted that both these lags are zero if one assumes that the date of the variable is equal to the time period when it is observed, as is standard for the single database (vintage) forecast exercises.

It should be emphasized that the information lag is a distinct concept from the ragged edge of real-time data; see Wallis (1986). The latter is a property of the database and is a consequence of individual time series in a real-time vintage being measured up to different time periods. For instance, interest rates may be measured up to the vintage date, while real GDP growth lags with one quarter, and some labor market variables such as wages with two quarters. The ragged edge directly affects the data available for estimation of model parameters and the conditioning information when forecasting with the models. The minimum information lag is influenced by the ragged edge since it depends on the dates for which historical measured values of all the forecasted variables are available. At the same time, the information lag concerns only the forecasted variables and may be selected by the user of the combination method.

To clarify the relevance of these concepts and the decision problems implied by them, consider the following example based on one-quarter-ahead density forecasts with a static optimal pool: Suppose the minimum information lag is equal to one quarter for the vector x in vintage τ, while the observation lag is equal to four quarters. This means that $x_{\tau-1}$ has a measured value $x_{\tau-1}^{(m)}$ for vintage τ and that similarly $x_{\tau-2}, x_{\tau-3}, \ldots$ have measured values for this vintage. By having a measured value it is understood that there are not any missing data for any element of x. Furthermore, an observation lag of four means that actual values of $x_{\tau-4}, x_{\tau-5}, \ldots$ are available at τ and are taken from vintages $\tau, \tau-1, \ldots$. Similarly, forecast densities of the current and all previous one-quarter-ahead forecasts of x are available for the M models at time τ, where each model makes use of data from the corresponding vintage. This means that the predictive likelihood values based on the actual values $p(x_{t+1}^{(a)}|\mathcal{I}_t^{(i)}, A_i)$ can be observed for $t = T, \ldots, \tau-5$. In addition, the predictive likelihood values based on the measured values $p(x_{t+1}^{(m)}|\mathcal{I}_t^{(i)}, A_i)$ can be observed for $t = T, \ldots, \tau-2$.

The user of a static optimal pool needs to make two decisions before determining the recursive weights for the pool at time τ: (i) which information lag to use among $l = 1, 2, 3, 4$; and (ii) whether to use the predictive likelihoods based on the actual values or on the measured values for $t = T, \ldots, \tau-4$. The decisions to these two issues determine the objective function for selecting the optimal weights. Since the actual values represent the "true values" we assume in the empirical exercise that the second decision always brings the predictive likelihood values for the actuals to the weight estimation problem. If an information lag longer than the minimum possible is selected, this means for our example that all $x_{\tau-j}^{(m)}$ for $j < l$ along with the predictive likelihood values based on these measured values are discarded when estimating the optimal weights at τ. For the possible choices of l it holds that the optimal weights at τ are selected

such that the log predictive score function

$$\tilde{S}_{T:\tau-l-1,1}^{(\text{SOP})} = \sum_{t=T}^{\tau-5} \log\left(\sum_{i=1}^{M} w_{i,1,\tau} p\big(x_{t+1}^{(a)}\big|\mathcal{I}_t^{(i)}, A_i\big)\right) + \sum_{t=\tau-4}^{\tau-l-1} \log\left(\sum_{i=1}^{M} w_{i,1,\tau} p\big(x_{t+1}^{(m)}\big|\mathcal{I}_t^{(i)}, A_i\big)\right),$$

is maximized with respect to $w_{i,1,\tau}$, $i = 1, \ldots, M$, and subject to having non-negative weights adding to unity. Notice that the first term on the right hand side involves a sum up to the vintage date (τ) minus the observation lag ($k = 4$) and the forecast horizon ($h = 1$), while the sum for the second term begins at the vintage date minus the observation lag (plus the forecast horizon minus 1) and ends at the vintage date minus the information lag (l) and the forecast horizon. Notice also that when $\tau \leq T + l$ the above log predictive score function for selecting weights cannot be determined. Initial values for the weights are then needed for these vintages and one candidate is $w_{i,1,\tau} = 1/M$ for all i.

In the empirical exercise we initially make the mechanical assumption that the information lag is equal to the observation lag, but also examine the more realistic case when the information lag is shorter than the observation lag. For the variables we forecast in the empirical analysis, the shortest possible information lag for quarterly data is one quarter for most vintages and two quarters for the remaining ones. Finally, the two lag concepts are applied to density forecasts in this paper, they are also relevant for point forecast combination methods with real-time data.

2.3. Dynamic Prediction Pools

Dynamic prediction pools, suggested by Del Negro et al. (2016), directly allow the weights to vary as well as to be correlated over time. While their setup is based on two models, Amisano and Geweke (2017) extends the dynamic prediction pool from two to three models. In fact, the approach in Amisano and Geweke allows for any finite number of models and it is for such a general case that we present dynamic prediction pools below. Accordingly, the number of models is, as before, equal to M and the log predictive score for the dynamic prediction pool is:

$$S_{T:T_h,h}^{(\text{DP})} = \sum_{t=T}^{T_h} \log\left(\sum_{i=1}^{M} w_{i,t+h|t} p_{t+h|t}^{(i)}\right), \tag{3}$$

where $w_{i,t+h|t}$ is the weight on model i for h-step-ahead density forecasts at t, where all weights are non-negative and sum to unity.

To model the time variation of the weights, we follow Amisano and Geweke (2017) and consider a parsimoniously parameterized M-dimensional process for the state variable

$$\xi_t = \rho\xi_{t-1} + \sqrt{(1-\rho^2)}\eta_t, \qquad t = T, \ldots, T_h, \tag{4}$$

where $0 \leq \rho \leq 1$ is a scalar and $\eta_t \sim$ i.i.d.$N(0, I_M)$.[6] The ρ parameter is referred to as a "forgetting factor" for dynamic pools by Del Negro et al. (2016) since with $\rho < 1$ there is

---

[6] For the implementation of the dynamic prediction pool in Del Negro et al. (2016), they have a univariate process similar to (4), but also allow for a drift parameter μ and a standard deviation σ. The process for ξ in (4) can be enriched in various ways, but for the sake of parsimony we only allow for one free parameter.

discounting of past information. The parameterization of ξ_t in (4) ensures that its covariance is the identity matrix when $\rho < 1$, while ξ_t is constant (static) otherwise.

The weights are determined from a logistic transformation of the individual elements of the state vector, $\xi_{i,t}$ which ensures that each element is non-negative and that the sum of the elements is unity:

$$w_{i,t} = \frac{\exp(\xi_{i,t})}{\sum_{j=1}^{M} \exp(\xi_{j,t})}, \quad i = 1, \ldots, M. \tag{5}$$

The vector w_t is consequently M-dimensional with individual entries given by the model weights. As pointed out by Amisano and Geweke (2017, Appendix E.4) the specification in (5) implies a symmetric prior across weights.

To estimate the log predictive score in (3) conditional on ρ, Amisano and Geweke (2017) follow the approach in Del Negro et al. (2016) and employ the *Bayesian bootstrap particle filter*; see, e.g., Gordon, Salmond, and Smith (1993) and Herbst and Schorfheide (2016) for details and further references. This filter is *initialized* as follows: At $t = T - 1$, draw N particles from the unconditional distribution of ξ_{T-1} and map these into $w_{i,T-1}$ using (5), while each particle is assigned equal weight; i.e., for $i = 1, \ldots, M$ and $n = 1, \ldots, N$

$$\xi_{T-1}^{(n)} \sim N(0, I_M),$$

$$w_{i,T-1}^{(n)} = \frac{\exp(\xi_{i,T-1}^{(n)})}{\sum_{j=1}^{M} \exp(\xi_{j,T-1}^{(n)})},$$

$$W_{T-1}^{(n)} = 1.$$

During the *recursions* of the bootstrap particle filter for $t = T, \ldots, T_h$, each iteration involves three steps: forecasting, updating, and selection. The *forecasting* step concerns propagating the N particles forward by drawing innovations $\eta_t^{(n)} \sim N(0, I_M)$ such that

$$\tilde{\xi}_t^{(n)} = \rho \xi_{t-1}^{(n)} + \sqrt{(1 - \rho^2)} \eta_t^{(n)},$$

$$\tilde{w}_{i,t}^{(n)} = \frac{\exp(\tilde{\xi}_{i,t}^{(n)})}{\sum_{j=1}^{M} \exp(\tilde{\xi}_{j,t}^{(n)})},$$

for $i = 1, \ldots, M$ and $n = 1, \ldots, N$. Next, the incremental weights are calculated as

$$\tilde{\omega}_t^{(n)} = p(x_t^{(m)} | \tilde{w}_t^{(n)}, \mathcal{I}_{t-h}^{(\mathcal{P})}, \mathcal{P}) = \sum_{i=1}^{M} \tilde{w}_{i,t}^{(n)} p(x_t^{(m)} | \mathcal{I}_{t-h}^{(i)}, A_i), \quad n = 1, \ldots, N,$$

where these weights depend on ρ via $\tilde{w}_t^{(n)}$, a vector with $\tilde{w}_{i,t}^{(n)}$ in element i, and with $\mathcal{I}_t^{(\mathcal{P})}$ being the joint information set of the pooled models. Notice that the incremental weights are formed from the h-steps-ahead predictive likelihoods of the individual models based on measured values of the predicted variables in period t, $x_t^{(m)}$.

The *updating* step consists in recomputing the weights according to

$$\tilde{W}_t^{(n)} = \frac{\tilde{\omega}_t^{(n)} W_{t-1}^{(n)}}{(1/N) \sum_{j=1}^{N} \tilde{\omega}_t^{(j)} W_{t-1}^{(j)}}.$$

Notice that the sum of the updated weights $\tilde{W}_t^{(n)}$ over all particles is equal to N. If all the weights from recursion $t - 1$ are equal, then the updated weights are proportional to the incremental weights and therefore the particle likelihood values.

For the *selection* step we first compute the effective sample size (ESS) according to

$$\text{ESS}_t = \frac{N}{(1/N) \sum_{n=1}^{N} (\tilde{W}_t^{(n)})^2}.$$

On the one hand, if $\text{ESS}_t < \delta^* N$ for a suitable value of the hyperparameter δ^*, where $0 < \delta^* < 1$, the particles are resampled with multinomial resampling, characterized by support points and weights $\{\tilde{\xi}_t^{(n)}, \tilde{w}_t^{(n)}, \tilde{W}_t^{(n)}\}_{n=1}^{N}$. Let $\{\xi_t^{(n)}, w_t^{(n)}, W_t^{(n)}\}_{n=1}^{N}$ denote a swarm of N i.i.d. draws where the weights are given by $W_t^{(n)} = 1$. On the other hand, if $\text{ESS}_t \geq \delta^* N$, the weights $W_t^{(n)} = \tilde{W}_t^{(n)}$ while the state variables $\xi_t^{(n)} = \tilde{\xi}_t^{(n)}$ and the corresponding model weights $w_t^{(n)} = \tilde{w}_t^{(n)}$.

The conditional predictive likelihood of the dynamic pool in recursion t is approximated with

$$p_{t+h|t}^{(\mathcal{P})}(\rho) = p(x_{t+h}^{(a)} | \mathcal{I}_t^{(\mathcal{P})}, \mathcal{P}; \rho) = \sum_{i=1}^{M} w_{i,t+h|t}(\rho) p(x_{t+h}^{(a)} | \mathcal{I}_t^{(i)}, A_i), \tag{6}$$

where the particle weights depend on the parameter ρ, and the weights $w_{i,t+h|t}^{(n)}$ are computed by iterating forward using the law of motion in (4). That is

$$w_{i,t+h|t}(\rho) = E[w_{i,t+h} | \mathcal{I}_t^{(\mathcal{P})}, \mathcal{P}; \rho]$$

$$\approx \frac{1}{N} \sum_{n=1}^{N} w_{i,t+h}^{(n)}(\rho) W_t^{(n)},$$

where for each particle n

$$\xi_{i,t+s}^{(n)}(\rho) = \rho \xi_{i,t+s-1}^{(n)} + \sqrt{(1-\rho^2)} \eta_{t+s}^{(n)},$$

$$w_{i,t+h}^{(n)}(\rho) = \frac{\exp(\xi_{i,t+h}^{(n)}(\rho))}{\sum_{j=1}^{M} \exp(\xi_{j,t+h}^{(n)}(\rho))},$$

for $s = 1, \ldots, h$, and where $\eta_{t+s}^{(n)}$ is a draw from an M-variate standard normal distribution.

In a real-time setting, the information lag needs to be taken into account. Consider the convenient, albeit mechanical, assumption that the information lag is equal to the observation lag. With annual revisions data, this means that the predictive likelihoods for the individual models are lagged four periods when computing the incremental weights. Since measured values of x may be available for periods $t - 3$, $t - 2$ and $t - 1$ in vintage t, a shorter information lag is feasible. Unless the measured values are equal to the actual values for these time periods, however, the bootstrap particle filter requires two loops, where for each vintage t the iterations

from T until t are (at least partly) revisited. The assumption that the information lag is equal to the observation lags means that the second loop can be avoided. Alternatively, it may also be skipped if one assumes that measured values are well approximated by the actual values, i.e., that the revisions are sufficiently small that they can be neglected.[7]

Amisano and Geweke (2017) apply the bootstrap particle filter over a fine grid of values for ρ and compute $\hat{\rho}_\tau$ by maximizing the log score

$$\hat{\rho}_{\tau,h} = \arg\max_{\rho} \sum_{t=T}^{\tau-h} \log\Big(p\big(x_{t+h}^{(m)} | \mathcal{I}_t^{(\mathcal{P})}, \mathcal{P}; \rho\big)\Big), \quad \tau = T, \ldots, T_h \tag{7}$$

where the predictive likelihood on the right hand side are computed as in (6), but with the measured value instead of the actual value. This means that the first period τ when the h-step-ahead predictive likelihood of the individual models can be observed occurs at $\tau = T+h$. Taking the real-time aspect fully into account means that the information lag, $l \leq k$, is added to this number. It follows that for all τ less than $T + h + l$, a unique value of ρ cannot be determined as there are no data on the predictive likelihoods available. This initialization problem may be dealt with by replacing the unobserved predictive likelihood values with a positive constant, such as $1/M$, with the consequence that all values of ρ from T up to $T + h + l - 1$ obtain the same log score when computing the weights. As the number of particles becomes very large, this amounts to giving all models the same weight.

With the sequence $\{\hat{\rho}_t\}_{t=T}^{\tau}$, the real-time log predictive score of the dynamic prediction pool is then estimated by

$$S_{T:\tau,h}^{(\text{DP})} = \sum_{t=T}^{\tau} \log\Big(p_{t+h|t}^{(\mathcal{P})}\big(\hat{\rho}_{t,h}\big)\Big).$$

According to Amisano and Geweke (2017), this procedure may be interpreted as a Bayesian analysis based on a flat (uniform) prior on ρ.

Resampling was originally employed by Gordon et al. (1993) to reduce the effects from sample *degeneracy*—a highly uneven distribution of particle weights—as this part of the selection step adds noise; see Chopin (2004). It also allows for the removal of low weight particles with a high probability and this is very practical as it is preferable that the filter is focused on regions with a high probability mass. However, this also means that resampling may produce sample *impoverishment* as the diversity of the particle values is reduced. The hyperparameter δ^* provides a 'crude' tool for balancing the algorithm against the pitfalls of degeneracy or impoverishment by ensuring that resampling takes place but does not occur 'too often'.[8]

---

[7] If only data on x from vintage t are used as measured values they are all subject to revision and the double loop has to be executed from period T for each vintage t. On the other hand, if actuals are used up to period $t-4$ and measured values from vintage t for periods $t-3$, $t-2$ and $t-1$, then the double loop would start in $t-4$ since the earlier computations were run for vintage $t-1$. Finally, if the measured values for $t-3$, $t-2$ and $t-1$ are approximated by the actual values, then the double loop can be dispensed with. For each of these cases, an information lag of one is applied.

[8] A more direct approach to combatting sample impoverishment is based on taking the particle values into account when resampling; see, e.g., Doucet and Johansen (2011) for discussions on the *resample-move* algorithm of Gilks and Berzuini (2001) and the *block sampling* algorithm of Doucet, Briers, and Sénécal (2006).

Del Negro et al. (2016) use a multinomial distribution for the selection step with $\delta^* = 2/3$, but as pointed out by, for example, Douc, Cappé, and Moulines (2005), this resampling algorithm produces an unnecessarily large variance of the particles. Moreover, and as emphasized by Hol, Schön, and Gustafsson (2006), ordering of the underlying uniform draws improves the computational speed considerably. The commonly used alternative resampling algorithms are faster and have a smaller variance of the particles. Systematic resampling, introduced by Kitagawa (1996) and also emphasized by Carpenter, Clifford, and Fearnhead (1999), is a commonly used approach as it is very easy to implement, comparatively fast, and, according to Doucet and Johansen (2011), as it often outperforms other sequential resampling schemes. It is a faster version of stratified resampling (Kitagawa, 1996), where instead of drawing N uniforms only one is required, while stratification and, simultaneously, sorting is dealt with via the same simple affine function. A drawback with systematic resampling is that it generates cross-sectional dependencies among the particles, which also makes it difficult to establish its theoretical properties; see Chopin (2004). For an overview of sequential resampling schemes see, e.g., Hol et al. (2006), who also discuss theoretical criteria for choosing between multinomial, stratified, systematic and residual resampling (suggested by Liu and Chen, 1998); Douc et al. (2005), who also study large sample behavior; and more recently Li, Bolić, and Djurić (2015), who also discusses distributed or parallel algorithms.[9]

2.4. Bayesian Model Averaging

BMA provides a coherent framework for accounting for model uncertainty; see Hoeting, Madigan, Raftery, and Volinsky (1999). The standard BMA weights rely on posterior model probabilities and therefore require the calculation of marginal likelihoods over a set of models which predict the same observables. The DSGE and VAR models we examine, however, do not satisfy this condition: the VAR models predict all nine observable variables comprising the full information set, while the DSGE models do not predict all variables.

However, an alternative BMA weighting scheme may be obtained by only using the predictive likelihood values of the variables of interest (x_t) and a prior for the weights; see Eklund and Karlsson (2007) for discussions on the general idea. Specifically, BMA weights may be obtained as in Del Negro et al. (2016, Section 3) such that

$$\hat{w}_{i,t,h} = \frac{\hat{w}_{i,t-1,h} \, p\big(x_t^{(m)} \big| \mathcal{I}_{t-h}^{(i)}, A_i\big)}{\sum_{j=1}^{M} \hat{w}_{j,t-1,h} \, p\big(x_t^{(m)} \big| \mathcal{I}_{t-h}^{(j)}, A_j\big)}, \tag{8}$$

for $t = T+1, \ldots, T_h$, with $\hat{w}_{i,T,h}$ denoting the prior predictive probability that $w_i = 1$. In this case, the model weights at t are built using only the predictive likelihood values up to period t. As long as $\hat{w}_{i,T,h} = 1$ for some model i does *not* hold, these BMA weights will be positive for

---

[9] Since the bootstrap particle filter will spend a considerable share of the computational time in the resampling stage, especially when δ^* is high, the precise implementation of the selected resampling scheme is also important; see also Warne (2019, Section 8.4) for some details on how to implement the standard sequential algorithms.

several models until the recursive log score of one model dominates the others sufficiently. In the empirical sections below, we primarily let $\hat{w}_{i,T,h} = 1/M$.

It should be kept in mind that the predictive likelihood generated BMA weights are based on the following assumption:

$$p\big(x_t | \mathcal{I}_{t-h}^{(i)}, A_i\big) = p\big(x_t | \mathcal{I}_{t-h}^{(\mathcal{P})}, A_i\big).$$

That is, the additional information available in $\mathcal{I}_{t-h}^{(\mathcal{P})}$ relative to $\mathcal{I}_{t-h}^{(i)}$ does not change the density forecast of x_t for any model $i = 1, \ldots, M$. This holds trivially for the two VAR models, but also for the three DSGE models since the "missing" variables in $\mathcal{I}_{t-h}^{(i)}$ are not predicted by these models.

The BMA weights in (8) are based on the assumption that $x_t^{(m)}$ is observed at t. As discussed in Section 2.2, the real-time dimension means the BMA weights need to be adjusted by lagging the predictive likelihoods on the right hand side by the information lag. In other words, we replace equation (8) with

$$\hat{w}_{i,t,h} = \frac{\hat{w}_{i,t-1,h} \, p\big(x_{t-l}^{(m)} | \mathcal{I}_{t-h-l}^{(i)}, A_i\big)}{\sum_{j=1}^{M} \hat{w}_{j,t-1,h} \, p\big(x_{t-l}^{(m)} | \mathcal{I}_{t-h-l}^{(j)}, A_j\big)}. \tag{9}$$

Like in the cases of the prediction pools, the first period when an h-step-ahead predictive likelihood value is observed occurs at $T + h + l$. For $t = T + 1, \ldots, T + h + l - 1$ we can therefore replace the predictive likelihood values in (9) with a positive constant such that $\hat{w}_{i,t,h} = \hat{w}_{i,T,h}$, the prior predictive probability of model i.

The predictive likelihood for the BMA combination is given by

$$p\big(x_{t+h}^{(a)} | \mathcal{I}_t^{(\mathcal{P})}, \mathcal{P}\big) = \sum_{i=1}^{M} \hat{w}_{i,t,h} \, p\big(x_{t+h}^{(a)} | \mathcal{I}_t^{(i)}, A_i\big),$$

from which it is straightforward to compute the log predictive score, denoted by $S_{T:T_h,h}^{(\text{BMA})}$, of this density forecast combination method.

2.5. Dynamic Model Averaging

Raftery, Kárný, and Ettler (2010) proposed a model combination method, called dynamic model averaging (DMA), where the weights of the log predictive score may be regarded as depending on a hidden Markov process, s_t, as in Waggoner and Zha (2012), but where the estimates of the Markov transition probabilities are approximated. Specifically, Raftery et al. (2010) suggest to estimate the weights as follows

$$w_{i,t+h|t} = \frac{\hat{w}_{i,t,h}^{\varphi^h}}{\sum_{j=1}^{M} \hat{w}_{j,t,h}^{\varphi^h}}, \tag{10}$$

where φ is a parameter such that $0 \le \varphi \le 1$. Notice that the weights $\hat{w}_{i,t,h}$ on the right hand side of equation (10) correspond to the weights from the recursive BMA calculation. Accordingly, if $\varphi = 1$ then DMA is identical to BMA, and if $\varphi = 0$ then DMA implies that the weights are equal $(1/M)$ for all time periods. The parameter φ is interpreted as a *forgetting factor*, where

lower values means that past forecast performance is given a lower weight; see also Koop and Korobilis (2012). Provided that $\varphi < 1$, it follows that the DMA weights approach the equal weights as h increases.

The predictive likelihood for the DMA forecast combination is given by

$$p\big(x_{t+h}^{(a)}|\mathcal{I}_t^{(\mathcal{P})},\mathcal{P}\big) = \sum_{i=1}^{M} w_{i,t+h|t}\,p\big(x_{t+h}^{(a)}|\mathcal{I}_t^{(i)},A_i\big),$$

from which the log predictive score, denoted by $S_{T:T_h,h}^{(\text{DMA})}$, can be directly computed.

Amisano and Geweke (2017) estimate the forgetting factor by recursively maximizing the log predictive score over a grid of φ values, similar to the case for ρ in Section 2.3. They suggest that the procedure can be given a Bayesian interpretation where the researcher assigns a flat (uniform) prior on φ. DMA is also considered by Del Negro et al. (2016), who consider three values of φ below but close to unity.

3. The DSGE and the VAR Models

3.1. The DSGE Models

We use three DSGE models. The first is that of Smets and Wouters (2007), as adapted to the euro area (labelled SW). This contains a continuum of utility-maximizing households and profit-maximizing intermediate good firms who, respectively, supply labor and intermediate goods in monopolistic competition and set wages and prices. Final good producers use these intermediate goods and operate under perfect competition.

The model incorporates several real and nominal rigidities, such as habit formation, investment adjustment costs, variable capital utilization and Calvo staggering in prices and wages. The monetary authority follows a Taylor-type rule when setting the nominal interest rate. There are seven stochastic processes: a TFP shock; a price and a wage markup shock; a risk premium (preference) shock; an exogenous spending shock; an investment-specific technology shock; and a monetary policy shock. The observed variables are: real GDP, real private consumption, real investment, employment, real wages, the GDP deflator (all transformed as 100 times the first difference of the natural logarithm), and the short-term nominal interest rate in percent.

The second model (SWFF) adds the financial accelerator mechanism of Bernanke, Gertler, and Gilchrist (1999) (BGG) to the SW model and augments the list of observables to include a measure of the external finance premium; see McAdam and Warne (2019) for details.[10] The final model (SWU) instead allows for an extensive labor margin, following Galí, Smets, and Wouters (2012), and adds the unemployment rate in percent to the set of observables. McAdam and Warne (2018) describes the models' structure and estimation properties in greater depth and provides a comparative impulse response analysis.

---

[10] A variant of the SWFF which includes long-term inflation expectations data for the US is used by, e.g., Del Negro and Schorfheide (2013), Del Negro, Giannoni, and Schorfheide (2015) and more recently Cai, Del Negro, Herbst, Matlin, Sarfati, and Schorfheide (2019).

3.2. THE VAR MODELS

The two BVAR models we consider in this paper make use of the priors discussed in Giannone et al. (2015, 2019). Below we first present the prior and posterior distributions conditional on a vector of hyperparameters and show the relation between the prior parameters and T_d dummy observations and when the observables are *not* subject to missing observations; see also Bańbura, Giannone, and Lenza (2015). The marginal likelihood conditional on the hyperparameters can then be computed analytically and acts as a likelihood function when the hyperparameters are estimated. To achieve this, a *hyperprior* for the hyperparameters is presented and we discuss how they can be estimated in this setting.

Before we continue, it should be stressed that the discussion below is based on complete datasets, i.e., when there are no missing observations of the observable variables. The real-time data vintages we use in the paper have a so-called ragged edge, with some variables being missing for the vintage date as well as for the quarter prior to the vintage date. To incorporate such datasets makes direct sampling of the VAR parameters impossible and further complicates the posterior analysis as an analytical expression of the marginal likelihood conditional on the hyperparameters is not available, with the effect that all these parameters need to be estimated simultaneously. The computational costs of dealing with the ragged edge can therefore be very high and for this reason a second best approach may be considered, where the dataset is trimmed during the parameter estimation step. We return to this issue in Section 3.2.5.

3.2.1. THE NORMAL-INVERTED WISHART BVAR MODEL

To establish notation, let y_t be an n-dimensional vector of observable variables with a VAR representation given by

$$y_t = \Phi_0 + \sum_{j=1}^{p} \Phi_j y_{t-j} + \epsilon_t, \quad t = 1, \ldots, T, \tag{11}$$

where $\epsilon_t \sim N_n(0, \Omega)$ and Φ_j are $n \times n$ matrices for $j \geq 1$ and an $n \times 1$ vector if $j = 0$. Let $X_t = [1 \; y_t' \; \cdots \; y_{t-p+1}']'$ be an $(np + 1)$-dimensional vector, while the $n \times (np + 1)$ matrix $\Phi = [\Phi_0 \; \Phi_1 \; \cdots \; \Phi_p]$ such that the VAR can be expressed as:

$$y_t = \Phi X_{t-1} + \epsilon_t. \tag{12}$$

Stacking the VAR system as $y = [y_1 \; \cdots \; y_T]$, $X = [X_0 \; \cdots \; X_{T-1}]$ and $\epsilon = [\epsilon_1 \; \cdots \; \epsilon_T]$, we can express this as

$$y = \Phi X + \epsilon. \tag{13}$$

The normal-inverted Wishart prior for (Φ, Ω) is given by

$$\text{vec}(\Phi) | \Omega, \alpha \sim N_{n(np+1)}\big(\text{vec}(\mu_\Phi), [\Omega_\Phi \otimes \Omega]\big), \tag{14}$$

$$\Omega | \alpha \sim IW_n(A, v), \tag{15}$$

where the prior parameters $(\mu_\Phi, \Omega_\Phi, A, v)$ are determined through a vector of hyperparameters, denoted by α.[11] Combining this prior with the likelihood function and making use of standard "Zellner" algebra, it can be shown that the conjugate normal-inverted Wishart prior gives us a normal posterior for $\Phi|\Omega, \alpha$ and an inverted Wishart posterior for $\Omega|\alpha$. Specifically,

$$\text{vec}(\Phi)\big|\Omega, y, X_0, \alpha \sim N_{n(np+1)}\big(\text{vec}(\bar{\Phi}), \big[(XX' + \Omega_\Phi^{-1})^{-1} \otimes \Omega\big]\big), \tag{16}$$

$$\Omega\big|y, X_0, \alpha \sim IW_n\big(S, T + v\big), \tag{17}$$

where

$$\bar{\Phi} = \big(yX' + \mu_\Phi \Omega_\Phi^{-1}\big)\big(XX' + \Omega_\Phi^{-1}\big)^{-1},$$

$$S = yy' + A + \mu_\Phi \Omega_\Phi^{-1}\mu_\Phi' - \bar{\Phi}\big(XX' + \Omega_\Phi^{-1}\big)\bar{\Phi}'.$$

The log marginal likelihood has an analytical expression which is given by

$$\begin{aligned}
\log p\big(y\big|X_0, \alpha\big) = &-\frac{nT}{2}\log(\pi) + \log\Gamma_n(T + v) - \log\Gamma_n(v) - \frac{n}{2}\log\big|\Omega_\Phi\big| \\
&+ \frac{v}{2}\log\big|A\big| - \frac{n}{2}\log\big|XX' + \Omega_\Phi^{-1}\big| - \frac{T+v}{2}\log\big|S\big|,
\end{aligned} \tag{18}$$

where $\Gamma_b(a) = \prod_{i=1}^b \Gamma([a - i + 1]/2)$ for positive integers a and b with $a \geq b$, while $\Gamma(\cdot)$ is the gamma function; see Appendix A for further details.

3.2.2. Sum-Of-Coefficients Prior

In this paper we consider two ways of parameterizing the prior parameters $(\mu_\Phi, \Omega_\Phi, A, v)$. The first approach is based on Giannone et al. (2015) with a Minnesota prior combined with the standard sum-of-coefficients prior by Doan, Litterman, and Sims (1984), and the dummy-initial-observation prior by Sims (1993). As pointed out by Sims and Zha (1998), the latter part of the prior was designed to neutralize the bias against cointegration due to the sum-of-coefficients prior, while still treating the issue of overfitting of the deterministic component; see also Sims (2000). This parameterization is henceforth called the SoC prior.

Specifically, the SoC prior can be implemented through $T_d = n(p+2)+1$ dummy observations by prepending the y ($n \times T$) and X ($np + 1 \times T$) matrices with the following:

$$y_{(d)} = \begin{bmatrix} \lambda_o^{-1}\text{diag}(\psi \odot \omega) & 0_{n \times n(p-1)} & \text{diag}(\omega) & \delta^{-1}\bar{y}_0 & \mu^{-1}\text{diag}(\psi \odot \bar{y}_0) \end{bmatrix},$$

$$X_{(d)} = \begin{bmatrix} 0_{1 \times np} & 0_{1 \times n} & \delta^{-1} & 0_{1 \times n} \\ \lambda_o^{-1}\big(j_p \otimes \text{diag}(\omega)\big) & 0_{np \times n} & \delta^{-1}\big(\imath_p \otimes \bar{y}_0\big) & \mu^{-1}\big(\imath_p \otimes \text{diag}(\bar{y}_0)\big) \end{bmatrix}, \tag{19}$$

where $\odot$ is the Hadamard product, i.e., element-by-element multiplication. The vector $\imath_p$ is a p-dimensional unit vector, while the $p \times p$ matrix $j_p = \text{diag}[1 \cdots p]$. Notice that the first $n(p+1)$

---

[11] For notational simplicity, the model assumptions (A_i), including any calibrated hyperparameters, are not explicitly specified as conditioning information.

columns of the matrices in (19) cover the Minnesota prior, the following column is the dummy-initial-observation prior, while the remaining n columns determine the sum-of-coefficients prior.

The hyperparameter $\lambda_o > 0$ gives the overall tightness in the Minnesota prior, the cross-equation tightness is set to unity, while the harmonic lag decay hyperparameter is equal to 2. The hyperparameter δ captures shrinkage for the dummy-initial-observation prior, where $\delta \to \infty$ gives the standard diffuse prior for Φ_0. The hyperparameter μ similarly determines shrinkage for the sum-of-coefficients prior, while the vector ω handles scaling issues. In this paper we focus on forecasting and let the each element of ω be given by the estimated innovation standard deviation from AR processes of order p for the corresponding observed variable. The vector ψ is the prior mean of the diagonal of Φ_1, and $\bar{y}_0$ is given by the pre-sample mean of y_t, i.e., $\bar{y}_0 = (1/p) \sum_{j=1}^{p} y_{j-p}$. This is consistent with the treatment in Bańbura, Giannone, and Reichlin (2010) and Giannone et al. (2019).[12]

The vector ψ is given by ι_n under the orthodox Minnesota prior (random walk prior mean), but can also be given by, for instance, a 0-1 vector as in Bańbura et al. (2010), where ψ_i is set to unity if y_{it} is a levels variable and to zero if it is a first differenced variable. For the SoC prior, we let $\psi_i = 1$ for all variables that appear in first differences in the measurement equations of the DSGE models and as levels variables in the VAR models, while the remaining elements have $\psi_i = 0.9$. It now follows that the three-dimensional vector of hyperparameters to be estimated is given by $\alpha = [\lambda_o \ \delta \ \mu]'$ under the SoC prior.

From, e.g., Bańbura et al. (2010) we find that the relationship between the dummy observations and the prior parameters $(\mu_\Phi, \Omega_\Phi, A, v)$ are:

$$\mu_\Phi = y_{(d)} X'_{(d)} \left(X_{(d)} X'_{(d)} \right)^{-1}, \qquad\qquad \Omega_\Phi = \left(X_{(d)} X'_{(d)} \right)^{-1},$$
$$A = \left(y_{(d)} - \mu_\Phi X_{(d)} \right) \left(y_{(d)} - \mu_\Phi X_{(d)} \right)', \qquad\qquad v = T_d - (np + 1).$$

If we make use of the expression for the number of degrees of freedom above, it follows that $v = 2n$ and the prior mean of Ω exists as $v > n+1$ when $n \geq 2$. However, the number of degrees of freedom can instead be selected as desired rather than taken literally from the dimensions of the dummy observation matrices. For example, the choice $v = n + 2$ is sufficient to ensure that the expectation of $\Omega|\alpha$ under the prior density exists and this is the choice we make in this paper for the SoC prior as well as for the prior discussed in Section 3.2.3.

Given the dummy observations in equation (19), simple analytical expressions for the prior location matrices μ_Φ and A can be shown to be

$$\mu_\Phi = \left[\left((\iota_n - \psi) \odot \bar{y}_0 \right) \ \text{diag}(\psi) \ 0_{n \times n(p-1)} \right],$$
$$A = \text{diag}(\omega)^2.$$

---

[12] An alternative approach is considered by, e.g., Giannone et al. (2015) who treat ω as a hyperparameter to be estimated.

Furthermore, since Ω_Φ only depends on the parameters affecting $X_{(d)}$, the prior covariance matrix of Φ does *not* depend on the vector ψ.

Letting $y_\star = [y_{(d)}\ y]$ and $X_\star = [X_{(d)}\ X]$, it can be verified that the posterior parameters can be conveniently expressed as

$$\bar{\Phi} = y_\star X_\star' \left(X_\star X_\star'\right)^{-1},$$

$$XX' + \Omega_\Phi^{-1} = X_\star X_\star',$$

$$S = \left(y_\star - \bar{\Phi}X_\star\right)\left(y_\star - \bar{\Phi}X_\star\right)'.$$

3.2.3. Prior for the Long Run

The second parameterization of the normal-inverted Wishart prior is based on the prior for the long run (PLR) suggested by Giannone et al. (2019). The PLR provides an alternative to the SoC prior for formulating the disbelief in an excessive explanatory power of the deterministic component of the model; see Sims (2000). Specifically, the PLR focuses on long-run relations, stationary as well as non-stationary, where economic theory can play an important role for eliciting the priors. The PLR does not impose the long-run relations but instead allows for shrinkage of the VAR parameters towards them.

Let B be an $n \times n$ nonsingular matrix with two blocks of rows

$$B = \begin{bmatrix} \beta_\perp' \\ \beta' \end{bmatrix}, \tag{20}$$

where β are $r \leq n$ potential cointegration relations (Johansen, 1996) and $\beta_\perp$ reflects coefficients on the $n - r$ possible stochastic trends, with $\beta'\beta_\perp = 0$ whenever $1 \leq r \leq n - 1$. For the PLR with a diffuse prior for the constant term (Φ_0) we replace the last $n+1$ columns of $y_{(d)}$ and $X_{(d)}$ in equation (19) such that

$$y_{(d)} = \begin{bmatrix} \lambda_o^{-1}\mathrm{diag}(\psi \odot \omega) & 0_{n \times n(p-1)} & \mathrm{diag}(\omega) & 0_{n \times 1} & B^{-1}\mathrm{diag}(\psi \odot B\bar{y}_0 \ominus \phi) \end{bmatrix},$$

$$X_{(d)} = \begin{bmatrix} 0_{1 \times np} & 0_{1 \times n} & \gamma^{-1} & 0_{1 \times n} \\ \lambda_o^{-1}\left(j_p \otimes \mathrm{diag}(\omega)\right) & 0_{np \times n} & 0_{np \times 1} & \left(\iota_p \otimes B^{-1}\mathrm{diag}(B\bar{y}_0 \ominus \phi)\right) \end{bmatrix}, \tag{21}$$

where element-by-element division is denoted by $\ominus$. The hyperparameter γ reflects overall tightness of Φ_0 such that a diffuse and improper prior is obtained when γ^{-1} is (arbitrarily close to) zero. The hyperparameter ϕ is an $n \times 1$ vector which captures shrinkage of the prior on the possibly non-stationary and stationary linear combinations of y in the rows of B. Since the PLR addresses the issue of the overfitting of the deterministic component, while also allowing for cointegration relations, there is no strong a priori reason for also including the dummy-initial-observation prior in this setup, other than it being an elegant approach for including a proper prior for the constant term of the VAR model.

Note that the original PLR is based on $\psi = \iota_n$, but we have introduced it here as a convenient way of allowing for non-unit means of the diagonal elements of Φ_1 also for this prior. As a consequence, it complements the treatment of possible cointegration relations, where the prior mean may otherwise imply a unit root. For instance, if a possible cointegration relation is a single variable, then having the corresponding ψ element set to some value less than one in absolute terms ensures that the prior mean of the VAR parameters is consistent with this variable being stationary. In this paper, we let $\psi_i = 0.8$ for such variables under the PLR; see also the specification of β below. Furthermore, we let $\gamma^{-1} = 0$ such that the prior for Φ_0 is diffuse and improper. How this affects the posterior distributions of the VAR parameters and the analytical expression of the marginal likelihood are discussed in Appendix A.[13]

The vector of unknown hyperparameters is given by $\alpha = [\lambda_o \ \phi']'$, with $n+1$ elements, while the matrix B is suggested by economic theory, such as from the three DSGE models considered in this paper. As pointed out by Giannone et al. (2019), the PLR simplifies to the sum-of-coefficients prior when $B = I_n$ and $\phi_i = \mu$ for $i = 1, \ldots, n$; see the last n rows of $y_{(d)}$ and $X_{(d)}$ in (19) and (21).

With the nine variables of y_t being ordered as real GDP, real private consumption, real total investment, GDP deflator inflation, total employment, real wages, the nominal short-term interest rate, the spread between the total lending rate and the policy rate, and unemployment, the DSGE models may be used directly to suggest the following non-stationary long-run relations:

$$
\beta'_\perp = \begin{bmatrix} 1 & 1 & 1 & 0 & 0 & 1 & 0 & 0 & 0 \\ 1 & 1 & 1 & 0 & 1 & 0 & 0 & 0 & 0 \end{bmatrix}.
$$

This means that the two potential stochastic trends are given by a technology trend shared by GDP, consumption, investment and wages, and a labor supply (population) trend shared by GDP, consumption, investment and employment. The possibly stationary long-run relations are similarly given by

$$
\beta' = \begin{bmatrix} -1 & 1 & 0 & 0 & 0 & 0 & 0 & 0 & 0 \\ -1 & 0 & 1 & 0 & 0 & 0 & 0 & 0 & 0 \\ -1 & 0 & 0 & 0 & 1 & 1 & 0 & 0 & 0 \\ 0 & 0 & 0 & 1 & 0 & 0 & 0 & 0 & 0 \\ 0 & 0 & 0 & 0 & 0 & 0 & 1 & 0 & 0 \\ 0 & 0 & 0 & 0 & 0 & 0 & 0 & 1 & 0 \\ 0 & 0 & 0 & 0 & 0 & 0 & 0 & 0 & 1 \end{bmatrix}.
$$

---

[13] For details, see equations (A.13)–(A.15) and (A.16), respectively.

These seven linear combinations yield (the log of) the consumption-output ratio, the investment-output ratio, the labor share, inflation, the short-term nominal interest rate, the spread, and unemployment.[14]

3.2.4. Hyperpriors and Posterior Inference

The use of hyperpriors is by no means new and has recently been employed in the BVAR models studied in the papers by Giannone et al. (2015, 2019) and Bańbura et al. (2015). Following Giannone et al. (2015), as hyperpriors for λ_o, δ and μ we use a Gamma distribution with mode 0.2, 1 and 1 (also as in Sims and Zha, 1998) and standard deviations 0.4, 1 and 1, respectively.[15] Furthermore, following Giannone et al. (2019), the hyperprior for each element of ϕ is Gamma with mode and standard deviation equal to 1.

By combining the marginal likelihood in (18) with the SoC prior for the hyperparameters, or the expression in (A.16) for the marginal likelihood with the PLR for the hyperparameters, the hyperparameters in the vector α can be estimated from the corresponding log posterior kernel. A numerical optimizer, such as `csminwel` by Chris Sims, may now be used to compute the posterior mode of α as well as a suitable covariance matrix, such as the inverse Hessian at the mode. To obtain posterior draws of α one may, for instance, apply the standard random-walk Metropolis algorithm using the mode estimates, a normal proposal density and a suitable scaling parameter for the covariance matrix such that the acceptance rate lies within a suitable interval. Once these draws are available, posterior draws of Φ and Ω may be obtained from their posterior distributions conditional on α.

3.2.5. Dealing with the Ragged Edge

To formally deal with the ragged edge property of real-time data vintages, the methodology discussed above is not feasible and needs to be replaced with a computationally heavier approach. Specifically, the expression of the likelihood function[16] is no longer valid as it assumes that all variables have observations for the full sample. The likelihood function can instead be computed recursively with a Kalman filter that supports missing observations; see, e.g., Durbin

---

[14] A possible contender to this setup is to follow Giannone et al. (2019) and instead consider also a third possible stochastic trend, given by a vector with unit coefficients on inflation and the short-term nominal interest rate and zeros elsewhere, i.e., a nominal stochastic trend. This means that the two vectors in β' above that pick these two variables (rows four and five) should be replaced with one vector taken as row five minus row four, providing a possibly stationary real interest rate.

[15] Recall that the gamma distribution has the following density

$$p_G(z|a,b) = \frac{1}{\Gamma(a)b^a} z^{a-1} \exp\left(\frac{-z}{b}\right),$$

with shape parameter $a > 0$ and scale parameter $b > 0$. The mean is here ab while the variance is ab^2. The mode is unique when $a > 1$ and is then given by $b(a-1)$. With mode denoted by $\tilde{\mu}$ and standard deviation by σ, it holds that $b = (\sqrt{\tilde{\mu} + 4\sigma^2} - \tilde{\mu})/2$, while $a = (\sigma/b)^2$. For the case with $\sigma = 1$ and $\tilde{\mu} = 1$, it follows that $b = (\sqrt{5} - 1)/2 \approx 0.6180$, $a = 1/b^2 \approx 2.6180$, and the mean is close to 1.6180. The other case with $\sigma = 0.4$ and $\tilde{\mu} = 0.2$ means that $b = (\sqrt{17} - 1)/10 \approx 0.3123$ and $a = (2/5b)^2 \approx 1.6404$, such that the mean is approximately equal to 0.5123.

[16] See, e.g., equation (A.4) in Appendix A.

and Koopman (2012, Chap. 4.10). This is technically uncomplicated, but the need to take missing data into account in a stepwise manner when computing the likelihood function means that an analytical expression for the marginal likelihood conditional on α is not available. The joint prior density of the parameters (Φ, Ω, α) can, of course, be computed and the product between it and the likelihood function yields the usual posterior kernel. Numerical optimization of all the parameters can now be applied to this kernel, yielding the posterior mode estimate of all parameters. Posterior sampling of the parameters can be conducted using, e.g., Markov Chain Monte Carlo (MCMC) or Sequential Monte Carlo (SMC) methods which, often, take the posterior mode estimate and the inverse Hessian at the mode as part of the tuning parameters for the selected posterior sampler.

While this procedure is formally valid, the dimension of the parameter space is typically large, making posterior mode estimation and posterior sampling cumbersome and time consuming. Moreover, this is expected to be numerically very challenging since restrictions on Ω (positive definite) and α (positive) must hold. Since the real-time data vintages used by, for instance, our study only have missing data for the last two time periods, one option is to discard these periods when estimating the parameters. Doing so would allow for the approach advocated by Giannone et al. (2015, 2019), which reduces the posterior mode estimation and MCMC or SMC posterior sampling dimension problems from having $n^2 p + n + \dim(\alpha)$ parameters to simply having $\dim(\alpha)$ parameters, while the VAR parameters can be obtained from direct sampling once the α parameters have been computed. The trade-off between using a formally valid approach with a high computational burden and a procedure based on the disposal of some information during the estimation stage for lower computational costs is expected to favor the latter case when n and p are large enough compared with the number of data points being disposed of. For the current study with $n = 9$ and $p = 4$, this amounts to having 333 fewer parameters in the latter case. From McAdam and Warne (2019, Table 4) the number of available observations on the different variables for the last time period is less than or equal to 2 of 9, while the corresponding number for the second last time period is 7 of 9. Hence, the number of data points being discarded is at most 9. It should be kept in mind, however, that the discarded data may be highly important when forecasting and may also influence the parameter estimates, especially when the discarded data is sufficiently different from the utilized data. The direct effect is avoided by including all the available vintage data during the forecast stage, while the indirect effect through the parameter estimates is the cost of discarding data during the estimation stage.

Once posterior draws of the VAR parameters are available, the predictive likelihood can be estimated using the approach advocated by Warne et al. (2017) and McAdam and Warne (2019), where the last two time periods of each data vintage are now included in the information set. In this paper we do not evaluate the costs of using the two approaches with respect to computational time and difference between the predictive likelihood estimates. To save valuable computational time, we opt for the second approach and to further save time, we do not use posterior draws

of the hyperparameters when sampling the VAR parameters from their posteriors, but fix them at the posterior mode estimates for each data vintage.

4. Estimation of the Models

In this section we discuss certain features concerning the recursive estimation of the BVAR models. The real-time euro area dataset is extensively discussed in McAdam and Warne (2019), including how these vintages can be extended back in time until 1970 using vintages from the area-wide model database; we refer the reader to this article as well as to Smets, Warne, and Wouters (2014) for details. Below, we use exactly the same sample of vintages from the euro area real-time database, i.e., from 2001Q1 until 2014Q4. The three DSGE models in McAdam and Warne (2019) are estimated using observations from 1985Q1, while 1980Q1–1984Q4 is used as a training sample. We also estimate the BVAR models using observations from 1985Q1, while the initialization vector X_0 is built from observations prior to this date. Specifically, the two BVAR models we study below have $p = 4$ lags such that X_0 is formed by observations from 1984. Details on the data transformations and the variables included in the various models are provided in the Appendix, Part C.

The predictive likelihoods of the DSGE models have already been estimated for this sample of real-time vintages and the Bayesian estimation approach is discussed in McAdam and Warne (2019). In their study, 750,000 posterior draws of the parameters of each DSGE model—using the random-walk Metropolis sampler—have been computed on an annual basis for the Q1 vintages, reflecting how often such models are typically re-estimated by policy institutions in practise. The Q1 parameter draws are then also used for the Q2 until Q4 vintages within the same year. Treating the first 250,000 draws as a burn-in period of the sampler, the predictive likelihoods for backcasts, nowcasts and up to eight-quarter-ahead forecasts have thereafter been estimated using 10,000 of the remaining 500,000 draws, where each used draw is separated by 50 draws; see also Warne et al. (2017) for additional information about the approach as well as the numerical precision of the predictive likelihood estimates using DSGE models.

The BVAR models comprise all nine observed variables that appear in the three DSGE models. While real GDP, private consumption, total investment, total employment and real wages appear as (100 times) the first differences of the natural logarithms of the data for these variables in the DSGE models, the BVAR models instead use (100 times) the natural logarithms of the data, i.e., the log-levels rather than the first differences of the logs. The other four observed variables (GDP deflator inflation, short-term nominal interest rate, the spread and the unemployment rate) are measured identically for both groups of models.

As already discussed in Section 3.2.5, the parameters of the BVAR models are estimated by trimming the data such that the last two time periods of the vintage are discarded. Furthermore, the posterior draws of the VAR parameters are obtained from their normal-inverted Wishart distributions by setting the α hyperparameters to its posterior mode value. In contrast to the DSGE models, we let the BVAR models be re-estimated for each vintage and we take

100,000 posterior draws. The backcasts, nowcasts and forecasts are based on the full vintage dataset, where the technical details are presented in Appendix B, as well as the estimation of the predictive likelihoods. Since the posterior draws are independent, all draws are made use of when estimating the predictive likelihoods for the BVAR models.

Before we turn to the empirical results on forecasting properties of the models, the recursive posterior mode estimates of the α hyperparameters are depicted in Figure 2 for the BVAR with the SoC prior (top) and the PLR (bottom). The former model has three hyperparameters and from the plots we find that the estimates of the overall Minnesota tightness hyperparameter, λ_o, vary between roughly 0.2 and 0.3 with an average of 0.26. The shrinkage hyperparameter for the dummy-initial-observation part of the prior, δ, typically takes values around 1.5 (the mean is 1.56) with most of the values below 1.5 up to 2005, and values above thereafter. The μ hyperparameter related to the sum-of-coefficients part is estimated at about 2.30 on average.

Turning next to the hyperparameters of the PLR case, we find that the recursive estimates of the λ_o parameter are similar to those for the SoC prior. Concerning the shrinkage hyperparameters on the long-run relations in the B matrix, we find that the ϕ_1, ϕ_2 and ϕ_4 are all very close to unity. Recall that these parameters reflect shrinkage for the two possibly non-stationary relations reflecting a technology and a labor trend, as well as the potential stationary investment-output ratio. The high stability of the posterior mode estimates around the prior mode for these hyperparameters reflects a lack of information from the (marginal) likelihood about these parameters.[17] Concerning the hyperparameter for the consumption-output ratio, ϕ_3, the recursive estimates are upward sloping with an average value of 0.96. Next, for the labor-share hyperparameter, ϕ_5, the estimates are below unity with an average of 0.55, suggesting more shrinkage than at the prior mode, with a fairly large drop in 2003 from 0.9 to around 0.4 and a jump up to roughly 0.7 in 2010.

The last four hyperparameters concern shrinkage for specific variables: inflation, the short-term nominal interest rate, the spread and the unemployment rate, respectively. The average posterior mode estimate of ϕ_6 is 0.08, with a mild upward trend for the recursive estimates. The remaining three hyperparameters all have larger average values of 2.35, 0.85 and 4.95, respectively. Overall, there is some variation for these hyperparameters and in the cases of ϕ_7, for the short-term nominal interest rate, an upward trending path consistent with less shrinkage over the sample. For the shrinkage hyperparameter related to the spread, ϕ_8, there are instead two jumps in the path around 2003 and 2005, respectively, until a new plateau of approximately 0.9 is reached.

---

[17] Specifically, if one plots the log marginal likelihood function for this BVAR model, fixing all hyperparameters at their posterior mode values except one (for anyone of the vintages) and making use of a suitable grid around the mode value for, say, ϕ_1 gives a very flat profile, while the corresponding log posterior kernel has the same shape as the underlying gamma prior.

5. Comparing the BVAR Models to the DSGE Models

5.1. Point Forecasts

The point forecast, given by the mean of the predictive density, is estimated by averaging the point forecast conditional on the parameters over the posterior draws; see, for example, McAdam and Warne (2019, Section 5.2) and Appendix B. The recursively estimated paths are displayed in so-called spaghetti plots in Figure 3 for the three DSGE models and the two BVARs, with the real GDP growth forecasts in Panel A (top) and the inflation forecasts in Panel B (bottom). The actual values are plotted with solid black lines, while the dashed lines are the recursive posterior estimates of the population mean of the two variables for the DSGE models. For the BVAR models, where some variables appear in levels rather than in first differences, the dashed lines instead trace out the vintage sample mean values of real GDP growth and inflation since 1995Q1.

Turning first to the real GDP growth forecasts in Panel A, the BVAR model forecasts tend to be lower than those obtained from the DSGE models. This is not only true in the aftermath of the Great Recession in late 2008, early 2009, but also prior to this episode. The mean forecast errors for the whole sample are shown in Table 1 and this visual observation is indeed confirmed as the mean errors concern the difference between the actual value and the point forecast. The smallest mean errors are generated by the BVAR model with the PLR, while those of the BVAR with the SoC prior are roughly 0.1 percentage points larger in absolute terms. Since the mean errors are all negative it follows that all five models over-predict real GDP growth on average with larger errors for the DSGE models than for the BVAR models.[18]

Concerning the inflation point forecasts in Panel B of Figure 3, the SW and SWU model forecast paths are, as pointed out by McAdam and Warne (2019), quite similar with a strong tendency of mean reversion over the forecast horizon. The point forecasts of the SWFF model are quite different with v-shaped paths. Turning to the BVAR models, the forecasts paths are flatter and more varied than those of the DSGE models. From the mean errors in Table 1, it can be seen that the DSGE models tend to under-predict inflation fore the shorter horizons and, in the cases of the SW and SWU models, over-predict inflation. As can also be inferred from the spaghetti-plots for the SWFF model, it under-predicts inflation, albeit with a decreasing error as the forecast horizon grows. By contrast, the mean errors of the BVAR models are all smaller in absolute terms than those for the DSGE models and suggest that the models weakly under-predict inflation. Recalling that both real GDP growth and inflation are measured in quarterly terms such that their values are comparable in terms of scale, the evidence in Table 1 suggests that the five models tend to forecast inflation better than real GDP growth.

---

[18] See McAdam and Warne (2019) for discussions on the finding that the DSGE models' point forecast paths tend to jump up somewhat after the Great Recession, while the path of posterior population mean estimates of real GDP growth is downward-sloping.

5.2. Density Forecasts

The predictive likelihood function of each DSGE model is estimated as discussed in McAdam and Warne (2019, Section 5.1),[19] while the Kalman filter framework for the BVAR models is presented in Appendix B; see also Warne et al. (2017) for additional discussions on this topic. The log predictive scores for the three DSGE and the two BVAR models based on the full sample of vintages (2001Q1–2014Q4) are provided in Table 2. For each horizon (h) and variable set (real GDP growth, inflation, and their joint forecast of real GDP growth and inflation) in a row, the log score values shown in the top are in deviation from the largest value, while the row below gives the largest value in the column of the corresponding model.

Starting with the joint real GDP growth and GDP deflator inflation density forecasts in columns 2–6, the SW or SWU typically has the highest log score for the shorter horizons, while the SoC or PLR model performs best for many of the longer forecast horizons. The SWFF model generally performs markedly worse than the other models, except for the backcast and, possibly, the eight-quarter-ahead forecast.

Turning next to the real GDP growth density forecasts in columns 7–11, it can be seen that for most horizons (all except for $h = 0, 1$), the PLR model obtains the largest value. For the shorter horizons, the SW model is ranked second among the five, while the SWU model comes in second for $h \geq 4$. The difference in values between the two BVARs and the SW and SWU models is overall not big, and we return to a probabilistic assessment of this issue when discussing the weighted likelihood ration tests of Amisano and Giacomini (2007).

Finally, the inflation forecasts in columns 12–16, the SWU model has the highest values for many horizons ($0 \leq h \leq 5$), while the SoC model ranks as second best for these horizons and ahead when $h = 6, 7$ and the SWFF performs best at the eight-quarter-ahead horizon. It is also noteworthy that the SWFF model performs very poorly for the shorter horizons, as also pointed out in McAdam and Warne (2019).

Overall, it appears to be a tight race between the DSGE and BVAR models, with the DSGE models possibly doing better when forecasting inflation and the BVARs with real GDP growth. Furthermore, the SW and SWU models tend to forecast both variables better than the BVARs for the nowcast and one-quarter-ahead horizon, while the BVARs succeed at the six- and seven-quarter-ahead horizons. Since the number of backcasts is very small for real GDP growth (3), small for inflation (16), and very small for the joint density forecasts (3), this horizon is excluded from the discussion below.

---

[19] Notice that the equation for the h-step-ahead covariance matrix of the state variables on page 558 of McAdam and Warne (2019) contains an error. It should read:

$$P_{T+h|T}^{(i)} = F^h P_{T|T}^{(i)} (F')^h + \sum_{j=0}^{h-1} F^j B B' (F')^j,$$

where the second term on the right hand side is missing in McAdam and Warne (2019); see also equation (B.27) in Appendix B.

The equality of the log predictive scores of two models can be tested formally using the weighted likelihood ratio tests advocated by Amisano and Giacomini (2007); see also Diks, Panchenko, and van Dijk (2011). The empirical evidence over the full forecast sample for the five models is presented in Figure 4; see also Appendix D, Tables D.1–D.4. The underlying test statistic is based on equal weights and the percentile values are plotted in the charts for ten model pairs over the nowcast and the one- to eight-quarter-ahead horizon, where the model pair is shown in the title of the chart. The values for the real GDP growth density forecasts are plotted as a solid red line, for GDP deflator inflation as a dashed blue line, and the joint real GDP growth and inflation density forecasts as a dash-dotted green line. It should be kept in mind that large percentile values favor the first model, while small values favor the second model.

The top four charts display percentile values when testing the BVAR with an SoC prior versus the three DSGE models and the PLR model. The following three charts give the values for the PLR model versus the DSGE models, and the last three the values for pairs of the different DSGE models. Concerning the two BVAR models when paired with the SW or SWU model, the percentile values are often close the center (50 percent), with the exception of the inflation forecasts with the PLR model. This is contrasted with the values obtains for both BVARs versus the SWFF model, where the results generally favor the BVAR model, except for the long-term inflation forecasts.

When testing the SoC model versus the PLR model, the formal evidence for the univariate forecasts is fairly strong, with the PLR being favored for real GDP growth and the SoC for inflation. Similarly, when pairing the DSGE models against one another the test values typically gives strong formal evidence that both the SW and SWU models are better than the SWFF for the full sample, again with the exception of the long-term inflation forecasts. Furthermore, when the SW model is paired with the SWU model the latter comes weakly on top, with the SW being stronger at the short-term real GDP growth forecasts, while the SWU outperforms the SW for the shorter-term inflation forecasts.

It is interesting to note that the formal test evidence involving a pair from the BVAR or from the DSGE model group is typically stronger, i.e. having low or high percentile values, than when one model from the BVAR group is paired with a model from the DSGE group, albeit with the SWFF model being an outlier as it typically performs worse than any of the other models. For example, the difference in log score between the PLR and the SoC models for four-quarters-ahead real GDP growth forecasts is 4.80 log-units while the difference between the PLR and the SWU model is 4.50 and, all else equal, the difference in log score between the SoC and the SWU of 0.30 is small. However, the percentile values for PLR versus SoC and versus SWU are 0.99 and 0.62, respectively. We therefore expect to find an event or several events within the forecast sample that can account for this difference in behavior.

It should be pointed out that the Amisano-Giacomini weighted likelihood ratio test can generate seemingly counter-intuitive results. Suppose that equal weights are applied to the N observations of the difference in log predictive likelihood for the model pair, with a lag truncation of zero for the Newey and West (1987) estimator of the asymptotic variance, as in Amisano and Giacomini (2007), then the test statistic is given by the sample mean of the difference in log predictive likelihood values divided by the square root of the sample mean of the squared difference in log predictive likelihoods divided by N. One may expect a test statistic to be larger when the average log score between two models is large rather than when it is tiny, but as the following example shows this need not be the case.

Suppose that the difference in log predictive likelihood between model 1 and model 2 is c for all time periods. For this case the value of the test statistic is equal to $\sqrt{N}$ for all c and, hence, it is invariant to such constants. Moreover, this particular test value is larger than the value obtained when the difference in log predictive likelihood is c for half of the observations and kc for the other half, with $k > 1$.[20] In fact, the larger k is, the lower is the test value, while simultaneously the value of the difference in log predictive score increases in k. More generally, an increase of the variability in the differences between log predictive likelihoods of a pair of forecasting methods dampens the absolute value of the weighted likelihood ratio test statistic and can thereby lower the overall small sample power of the test, unless the increased variability is at least matched by a larger difference in average log predictive score.

Recursive estimates of the average log scores for the joint density forecasts of real GDP growth and inflation over the real-time vintages from 2001Q1 until 2014Q4 are shown in Figure 5. Each chart displays the five models for a given horizon with the SW model being represented by a solid red line, the SWFF model with a dark blue dash-dotted line, the SWU model with a green dashed line, the SoC BVAR with a rose pink dash-dotted and the PLR with a light blue dashed line. The horizontal axis in the panels represents the dating of the predicted variables, while the average log predictive score for a model in that period is based on all the vintages dated up to h periods prior to the date. Concerning the DSGE models it can be seen that the paths look quite similar with the SWFF model path shifted down from the other two. The average log score for each DSGE model is fairly constant with the downward shift in 2008Q4. The BVAR models, on the other hand, display an upward trending behavior until 2008Q4, when a large drop occurs, before the upward trending path begins again in the aftermath of the Great Recession.

The most striking feature of the charts in the figure is the size of the drop in average log score of the BVARs compared with the DSGE models. The latter models lose roughly twice as much in average log score as the latter models. For example, for the vintage 2008Q3 the one-quarter-ahead log predictive likelihood value for the SW and SWU models is somewhat larger than -4 log units, while it is less than -11 for the BVAR models. The two-quarter-ahead log predictive likelihood is around -7 for these two DSGE models and below -17 for the BVAR models. In

---

[20] For this stylized case, the test statistic is equal to $[(1+k)/\sqrt{2(1+k^2)}]\sqrt{N}$. If we consider $k \geq 0$, this function is increasing in k when $0 \leq k < 1$ with a maximum at 1 and is decreasing in k for $k \geq 1$.

fact, the relative losses for the BVAR models are such that the model ranking changes from the BVAR models obtaining a higher average log score than the DSGE models, to the SW and SWU overtaking both BVARs. It is only towards the end of the vintage sample that the BVARs regain higher log scores for some of the forecast horizons.

Moving to the recursive average log scores for the real GDP growth density forecasts in Figure 6, the pattern in connection with the onset of the Great Recession is again present. The loss in average log predictive score for the BVAR models is nearly one log unit, while it is a little less than half a log unit for the DSGE models. As a consequence, the BVAR models at least temporarily lose their top rankings to the SW and SWU models

Turning to the recursive average log scores for the inflation forecasts in Figure 7, the DSGE models often perform better than the BVAR models, especially for the one-quarter to four-quarter-ahead horizons. It is also notable that there is little or no effect on the short-term density forecasts from the drop in inflation during the first half of 2009, while the medium- and longer-term forecasts display a visible, albeit modest, drop in average log score for all models except the SWFF model, which includes the BGG type of financial frictions. This result is particularly interesting since the BVAR models have access to the same data on the external finance premium, yet they are unable to utilize this information as fruitfully as the SWFF model does when forecasting inflation over 2009Q1–Q2, even two-years-ahead.

To analyse what may underlie the large drop in log score of the BVAR models relative to the DSGE models, Table 3 provides prediction errors (PEs), predictive variances (PVs) and log predictive likelihoods (LPLs) over the various horizons when the objective is to predict real GDP growth in 2008Q4 and in 2009Q1. Since the log predictive likelihood is expected to be well approximated by a Gaussian likelihood function,[21] the cause for the large drop in log score is due to prediction errors, the predictive variance or, possibly, both.

In the case of 2008Q4, the sizes of the prediction errors for the BVAR models and the DSGE models are similar in size, with all models greatly over-predicting actual quarterly real GDP growth. Moreover, there are no major differences between the prediction errors based on the vintage underlying the forecast, especially in the case of the BVARs. For example, the SoC model forecasts in 2006Q4 ($h = 8$) are roughly of the same magnitude as those made in 2008Q3. The only possible exception concerns the SWFF model, which has somewhat larger errors in absolute terms than the other models. Turning to the predictive variances, the estimates from the BVAR models are nearly three times smaller than those from the DSGE models. Hence, the considerably smaller log predictive likelihoods of the BVAR models in 2008Q4 can be almost fully accounted for by their narrow predictive densities.

---

[21] Based on the evidence presented in McAdam and Warne (2019), the predictive likelihood of each one of the three DSGE models is well approximated by a normal density based on the prediction error and the predictive variance, albeit that the approximation error is larger when the value of the log predictive likelihood is smaller. Similar results were also obtained in Warne et al. (2017) when comparing a DSGE model to DSGE-VARs and, in particular, a BVAR model based on the methodology in Bańbura et al. (2010).

Concerning real GDP growth in 2009Q1, the same explanation is supported by the estimates in Table 3. Overall, the prediction errors are larger than in 2008Q4 while the predictive variances are broadly the same for all models, with the consequence that the log predictive likelihoods are much smaller for this quarter. Nevertheless, the explanation for the much larger drop in log predictive score for the BVARs than for the DSGE models is the predictive variance. The small predictive variances of the BVARs are beneficial in terms of log score prior to the Great Recession since the prediction errors are modest. However, the punishment is also severe for when these over-confident models fail to predict large changes to the variables of interest. Still, the lower predictive variances of the BVARs is also the reason why these models recover their losses relative to the DSGE models once the Great Recession is over.

6. Forecast Combination Results

6.1. Comparing the Models to the Combination Methods

Forecast combinations offer an opportunity for combining individual model density forecasts such that the combination provides a superior forecast. An indicator for such combinations to exist is that the density forecasts of the individual models are not dominated by one model. The joint real GDP growth and GDP deflator inflation forecasts display time varying top ranks among the five models and similarly for real GDP growth. Concerning the inflation density forecasts, however, some horizons at the shorter term have a dominant model throughout the forecast sample; see, e.g., the three-quarter-ahead forecasts in Figure 7 with the SWU in a dominant position. Even so, this model does not dominate the other models in terms of log predictive likelihood for each time period, and it is therefore possible, albeit difficult, for a combination scheme to outperform the SWU model.

The five combination methods discussed in Section 2 will be applied below for the DSGE and BVAR models and, as the default value, we let the information lag follow the actuals release lag, the observation lag, and be equal to four quarters ($k = 4$) for the SOP, the DP, the BMA and the DMA combination methods. Since data releases of the predicted variables are available prior to the annual revision data release, albeit with at least one lag, we shall also examine the case when the information lag is exactly one quarter for real GDP growth and inflation; see Section 6.4.1.

Concerning the dynamic prediction pool, the δ^* parameter is given by 0.90 in the Bayesian bootstrap filter. This means that an effective sample size below 90 percent of the number of particles (N) results in resampling during the selection step of the filter. The size of the latter parameter is 10,000 particles, while the grid for the ρ parameter, reflecting persistence of the dynamic pool weights, is given by $\rho \in \{0.01, 0.02, \ldots, 0.99\}$.[22] The initial values of the weights are, by construction, equal to $1/5$ for large N and these weights are used until the first time

---

[22] Del Negro et al. (2016) use 5,000 particles in their study with $\delta^* = 2/3$ and 10,000 posterior draws of ρ, via the random-walk Metropolis algorithm. We have checked the dynamic prediction pool results for alternative values of δ^*, namely, 0.8 and 2/3. This did not have a notable impact on the resulting log predictive scores.

period when historical predictive likelihood values are available. With an information lag of four quarters, this occurs in period $h + 4$ of the forecast sample.

The other combination methods that allow for time-varying weights are initialized by setting them to 1/5 for each model; in Section 6.4.2 we shall analyse in some details the importance of the initial values of the resulting log scores. Furthermore, and as mentioned in Section 2.5, we follow the approach in Amisano and Geweke (2017) and estimate the DMA forgetting factor, φ, and we have opted to set its grid to $\varphi \in \{0.01, 0.02, \ldots, 0.99\}$, keeping in mind that small values approximate the equal weights density forecasts and large are close to BMA.

The full forecast sample log predictive scores of the five individual models, equal weights (EW), SOP, BMA and DMA combination methods are displayed in Figure 8 in deviation from the log score of the dynamic pool. The top left panel displays the results for the joint real GDP growth and inflation density forecasts, where the five DSGE and BVAR models are plotted with unchanged linestyles and colors relative to the earlier graphs. The four combination methods are given by the grey dashed line for EW, black dotted line for SOP, grey solid line for DMA and black dash-dotted line for DMA, while the zero line represents the dynamic pool. It can be seen from the chart that nearly all combination methods and individual models obtain a lower log score than DP for all horizons, with EW typically being in second place; the exceptions are EW for the outer two horizons. The differences between EW and SOP are quite small, ranging from around -3.13 log units at the one-quarter-ahead horizon to 0.07 at the seven-quarter-horizon. Overall, the gaps in log score between the four combination approaches, the five models and DP decrease with the forecast horizon.

Turning to real GDP growth in the top right panel, the picture is broadly similar, with the DP and EW forecast combinations at the forefront while the individual models are ranked below them. As in the joint density forecast case, the DMA approach obtains higher log scores than the BMA approach. The SOP approach ranks above the DMA for the shorter horizons and below both for the longer horizons.

Moving to the inflation density forecasts in the bottom left panel, an individual model is ranked first for most horizons, with the exception of the seven-quarter-ahead forecasts and the EW. For the shorter horizons, the SWU ranks first, while the SoC prior BVAR and the SWFF are competitive at the longer horizons. For the shorter terms, the SOP ranks first among the combination approaches and DP and EW obtain the lowest scores, while the picture is reversed at the longer horizons. Overall, the combination approaches result in log predictive scores within a range of 3 to -2 log units relative to the DP. Over the shorter horizons, the SOP fares best among the five methods, while over the longer horizons it obtains the lowest score.

The equality of the log predictive scores of the DP and five individual models and the four alternative combination methods are formally tested with the Amisano and Giacomini weighted likelihood ratio test and the percentile values are shown in Figure 9. It is noteworthy that the DP is strongly favored to the SW and SWFF models for the joint real GDP growth and

inflation forecasts and the marginal real GDP growth forecasts, while the formal test evidence is somewhat weaker regarding the SWU model at the longer horizons. Concerning the inflation forecasts, the evidence favoring the SWU model is strong, except for the longer horizons. When comparing the DP to the BVAR models, the percentile values are generally closer to the middle region, apart from the comparison with the PLR and the marginal inflation forecasts from the two-quarter-ahead horizon and further out.

Turning to the comparisons with the other combination methods, the DP is favored to the EW approach for the joint forecasts over the shorter term and generally the real GDP growth forecasts, excluding the nowcasts, as well as the short term inflation forecasts. At the same time, the formal evidence when comparing the DP to the SOP is somewhat weaker, especially the real GDP growth forecasts. In view of the differences in log score shown in Figure 8, it is perhaps somewhat surprising that the evidence in favor of the DP is weaker when examined to the SOP than to the EW. The discussion in Section 5.2 may be recalled and the reason for these seemingly counter-intuitive results is simply that the numerical standard error is substantially larger for the SOP tests than for the EW tests.

Concerning the model averaging methods, the test evidence is quite similar for both combination schemes, with the DP being favored for the joint and the real GDP growth forecasts, and especially the shorter term, although the percentile values tend to be somewhat larger when comparing DP to BMA than to DMA. Regarding inflation and the shorter term, the percentile values are close to zero, thereby favoring BMA and DMA, respectively, over the DP.

To examine the behavior of the combination methods in more detail, the recursively estimated average log predictive scores of the joint density forecasts of the models and combination methods are plotted in Figure 10. To highlight the differences, the results are again shown in deviation from the recursive estimates of the average log predictive scores for the dynamic prediction pool, i.e., the zero line represents to DP. Concerning the EW method, the deviations from zero are small, especially for the longer horizons, while for the SOP combination the differences are occasionally highly varying and cross the zero line. Similar behavior is also recorded for the BVAR models, while the differences to the SW and SWU models are often positive until early 2005 and negative or very small thereafter. Recalling that the percentile values for the full sample weighted likelihood ratio tests in Figure 9 are close to unity, these results can broadly be understood from the discussion above and the impact of variability on the numerical standard error.[23]

6.2. MODEL WEIGHTS

The empirical evidence presented so far gives fairly convincing support for the usefulness of combination methods in a real-time density forecast comparison exercise. It is therefore of interest to learn how the weights of the five models develop over time, also relative to the

---

[23] The recursive estimates of the average log predictive scores for real GDP growth and inflation separately and relative to the estimates from the DP are shown in Figures D.1–D.2 of Appendix D.

other combination methods. The weights for the joint density forecasts of real GDP growth and inflation with the dynamic prediction pool are shown in Figure 11.[24] In addition, the sample mean, standard deviation, minimum and maximum of the estimated weights are shown in Table 4 for selected horizons.

Turning first to the estimated paths of the DP weights, recall that an information lag of four quarters is assumed. Each plot in Figure 11 therefore starts at the (large sample) initial value for $h + 4$ quarters before the weights can vary; see equation (7) and the discussion below it. The horizontal axis of the panels represents the dating of the predicted variables, such that 2008Q4 concerns the weights used for the density forecast of real GDP growth and inflation in 2008Q4. Notice that the weights of the SW and SWU models tend to increase slightly when the first data on predictive likelihood values are assumed to be available, while the remaining weights move down slightly. After this short phase, the weights of the DSGE models trend downward while those of the BVAR models trend upward gradually. This patterns is more pronounced for some of the shorter forecast horizons, with the weight on the SWFF model dropping below 10 percent and those of the BVARs occasionally reaching above 35 percent.

To pinpoint where, for example, information about 2008Q4 affects the four-quarter-ahead density forecast weights, eight periods must be added, i.e., the weight estimates for the density forecast of 2010Q4. Based on the weight paths in Figure 11, the impact of the Great Recession on the model weights is notable.[25] However, the changes in the weights are not dramatic with all models obtaining fairly large weights throughout the forecast sample. For example, at the four-quarter-ahead horizon the combined weight of the DSGE models is just below 50 percent at the end of the forecast sample, with the SWU having the largest weight and the SWFF the smallest. Furthermore, at the eight-quarter-ahead horizon, all model weights have essentially returned to the large sample initial values. The explanation for the slowly changing model weights of the DP is the high persistence of the underlying process, represented by ρ. The recursive posterior estimates of this parameter are displayed in Appendix D (see Figure D.14) and they mainly hover around 0.99, the largest value in the estimation grid.

Table 4 provides summary statistics of the DP weights for selected horizons, as well as of the other methods that support time-varying weights. It is striking how much lower the sample standard deviations of the DP weights are compared with, in particular, the SOP weights. Furthermore, the range of values is quite narrow for the DP, while the SOP frequently has the full range of possible weight values. The two model averaging methods also have large standard deviations compared with the DP and much wider ranges, albeit not as wide as the SOP. Based on the summary statistics, the behavior of the BMA and DMA in terms of their weights is

---

[24] The weights for the two marginal cases of real GDP growth and inflation with the DP as well as all the estimated weights based on the other three methods (SOP, BMA and DMA) are located in Appendix D; see Figures D.3–D.13.

[25] The impact of the Great Recession on the model weights of the static prediction pool as well as the Bayesian and dynamic model averaging combination methods is very distinct and is consistent with the information lag; see Appendix D, e.g., Figures D.5, D.8 and D.11, respectively.

more alike compared to results obtained for the dynamic and the SOP, especially at the longer horizons. As might be expected, this is mainly due to the posterior estimates of the forgetting factor, φ, being close to unity for these cases; see Appendix D, Figure D.17.

To summarize, the weights of the most successful density forecast combination method over the full forecast sample, the DP, vary moderately over time, less as the forecast horizon increases, and gives substantial weight to all models. By construction, the EW method shares these properties which help to explain its relative success over the other combination methods, whose weights are volatile and cover a wider range of values.[26] Furthermore, we have found in Section 6.1 that the longer the forecast horizon is, the more difficult it is for the combination methods to beat the EW combination; see, e.g., Figure 8. In the case of the DP, this can be understood from the increased discounting (ρ^h) that comes with longer horizons. Technically, this means that the inherent equal-weights force is strengthened as h becomes larger and, hence, that the DP resembles the EW combination more and more. At the same time, this property also reflects well the idea that a predictive likelihood value used to predict far into the future has a lower information value than a predictive likelihood value used for a shorter-term forecast.

6.3. Upper and Lower Bounds For Density Forecasts

The model weights for any density forecast combination method are formed using information available at the time the density forcast is made. One question that comes to mind when comparing density forecast is: given the models at hand, what is the best result that could have been obtained by combining them? Likewise, we may ask: what is the worst result that could have occurred? The answers to these questions give the user an upper and a lower bound for density forecast combination based on the M models being considered.

It is straightforward to construct both bounds *ex post* when the log score is used as the scoring rule. Specifically, the upper and lower bounds for each forecast horizon are obtained by collecting the maximum and the minimum of the log predictive likelihoods of the M models in each time period and adding these "optima" as the log scores of the upper and lower bound combinations, respectively. That is, the upper and the lower bound of the log scores are given by

$$S_{T:T_h,h}^{(U)} = \sum_{t=T}^{T_h} \max_{i=1,\ldots,M} \log\left(p_{t+h|t}^{(i)}\right), \tag{22}$$

$$S_{T:T_h,h}^{(L)} = \sum_{t=T}^{T_h} \min_{i=1,\ldots,M} \log\left(p_{t+h|t}^{(i)}\right). \tag{23}$$

From the perspective of a forecaster combining models in real time, however, these bounds are, as T_h increases, close to probability zero events as they involve always picking the winner or

---

[26] It is noteworthy that DMA approximates the equal (fixed) weights method when the forgetting factor is low. However, despite the fact that very low values of φ are allowed for when estimating this factor, the posterior mode estimates are always in the upper most part of the considered grid.

the loser. They nevertheless form natural benchmarks when comparing density forecasts. The spread between the upper and lower bounds gives a measure of how much room exists for the log score of any combination method using the same models and forecast sample. Moreover, the difference between the upper bound and the log score of the best model is the interval available to combination methods for improving on the model forecasts. Should this interval be "too narrow", it may be prudent to consider additional forecasting models before carrying out a combination exercise.[27]

The the recursively estimated log scores for the five combination methods and the recursive average lower bound for the joint real GDP growth and inflation density forecasts are plotted in Figure 12 in deviation from the recursive average upper bound.[28] This means that the upper bound is equal to zero. Since the log scores concern recursive averages, the distances of their paths from the upper bound are not always increasing, but can also approach this bound, as in the case of the SOP in the wake of the Great Recession. Concerning the average differences between the upper and lower bounds, note that it tends to decrease with the forecast horizon. The average interval is close to unity for the eight-quarter-ahead forecasts towards the end of the forecast sample, while for nowcasts and up to the three-quarter-ahead forecasts the difference is around 1.5 log units. The main explanation for this appears to be the real GDP growth forecasts which cover the negative growth rate in 2001Q4, where the BVAR models in particular have very low scores which are submitted to the lower bound.[29] In addition, from the graphs in Figures 6 and 7 it appears that this behavior of the log scores is mainly due to the real GDP growth forecasts. Furthermore, the recursive average log scores of the five combination methods tend to lie closer to the upper bound than the lower bound with the best combinations being around 2/3's up from the lower bound at the end of the forecast sample. Hence, given the pool of models available, there is room for improvement for combination methods and, from the perspective of these bounds, the gains from using the best combination methods over the best models are modest.

6.4. Sensitivity Analysis

The combination methods depend on specific assumptions that may affect the outcome of the empirical exercises above. First, the information lag $l = 4$ is mechanical as it follows exactly the observation lag and it neglects the fact that the information lag for real GDP growth and inflation for the euro area RTD is often only one quarter. To simplify computational issues

---

[27] What constitutes a "too narrow" interval is subjective, but it is nevertheless not hard to imagine cases where near consensus can be reached.

[28] The results for the marginal real GDP growth and inflation forecasts are shown in Appendix D, Figures D.20 and D.21, respectively. Similarly, upper and lower bounds graphs for the models instead of the combinations are shown in Figures D.22–D.24.

[29] This may be inferred from Figure 5 where the paths of the average log scores prior to 2005 for the models are more volatile with greater deviations between the best (DSGE) and the worst (BVAR) model for the shorter-term forecasts than for the longer-term forecasts. This is especially true for the negative real GDP growth in 2001Q4, a period which is covered by the density forecasts up to three-quarters-ahead but not by the longer-term forecasts.

and make comparisons less complex, we consider the case of $l = 1$ with the measured values given by the actuals rather than taken from the corresponding vintage. Consequently, the underlying log predictive likelihoods of the DSGE and BVAR models are not re-estimated for the three additional time periods per vintage and horizon, but instead the timing of the available information is shifted backwards.

Second, all methods are based on having equal initial values of the model weights in one form or another. Given that the sample is relatively short, this may have an effect on the outcome. For this reason, as well as to have an instrument for explicitly assessing the importance of including a model with financial frictions in the pool of models, the case when the weight on the SWFF model is initialized at zero and when the other models receive an initial weight of $1/4$ will be examined. For the fixed weight approach we likewise study the case when the weight is zero on the SWFF model and $1/4$ on the remaining four models.

6.4.1. The Information Lag

The information lag for real GDP growth and GDP deflator inflation data is often one quarter for the euro area RTD. For the former variable it is two quarters in three out of 56 cases and for the latter variable in 16 cases; see McAdam and Warne (2019, Table 4). With $l = 1$, we assume that the measured data are well approximated by the annual revisions actuals, i.e., for vintage t we let $x_{t-j}^{(m)} = x_{t-j}^{(a)}$ for $j = 1, 2, 3$, with the consequence that the predictive likelihood values of the individual models do not need to be recomputed for these periods.[30] Instead, we can simply append three already estimated h-step-ahead predictive likelihood values to the information set used to compute the weights at each point in time during the forecast sample. It follows that the recursively obtained weights on the models for the SOP and the two model averaging methods are not affected by the information lag other than by shifting the weights back in time three time periods and by allowing for three new sets of weights at the end of the forecast sample. In the case of the DP, the effect of the shorter information lag is also a simple time shift of the weights, provided that the number of particles, N, is large enough.

Table 5 shows the full sample log predictive scores of the joint real GDP growth and inflation density forecasts for the combination methods with time-varying weights. It is notable that mainly the short-term horizons are affected by the shortened information lag for all methods except the DP. In particular, substantially higher log scores are recorded for the nowcast of the SOP and the two model averaging approaches, while the differences are smaller at the four-quarter-ahead horizon and thereafter. Furthermore, the DP still obtains the largest log

---

[30] It should be kept in mind that the *relative impact* on the predictive likelihood from the revisions is unlikely to be substantial enough to affect the overall conclusions from the exercise in this section. For example, having some information about the real GDP growth in 2008Q4 when computing model weights in 2009Q1 is likely to have a great impact on the combined predictive likelihood of the shorter term forecasts for the combination methods that react strongly to new information, regardless of the precise value given to real GDP growth in 2008Q4. For example, the actual value of real GDP growth in 2008Q4 is -1.89 percent, while the measured value for this quarter from the 2009Q1 vintage is -1.48 percent, both values representing strong negative growth.

predictive score among the four methods, with the exception of the nowcast where DMA has a somewhat larger value.

The improvement in log predictive scores based on the shorter information lag is mainly due to being able to react earlier to the large forecast errors in real GDP growth recorded for the BVARs at the onset of the Great Recession. The full sample log scores for real GDP growth and inflation separately are located in Appendix D, Table D.7, and the pattern recorded in Table 5 also applies to the log predictive scores for real GDP growth, while the log scores of inflation are only marginally affected by the shorter information lag. The reason for the improvement in log scores with the shorter information lag can also be inferred by plotting the difference between the recursively estimated log predictive scores; see Figure 13. For the static prediction pool the improvement for the nowcast is approximately 18 log units and it occurs in 2009Q1 by having access to the log predictive likelihood for 2008Q4. Based on the model values for that quarter, the SOP approach leads to lower weights on the BVARs, especially the PLR, and a larger weight on the SW model at an earlier date. The BMA and DMA combination methods also gain in log score from the more timely information regarding real GDP growth at the onset of the Great Recession, although the impact on the log score is somewhat less pronounced than for the SOP.

Concerning the two-quarter-ahead to eight-quarter-ahead density forecasts, a shorter information lag does not always improve the log score. The full sample log scores of BMA are, with the exception of $h = 6$, lower for the shorter information lag, while it generally improves the log score for DMA. For the recursive estimates, the picture is more complex with all combinations displaying both gains and losses for some time periods and some horizons.

It is also striking how little the recursive log score of the DP is affected by the information lag. From Table 4 we know that its weights are substantially less volatile than those of the other combination methods and, hence, shifting the weights back in time only has a moderate effect on the log score. This applies to all forecast horizons and explains why the DP is robust to the choice of information lag for the euro area RTD vintages of 2001Q1 until 2014Q4.

6.4.2. The Initial Weights

Changing the initialization from equal weights to some other weighting scheme is straightforward when applying the static prediction pool as well as BMA and DMA. For the DP, the weight initialization depends on the parameters of the underlying process, ξ_t, as well as on the information available through the model predictive likelihood values. The default parameterization of ξ_t favors the propagation of equal weights through the initialization of ξ_{T-1} and the innovation η_t.

The predictive likelihood values of the models are initially set to a constant, such as unity or $1/M$, for the time periods $t = T, \ldots, T + h + l - 1$ due to the information lag, l, and the forecast horizon, h, delaying when actual realizations of the model predictive likelihoods can be observed. When the number of particles is large enough, this initialization period means that

the model weights estimator

$$\frac{1}{N}\sum_{n=1}^{N} w_{i,t+h|t}^{(n)}(\rho) W_t^{(n)} \approx \frac{1}{M}, \quad t = T, \dots, T+h+l-1.$$

One way to influence the weights during this initialization phase is to feed the bootstrap particle filter with alternative predictive likelihood values. For instance, the case when the SWFF model should be given zero initial weights while the other four models each have the weight $1/4$ can, partially, be implemented by setting the predictive likelihood values of the models equal to these weights during the first $h+l$ periods. The reason why this only partially changes the weights to the desired values is related to the initialization of ξ_{T-1} and to the assumption about η_t. Since both vectors are assumed to be standard normal, it follows that for large N, the large sample average of $w_{i,T-1} = 1/5$ and similarly for the candidate model weights $\tilde{w}_{i,t}$ at the beginning of the forecasting step in the Bootstrap filter. The expected value of the incremental weights in period T, $\tilde{\omega}_T$, is therefore given by the weighted average of the predictive likelihood values ($1/5$).

During the updating step, the particles are given a candidate re-weighting scheme, $\tilde{W}_T^{(n)}$, based on the old particle weights (unity) and the incremental weights. This candidate scheme will not favor equal weights since the predictive likelihood value of those particles based on a low weight on the SWFF model will achieve a larger predictive likelihood than average. For the selection step, two possibilities exist, but with similar outcomes. If the effective sample size remains above the selected threshold size, $\delta^* N$, the re-weighted candidate scheme of particle weights will be applied to the candidate model weights when estimating the model weights that are used to compute the predictive likelihood for the nowcast and the h-quarter-ahead forecasts. The corresponding model weights will have values less than $1/5$ for the SWFF model but greater than zero since the candidate model weights have mean $1/5$. The other models will obtains approximately equal values somewhat larger than $1/5$. On the other hand, if the effective sample size is below the threshold size, resampling occurs based on the swarm of candidate model and particle weights where model weights for particles with larger particle weights have a greater chance of survival, i.e., those with a low weight on the SWFF model. Again, the result is that average model weight has a value less than $1/5$ for the SWFF model but greater than zero, while the average model weights on the other four models are approximately equal and somewhat larger than $1/5$.

The inherent equal-weights force of ξ_t through its initialization and η_t can be guided towards other steady-state weights by tuning its distribution. One option is to change the mean of the normal distribution from zero to, say, -1.96 for the models where we wish to consider an initial weight close to zero. Since the purpose is to aim at a particular vector of near fixed weights during the first $h+l$ time periods of the forecast sample, the mean of the normal distribution need only be swapped during this period. Thereafter, the zero mean value is applied again, bearing in mind that the η_t random draws again push the DP weights towards equal weights. In

this section, we consider the case when the mean of ξ_{T-1} and η_t are equal to -1.96 for the SWFF model and zero for the other models. This not only ensures that the weight on the SWFF model is relatively close to 0 while the other weights are close to $1/4$ up to time period $T + h + l - 1$, but it also allows the $\xi_{i,t}$ process for the SWFF model to recover thereafter, provided that its predictive likelihood values give sufficient support for the model. Furthermore, by limiting the number of periods for the change of η_t to the initial $h + l$ periods of the forecast sample, it follows that this also applies when iterating the ξ_t process forward when computing the h-step-ahead weight.[31]

The full sample log predictive scores for the alternative initialization scheme with "zero weight" on the SWFF model and equal weights on the other models are shown in Table 6 for the joint real GDP growth and inflation case.[32] The fixed weights cases in the table are denoted FW since this covers both the EW combination and the combination with zero weight on the SWFF model. It is striking that the log scores of all combination methods are positively affected by having a zero initial weight on the SWFF model, with the exception of the SOP nowcasts. The fixed weight combination scheme obtains the highest log score for all horizons when the SWFF model is excluded and the improvement is particular notable for the shorter horizons. Although the DP also records substantial gains, they are not sufficiently large for the combination approach to retain its first rank. The smallest improvements are recorded for the SOP, where by construction the selection of weights does not depend on lagged weights.

The differences for the recursively estimated log scores of the two initialization cases are displayed in Figure 14.[33] The SOP and BMA typically both obtain their total gain from the initialization sample since the differences in log scores are nearly constant thereafter for all horizons. Furthermore, the fixed weight and DP both display drops in their gains at the onset of the Great Recession, suggesting that excluding the SWFF model (FW) or, at least, giving it a lower weight (DP) has a negative impact on the log predictive likelihoods of these combination methods during this period. This result is explained by having larger weights on the BVAR models when the SWFF model receives a lower weight. Furthermore, it is interesting to note that the DMA log scores improve relative to the benchmark case at the onset of the Great Recession for the short-term forecasts. This is mainly explained by DMA having larger weights on the SW and SWU models and lower on the SWFF model during this episode, while those on the BVAR models are largely unaffected.

Formal test results for the hypothesis that the log predictive score of the SWFF zero and the equal weights initialization are equal are displayed in Figure 15 for the five combination methods. With the exception of the inflation density forecasts and the SOP, the empirical evidence from

---

[31] This implementation is equivalent to introducing a time-varying drift-term into the equation for $\xi_{i,t}$, when i is the SWFF model, and having a zero mean for the distributions of ξ_{T-1} and η_t.

[32] The full sample results for real GDP growth and GDP deflator inflation separately are shown in Tables D.8 and D.9, respectively. The information lag is given by the default value of four lags for annual revisions data.

[33] The recursive estimates for real GDP growth and GDP deflator inflation separately are plotted in Figures D.27 and D.28, respectively.

the Amisano and Giacomini tests strongly favors the SWFF zero initialization for all methods and horizons. In the case of the SOP, the joint and the real GDP growth nowcasts test results yield percentile values around 50 percent, suggesting that the two initialization alternatives yield equal log scores. For the inflation density forecasts and with the exception of the SOP, the percentile values are large for the short-term and small for the long-term, thereby supporting setting the initial weight on the SWFF model to zero in the former case and being indifferent or preferring equal initial weights in the latter case.

The posterior model weights for the joint real GDP growth and inflation density forecasts using the DP and the SWFF zero initialization are displayed in Figure 16. The grey lines in the panels are the posterior weights based on the equal weights initialization; see also Figure 11. The SWFF zero initialization method we have proposed for the DP indeed provides the intended properties, i.e., close to zero weights during the first $h + l$ periods of the forecast sample and a chance to recover thereafter. The largest weights on the SWFF model during the initial periods are obtained for the nowcasts, while in general the weights on this model gradually become larger over the sample, especially for the longer term forecasts. The weights on the other models shift proportionally relative to the equal weights initialization to offset the lower weight on the SWFF model, and with the shift becoming smaller as the weight on the SWFF model depends less on the selected initialization method.[34]

7. Summary And Conclusions

This paper examines density forecast combinations of three DSGE models (the Smets and Wouters variants: SW, SWFF and SWU) and two BVARs (sum-of-coefficients, SoC, and prior for the long run, PLR) to compare five methods: fixed weights, static optimal and dynamic prediction pools, as well as Bayesian and dynamic model averaging. The models are estimated on real-time euro area data and the forecasts cover the sample 2001–2014, focusing on inflation, real GDP growth and their joint forecast. The main findings from the methodological presentation and the empirical exercises fall under two broad themes: (1) assessing model combinations in real time, and (2) assessing model combinations over multi-step horizons.

Concerning the first theme, the literature on density forecast combinations has, to our knowledge, omitted important characteristics of the real-time data dimension. Apart from fixed-weight combinations, model weights are computed using information about each model's past predictive performance. In a real-time context, model weighting emerges when outcomes are imperfectly known. This implies that the predictive likelihoods for models should be suitably lagged when computing the model weights. To that end, we introduce the terms *observation lag* and *information lag* to clarify the different time shifts involved for performance and weighting computations. The former term denotes the time difference between the date of a variable and the vintage its actual value is taken from, while the latter term gives the time difference between the date of a

---

[34] The posterior model weights for the marginal real GDP growth and inflation density forecasts subject to the SWFF zero initialization are displayed in Figures D.29–D.30 for the DP.

variable and the vintage a measured value is taken from. While the information lag affects the data available when computing model weights for predictions, the observation lag concerns the predictive performance of a combination method in a forecast comparison exercise. Depending on which actual values are selected, the measured data used for the model weight assessment may differ from the actual values since earlier releases of the variables may be available prior to the selected actual value. This stands in contrasts to the standard case of a single database, where both lags are zero and this distinction is suppressed.

Regarding the weighting structure itself, for the real GDP growth and joint forecasts, the DP and EW generally perform better than the other combination methods and the individual models. For inflation, the picture is more fluid with DSGE models typically obtaining higher log scores than the BVARs and the combination methods. Over short horizons, the SOP fares well, but loses out thereafter to EW and the DP. Overall, the DP performs well. An analogue of this can be gauged by the range of weights used by the different combination schemes. Whilst the DP generates a relatively narrow range with all models being influential, the SOP exploits the full support from zero to one, as do, to a lesser extent, BMA and DMA.

Another dimension in which the DP is robust (and, for instance, the SOP may not be) is with respect to the information lag. Shortening the lag from four quarters to one quarter has minimal effect on the log score of the DP, but dramatically lowers it for the other methods and especially so for the SOP—although this improvement abates after two or more step-ahead-forecasts. The gain is mainly due to being able to react earlier to the large real GDP growth *standardized* forecast errors for the BVARs at the onset of the Great Recession. This illustrates the case where better models (SW and SWU) are under-utilized since the historical performance of the BVARs is maintained by the long information lag. The treatment of this lag in real-time applications, therefore, reveals a trade-off in combination schemes as to the degree to which they react quickly or slowly to the most recently available information.

The second theme concerns the assessment of model combinations over multi-step horizons. Density forecast combinations are often conducted in a one-step-ahead environment yet, in our exercises, we demonstrate that models' predictive performance is horizon and variable specific. For instance the BVARs generally forecast real GDP growth better than the DSGEs, whereas for inflation it is the reverse. Taking this at face value, we may therefore be inclined to discard some models (à la BMA), or at least discard some model types.

In a rich model combination framework, however, the pitfalls of such a strategy become readily apparent. For instance some models, like SWFF, perform well for inflation but only at long horizons, whereas others, like SWU, see their initially strong inflation predictive performance recede as the forecast horizon increases. Likewise for real GDP growth, the SW performs well over the shortest horizons, before the PLR overtakes its first rank among the individual models thereafter, while the SWU becomes more attractive over the longer horizons. The bottom line is that the more one engages in a multi-step, multivariate predictive setting, the more likely it

is that a set of different models contain information that can be usefully combined.[35] A variant on this theme, and indeed a validation of it, can also be seen in our exercises to initialize to zero the weight on the SWFF model. This has a bearing on the weighting of the other models, but also does not preclude the eventual return of SWFF to predictive and combinatory usefulness.

Finally, our exercises can be extended in a number of directions. First of all, when shortening the information lag from four to one, we assume that the additional measured values of the predicted variables that are required to compute the predictive likelihoods for the resulting time periods are equal to the actual values. This is a convenient assumption when computing the weights as it implies that the models' predictive likelihood values based on the actuals can simply be shifted back in time. Instead, one may consider using the measured values for each given vintage, thereby requiring additional calculations for each real-time vintage. For most vintages, all three such values are available while two values exist for the remaining vintages. In addition, the minimum information lag need not be the same for all variables. The assumption that the actual values approximation for the shortened information lag case does not distort the results much is, for example, based on the observation that the revisions to the predicted variables are quite small compared with the predictive variances, also for the Great Recession. Second, the setup of the DP involves an inherent equal-weights force through the innovation process. In one of our exercises, we introduce a parameterization which gives a low weight on the SWFF model over the initialization phase, i.e., until predictive likelihood values from the forecast sample can be observed. An alternative approach is to ignore the underlying VAR-process associated with the SWFF model over the initialization sample, thereby effectively forcing its weight to zero. Furthermore, the VAR process itself can receive a richer parameterization relative to the case of one common autoregressive parameter and common unit innovation variance by allowing for some model-dependent parameters. For instance, one may allow for different rates of mean reversion or different means, thereby permitting model-weights to react individually to past performance as well as for the long-run forecast model weights to deviate from equal weights. It might also be an interesting robustness exercise to extend our analysis to a wider set of models, for instance to reduded-form models such as the random walk implementation in Warne et al. (2017), BVARs with stochastic volatility as in Clark (2011) and to dynamic factor models. We leave these issues open for future research.

---

[35] Another interesting conclusion is that DSGE models—whose performance around the Great Recession attracted particular criticism; see Kocherlakota (2010) for a discussion—appear quite competitive compared with less theory-constrained models, such as BVARs. In the wake of the Great Recession, all models incur large forecast errors, but "recover" their predictive abilities to varying degrees afterwards. This realization further bolsters the case against a narrow model selection.

TABLE 1: Mean errors based on predictive mean as point forecast for the sample 2001Q1–2014Q4.

| | Real GDP growth | | | | | Inflation | | | | |
| | DSGE | | | BVAR | | DSGE | | | BVAR | |
h	SW	SWFF	SWU	SoC	PLR	SW	SWFF	SWU	SoC	PLR
-1	0.045	−0.337	−0.218	−0.243	−0.139	0.154	0.227	0.136	0.116	0.089
0	−0.168	−0.388	−0.279	−0.200	−0.142	0.067	0.228	0.039	0.051	0.023
1	−0.382	−0.595	−0.439	−0.234	−0.162	0.028	0.278	0.004	0.054	0.017
2	−0.472	−0.655	−0.490	−0.256	−0.164	−0.018	0.284	−0.040	0.058	0.018
3	−0.502	−0.666	−0.486	−0.280	−0.173	−0.064	0.270	−0.084	0.067	0.022
4	−0.488	−0.650	−0.443	−0.287	−0.174	−0.113	0.241	−0.132	0.064	0.016
5	−0.467	−0.637	−0.400	−0.298	−0.183	−0.155	0.211	−0.172	0.062	0.015
6	−0.440	−0.622	−0.358	−0.306	−0.192	−0.186	0.185	−0.202	0.064	0.019
7	−0.411	−0.607	−0.318	−0.306	−0.195	−0.215	0.155	−0.231	0.058	0.016
8	−0.380	−0.587	−0.279	−0.296	−0.186	−0.238	0.129	−0.252	0.054	0.015

TABLE 2: Log predictive scores for backcasts, nowcasts and one-to eight-quarter-ahead forecasts over the vintages 2001Q1–2014Q4, with $h = -1$ being the backcast horizon and $h = 0$ the nowcast horizon.

	Real GDP growth & inflation					Real GDP growth					Inflation				
	DSGE			BVAR		DSGE			BVAR		DSGE			BVAR	
h	SW	SWFF	SWU	SoC	PLR	SW	SWFF	SWU	SoC	PLR	SW	SWFF	SWU	SoC	PLR
−1	−3.90	−5.07	−3.70	−0.20	0.00	−1.53	−1.73	−1.59	−0.26	0.00	−2.90	−7.51	−2.37	−0.11	0.00
					−5.30					−0.79					−1.59
0	0.00	−25.57	−2.40	−5.88	−5.11	0.00	−5.46	−6.05	−5.03	−2.72	−3.87	−23.49	0.00	−1.37	−2.67
	−36.77					−46.18							13.30		
1	−0.06	−39.12	0.00	−0.62	−0.24	0.00	−9.33	−3.48	−2.36	−0.07	−3.36	−27.57	0.00	−1.32	−2.82
			−48.39			−56.53							11.21		
2	−0.99	−38.88	0.00	−2.10	−4.03	−0.98	−10.05	−2.62	−2.41	0.00	−2.67	−24.94	0.00	−2.58	−6.35
			−53.75							−58.58			7.10		
3	−2.02	−34.05	0.00	−0.70	−1.98	−4.28	−12.31	−4.37	−3.53	0.00	−2.37	−20.48	0.00	−1.83	−6.02
			−57.72							−56.40			2.93		
4	−2.18	−26.89	−0.19	−0.55	0.00	−5.52	−13.24	−4.50	−4.80	0.00	−1.48	−13.96	0.00	−0.82	−5.04
					−59.47					−53.99			−0.90		
5	−2.39	−21.84	0.00	−1.70	−1.86	−5.11	−12.96	−2.86	−4.65	0.00	−0.78	−9.12	0.00	−1.02	−5.53
			−60.01							−52.78			−3.71		
6	−2.65	−17.16	−0.08	0.00	−1.56	−4.10	−11.87	−1.32	−3.59	0.00	−1.30	−5.56	−0.89	0.00	−5.20
				−61.11						−52.50				−5.63	
7	−1.87	−11.32	−0.03	0.00	−1.15	−4.23	−12.19	−1.48	−4.03	0.00	−1.21	−0.96	−1.54	0.00	−5.34
				−62.71						−50.90				−7.80	
8	−1.54	−8.05	−0.63	0.00	−2.31	−2.74	−11.26	−0.70	−2.39	0.00	−3.16	0.00	−3.81	−1.87	−6.94
				−63.57						−50.47		−8.15			

NOTES: The log scores are displayed in deviation from the largest value for a given forecasted vector of variables and horizon. The largest log score is shown in the row below for the model which achieves this value.

TABLE 3: Predictions error, variance and log predictive likelihood of real GDP growth in 2008Q4 and 2009Q1.

| | | 2008Q4 | | | | | 2009Q1 | | | | |
| | | DSGE | | | BVAR | | DSGE | | | BVAR | |
h	Type	SW	SWFF	SWU	SoC	PLR	SW	SWFF	SWU	SoC	PLR
	PE	−1.85	−2.13	−2.03	−1.98	−1.93	−1.81	−1.82	−2.74	−2.37	−2.32
0	PV	0.45	0.46	0.42	0.15	0.14	0.48	0.50	0.43	0.19	0.18
	LPL	−4.30	−5.42	−5.32	−12.05	−12.10	−3.95	−3.96	−8.92	−13.41	−13.41
	PE	−1.92	−2.31	−1.99	−2.26	−2.27	−2.69	−3.00	−2.80	−2.71	−2.69
1	PV	0.54	0.55	0.59	0.20	0.18	0.54	0.55	0.59	0.20	0.19
	LPL	−3.98	−5.38	−4.00	−11.92	−12.67	−7.07	−8.46	−7.12	−16.06	−16.22
	PE	−2.11	−2.41	−2.08	−2.25	−2.26	−2.68	−3.06	−2.72	−2.80	−2.79
2	PV	0.56	0.56	0.64	0.22	0.20	0.56	0.56	0.64	0.21	0.20
	LPL	−4.54	−5.69	−4.04	−10.88	−11.67	−6.79	−8.61	−6.33	−16.06	−17.39
	PE	−2.25	−2.51	−2.28	−2.29	−2.24	−2.79	−3.09	−2.78	−2.82	−2.80
3	PV	0.57	0.57	0.66	0.23	0.21	0.57	0.57	0.66	0.22	0.20
	LPL	−4.97	−6.08	−4.64	−10.51	−10.99	−7.19	−8.72	−6.40	−15.10	−16.46
	PE	−2.23	−2.55	−2.17	−2.28	−2.17	−2.92	−3.18	−2.93	−2.89	−2.82
4	PV	0.59	0.60	0.68	0.24	0.21	0.58	0.57	0.67	0.24	0.21
	LPL	−4.85	−6.06	−4.16	−10.22	−10.19	−7.74	−9.15	−6.96	−14.93	−16.04
	PE	−2.30	−2.58	−2.14	−2.21	−2.15	−2.89	−3.20	−2.81	−2.90	−2.78
5	PV	0.59	0.60	0.69	0.25	0.22	0.59	0.60	0.69	0.24	0.22
	LPL	−5.07	−6.17	−4.02	−9.09	−9.99	−7.45	−8.97	−6.29	−14.68	−15.16
	PE	−2.37	−2.58	−2.24	−2.24	−2.11	−2.94	−3.23	−2.78	−2.83	−2.76
6	PV	0.60	0.60	0.70	0.25	0.22	0.60	0.60	0.70	0.25	0.22
	LPL	−5.31	−6.14	−4.30	−9.26	−9.44	−7.68	−9.08	−6.13	−13.02	−14.97
	PE	−2.36	−2.62	−2.23	−2.21	−2.08	−3.01	−3.22	−2.88	−2.84	−2.72
7	PV	0.60	0.60	0.71	0.25	0.22	0.60	0.60	0.71	0.26	0.22
	LPL	−5.22	−6.29	−4.23	−8.91	−9.21	−7.95	−9.05	−6.42	−13.35	−14.32
	PE	−2.29	−2.65	−2.24	−2.23	−2.10	−2.98	−3.25	−2.86	−2.83	−2.70
8	PV	0.63	0.63	0.71	0.26	0.23	0.60	0.60	0.72	0.26	0.22
	LPL	−4.82	−6.19	−4.29	−8.85	−9.15	−7.78	−9.18	−6.30	−12.78	−14.12

NOTES: The three types of predictive distribution estimates are: prediction error (PE), predictive variance (PV) and log predictive likelihood (LPL). The forecast horizon, h, determines which euro area RTD vintage was used to predict real GDP growth in 2008Q4 and 2009Q1, respectively. For example, $h = 4$ when predicting the outcome in 2008Q4 implies that the 2007Q4 vintage was employed. The actual values of quarterly real GDP growth in 2008Q4 and 2009Q1 are given by −1.89 and −2.53 percent, respectively.

TABLE 4: Summary statistics of the weights on the DSGE and BVAR models for density forecast combination methods of real GDP growth and inflation over the vintages 2001Q1–2014Q4.

h	model	DP				SOP				BMA				DMA			
		mean	std	min	max	mean	std	min	max	mean	std	min	max	mean	std	min	max
0	SW	0.190	0.054	0.108	0.313	0.121	0.140	0.000	0.362	0.406	0.426	0.000	0.990	0.241	0.287	0.002	0.937
	SWFF	0.122	0.039	0.074	0.200	0.014	0.052	0.000	0.200	0.022	0.056	0.000	0.200	0.040	0.055	0.000	0.200
	SWU	0.168	0.035	0.118	0.246	0.144	0.302	0.000	1.000	0.108	0.155	0.000	0.507	0.149	0.146	0.002	0.472
	SoC	0.254	0.054	0.181	0.365	0.155	0.188	0.000	1.000	0.175	0.159	0.000	0.476	0.254	0.169	0.000	0.577
	PLR	0.267	0.059	0.180	0.366	0.565	0.326	0.000	1.000	0.289	0.281	0.000	0.776	0.317	0.219	0.000	0.740
1	SW	0.173	0.037	0.106	0.225	0.048	0.146	0.000	1.000	0.258	0.218	0.000	0.594	0.212	0.206	0.002	0.618
	SWFF	0.108	0.041	0.068	0.200	0.018	0.058	0.000	0.200	0.025	0.061	0.000	0.200	0.026	0.060	0.000	0.200
	SWU	0.182	0.038	0.112	0.252	0.252	0.311	0.000	1.000	0.268	0.204	0.000	0.562	0.201	0.172	0.002	0.494
	SoC	0.261	0.049	0.176	0.369	0.129	0.193	0.000	0.708	0.168	0.148	0.000	0.446	0.244	0.171	0.000	0.568
	PLR	0.275	0.064	0.179	0.407	0.552	0.380	0.000	1.000	0.281	0.278	0.000	0.765	0.317	0.223	0.000	0.677
4	SW	0.186	0.021	0.145	0.222	0.109	0.262	0.000	1.000	0.189	0.135	0.000	0.381	0.176	0.120	0.004	0.380
	SWFF	0.144	0.032	0.100	0.200	0.031	0.072	0.000	0.200	0.040	0.074	0.000	0.200	0.051	0.076	0.000	0.225
	SWU	0.202	0.037	0.142	0.282	0.152	0.186	0.000	1.000	0.284	0.268	0.000	0.756	0.238	0.225	0.002	0.729
	SoC	0.241	0.044	0.197	0.342	0.585	0.376	0.000	1.000	0.298	0.260	0.001	0.748	0.298	0.214	0.000	0.685
	PLR	0.227	0.032	0.182	0.282	0.124	0.222	0.000	1.000	0.190	0.143	0.000	0.454	0.236	0.147	0.000	0.482
8	SW	0.198	0.011	0.172	0.228	0.182	0.323	0.000	1.000	0.262	0.200	0.019	0.612	0.185	0.083	0.061	0.512
	SWFF	0.182	0.027	0.129	0.242	0.050	0.087	0.000	0.200	0.067	0.085	0.000	0.200	0.143	0.129	0.001	0.490
	SWU	0.202	0.027	0.167	0.305	0.148	0.156	0.000	0.432	0.198	0.150	0.003	0.510	0.185	0.140	0.026	0.696
	SoC	0.216	0.030	0.178	0.273	0.536	0.359	0.000	1.000	0.297	0.264	0.004	0.793	0.282	0.189	0.001	0.624
	PLR	0.204	0.013	0.168	0.235	0.084	0.102	0.000	0.453	0.176	0.114	0.000	0.413	0.205	0.090	0.000	0.374

NOTES: The density combination methods are: dynamic prediction pool (DP), static optimal prediction pool (SOP), Bayesian model averaging (BMA), and dynamic model averaging (DMA).

TABLE 5: Log predictive scores of joint real GDP growth and GDP deflator inflation for nowcasts and one-to eight-quarter-ahead forecasts of four combination methods based on different information lags over the vintages 2001Q1–2014Q4.

h	l	SOP	DP	BMA	DMA
0	1	-29.59	-29.13	-38.29	-27.89
	4	-47.13	-30.85	-49.83	-40.86
1	1	-51.97	-40.44	-57.71	-43.48
	4	-55.23	-41.18	-58.09	-47.40
2	1	-48.87	-48.26	-62.18	-49.40
	4	-50.20	-49.18	-61.21	-51.92
3	1	-63.11	-53.18	-66.38	-57.67
	4	-65.54	-53.79	-65.95	-57.94
4	1	-62.28	-55.27	-66.06	-60.02
	4	-64.25	-55.78	-65.30	-60.96
5	1	-64.61	-57.32	-65.09	-59.72
	4	-64.77	-57.63	-64.97	-61.36
6	1	-65.25	-58.70	-65.43	-61.93
	4	-64.84	-58.80	-65.00	-62.45
7	1	-65.62	-59.63	-64.95	-62.87
	4	-66.05	-59.62	-65.58	-63.55
8	1	-66.34	-60.46	-65.42	-62.49
	4	-66.83	-60.38	-65.27	-62.34

TABLE 6: Log predictive scores of joint real GDP growth and GDP deflator in-
flation for nowcasts and one-to eight-quarter-ahead forecasts of five
combination methods based on different initializations over the vin-
tages 2001Q1–2014Q4.

h	Initial weights	FW	SOP	DP	BMA	DMA
0	SWFF zero	−27.53	−47.14	−29.21	−49.37	−38.30
	Equal	−31.61	−47.13	−30.85	−49.83	−40.86
1	SWFF zero	−38.28	−54.83	−38.75	−57.44	−45.46
	Equal	−44.31	−55.23	−41.18	−58.09	−47.40
2	SWFF zero	−45.33	−49.71	−46.34	−60.49	−49.51
	Equal	−51.05	−50.20	−49.18	−61.21	−51.92
3	SWFF zero	−49.98	−65.00	−51.21	−65.21	−56.71
	Equal	−55.02	−65.54	−53.79	−65.95	−57.94
4	SWFF zero	−52.36	−63.65	−53.40	−64.49	−59.66
	Equal	−56.60	−64.25	−55.78	−65.30	−60.96
5	SWFF zero	−54.50	−64.17	−55.50	−64.15	−59.64
	Equal	−58.04	−64.77	−57.63	−64.97	−61.36
6	SWFF zero	−56.10	−64.24	−57.05	−64.26	−60.60
	Equal	−58.99	−64.84	−58.80	−65.00	−62.45
7	SWFF zero	−57.52	−65.43	−58.32	−64.90	−61.60
	Equal	−59.56	−66.05	−59.62	−65.58	−63.55
8	SWFF zero	−58.98	−66.20	−59.48	−64.75	−60.56
	Equal	−60.38	−66.83	−60.38	−65.27	−62.34

NOTES: The initial weight scheme denoted "SWFF zero" has equal weights 1/4 on the SW, SWU, BVAR
SoC and BVAR PLR models and weight 0 on the SWFF model, except for the dynamic pool, where the
initialization scheme is random but where the weights approximate such fixed weights on average. The initial
weight scheme "Equal" gives weight 1/5 to each model during the initialization sample. For the fixed weight
(FW) combination method the weights are constant at the "initial weights".

FIGURE 1: Illustration of the real-time information lag, l, and observation lag, k, for forecast combination methods, with $l \leq k$.
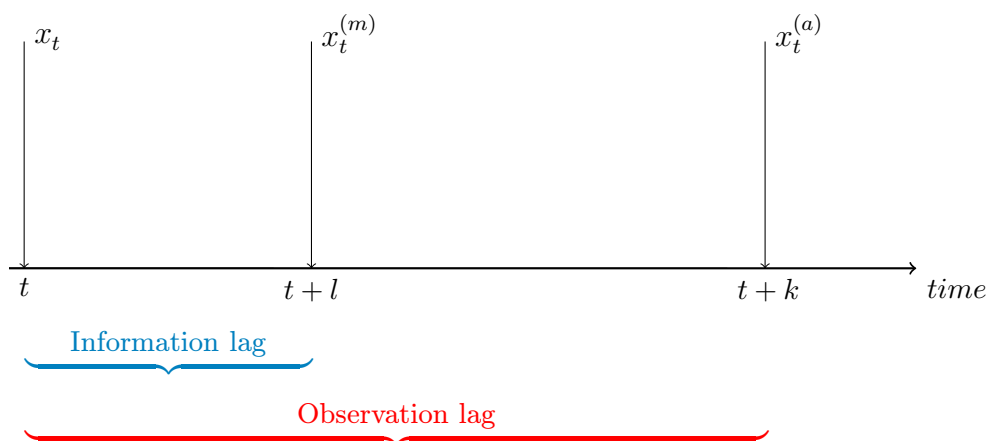
NOTES: The actual (or "true") value of x in period t is denoted by $x_t^{(a)}$ with $t + k$ being the time period when this value can be observed. The measured value of x in period t is $x_t^{(m)}$ with $t + l$ being the vintage its value is taken from.

FIGURE 2: Recursive posterior mode estimates of the hyperparameters of the BVAR models for 2001Q1–2014Q4.

SoC Model

λ_o

δ

μ

PLR Model

λ_o

ϕ_1

ϕ_2

ϕ_3

ϕ_4

ϕ_5

ϕ_6

ϕ_7

ϕ_8

ϕ_9
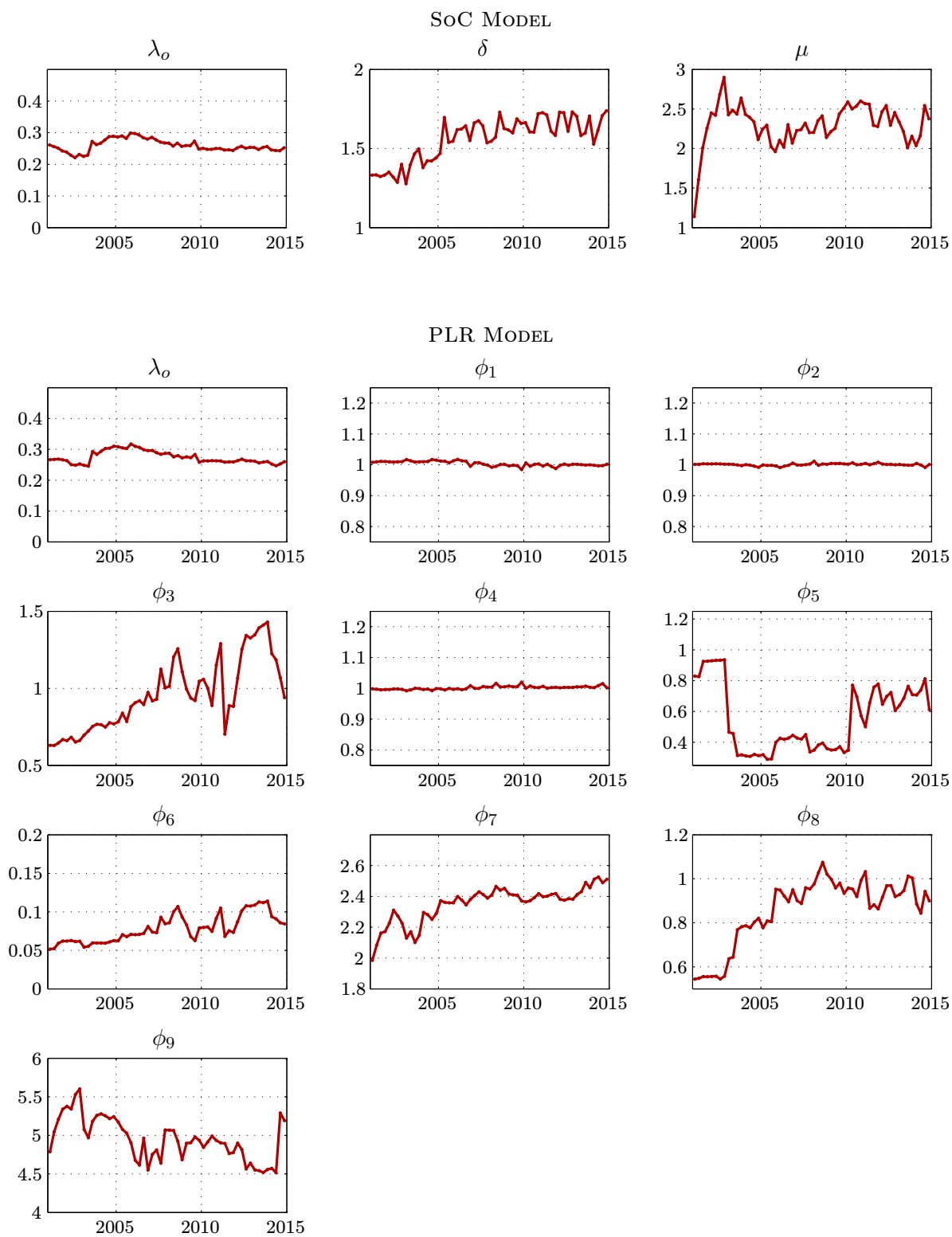
FIGURE 3: Recursive point backcasts, nowcasts and forecasts of real GDP growth and GDP deflator inflation using the RTD vintages 2001Q1–2014Q4.

A. Real GDP Growth

B. GDP Deflator Inflation
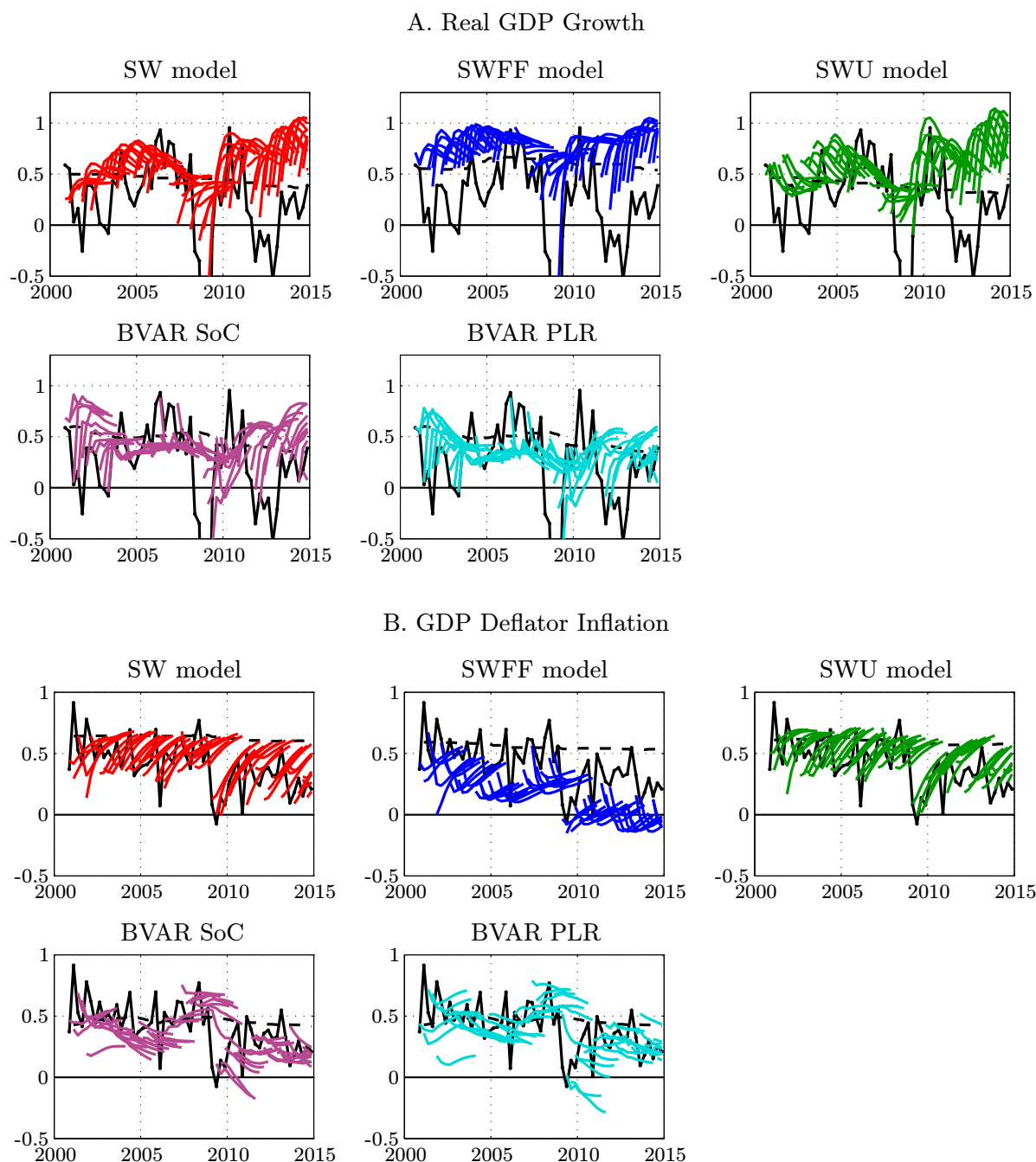
NOTES: The actual values are plotted as solid black lines. Recursively estimated posterior mean values of mean real GDP growth and mean inflation are plotted as dashed lines using the DSGE models. By contrast, the dashed lines are vintage sample mean values since 1995Q1 of real GDP growth and inflation for the BVAR plots.

FIGURE 4: Percentile values of the Amisano-Giacomini weighted likelihood ratio tests for the equality of the average log predictive scores of ten BVAR and DSGE model pairs for the sample 2001Q1–2014Q4.
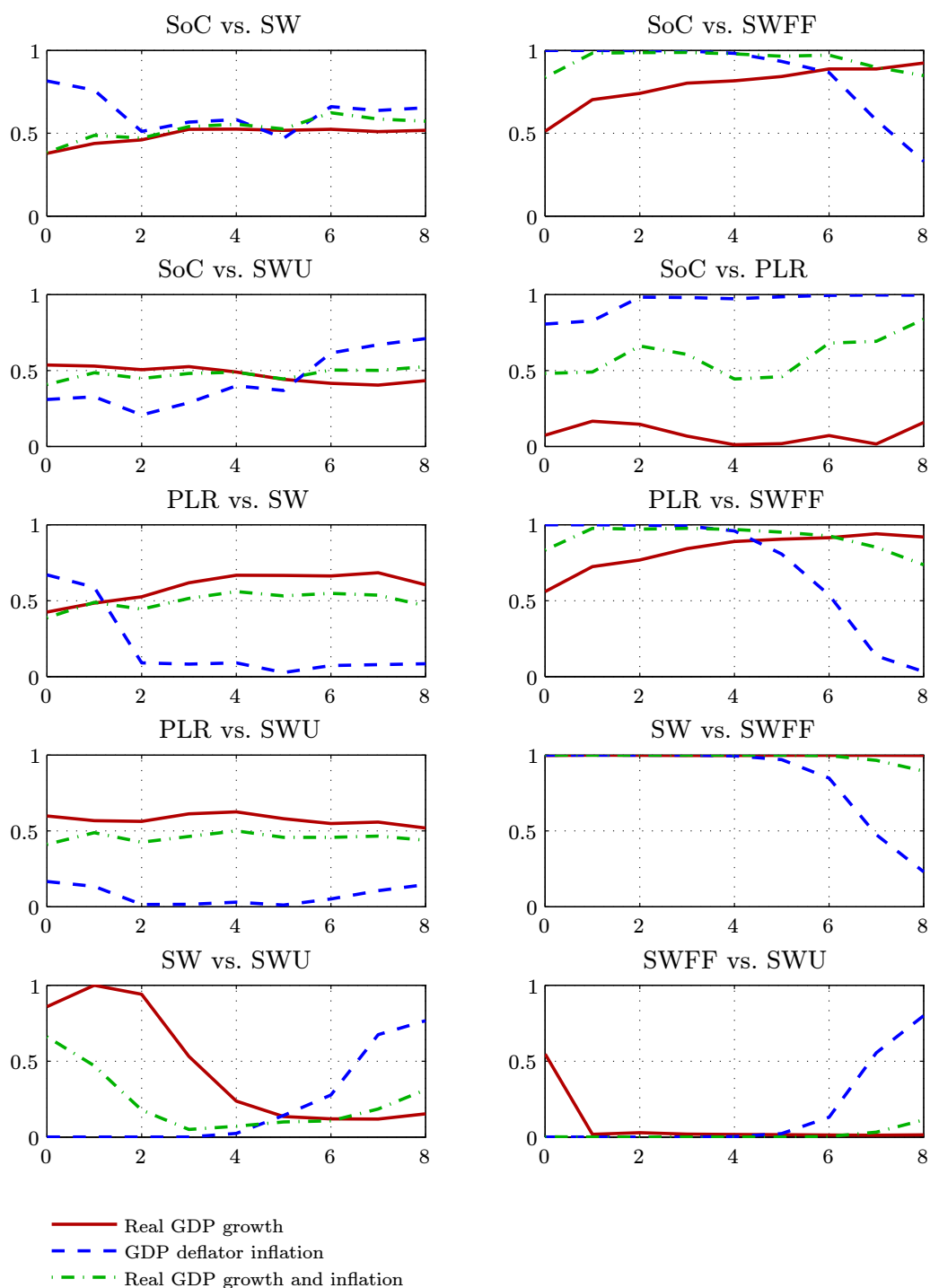
NOTES: The test statistics have been computed with equal weights and using the Bartlett kernel for the HAC estimator (Newey and West, 1987). Following Amisano and Giacomini (2007) we use a short truncation lag, but rather than using their selection of zero lags we use one lag. The percentile value of the test statistic is taken from a standard normal distribution, where large percentile values favor the first model of the test and small percentile values the second model.
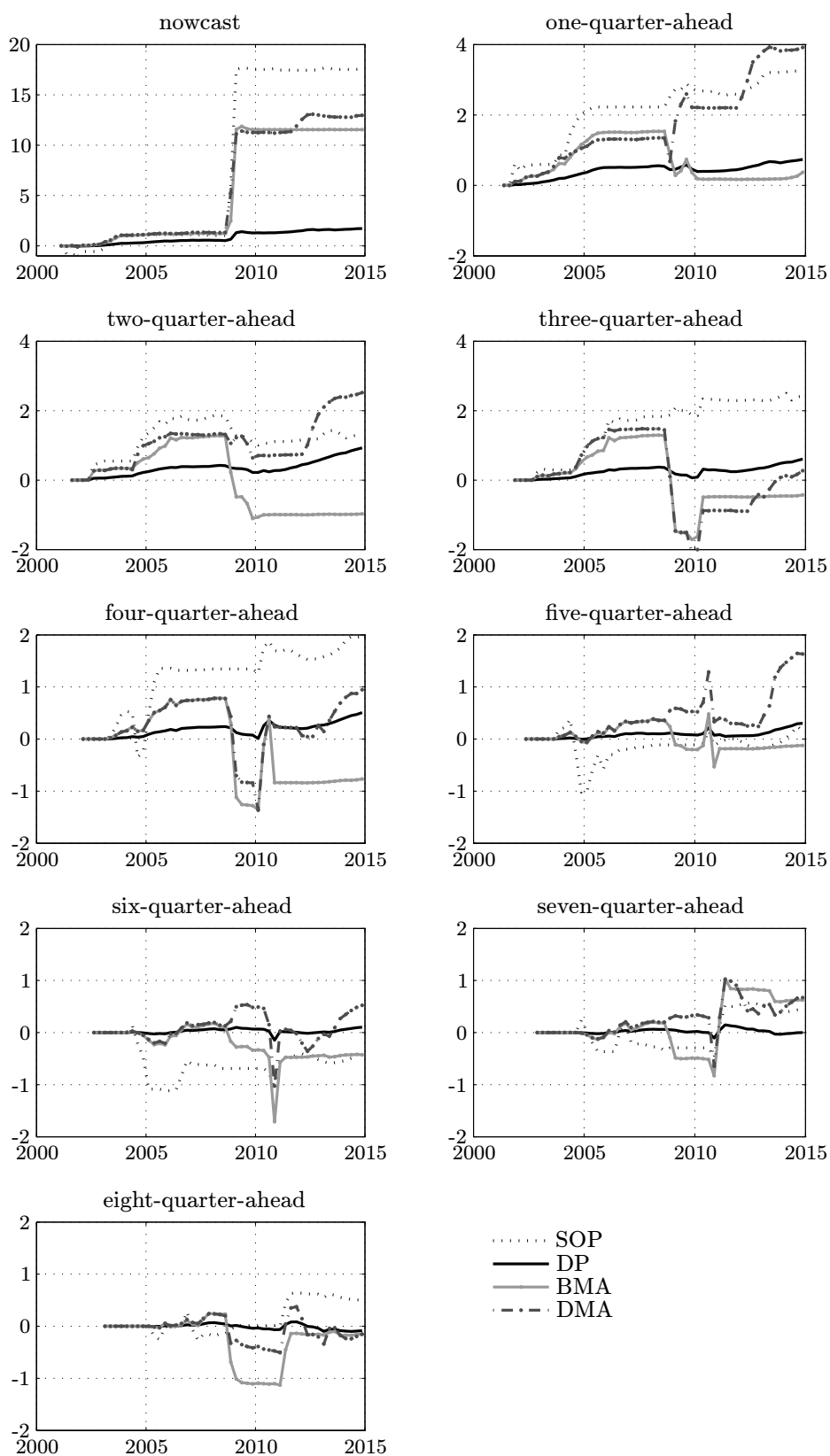
FIGURE 5: Recursive estimates of the average log predictive scores of joint real GDP growth and GDP deflator inflation for the vintages 2001Q1–2014Q4.
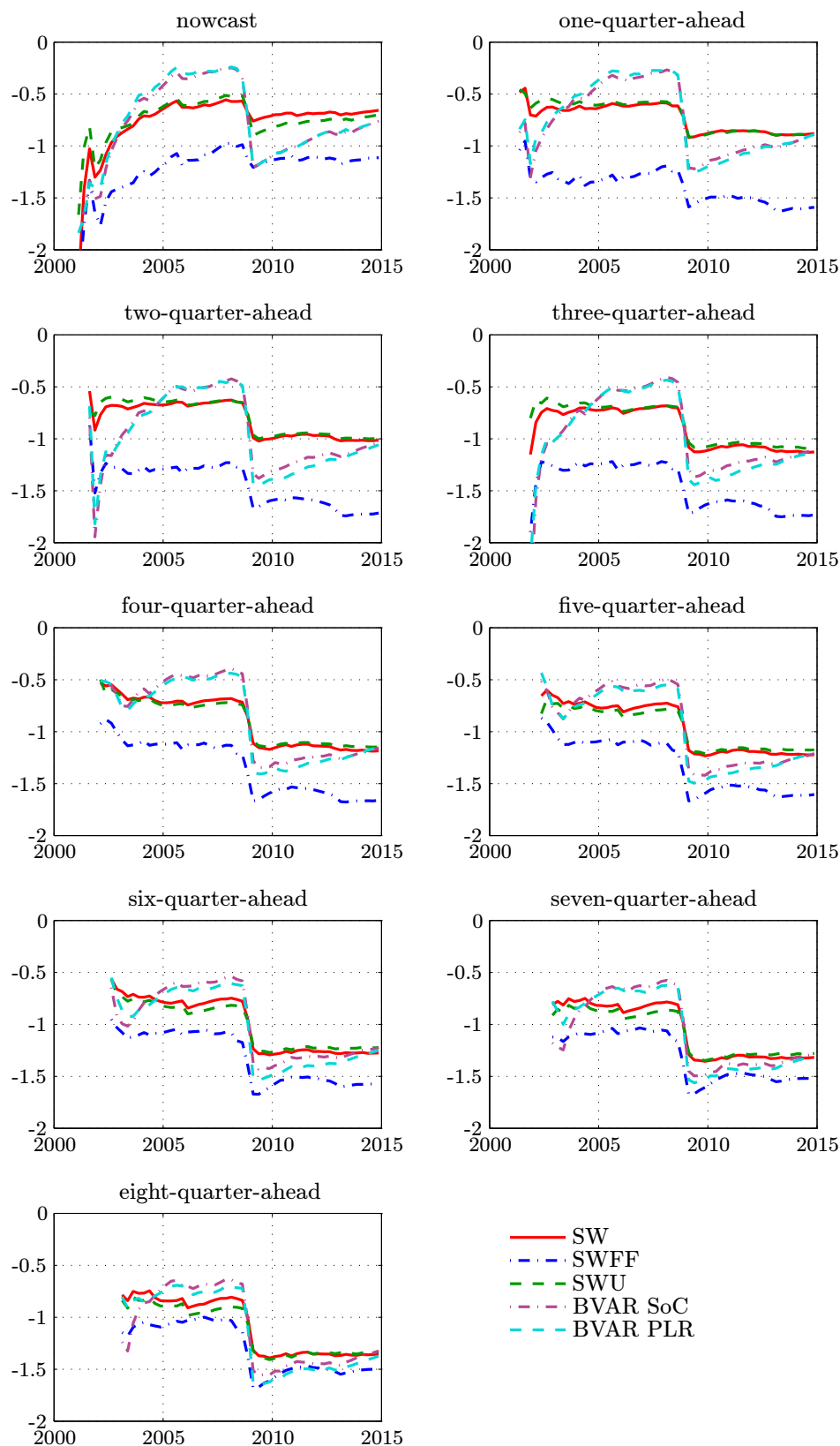
FIGURE 6: Recursive estimates of the average log predictive scores of real GDP growth for the vintages 2001Q1–2014Q4.
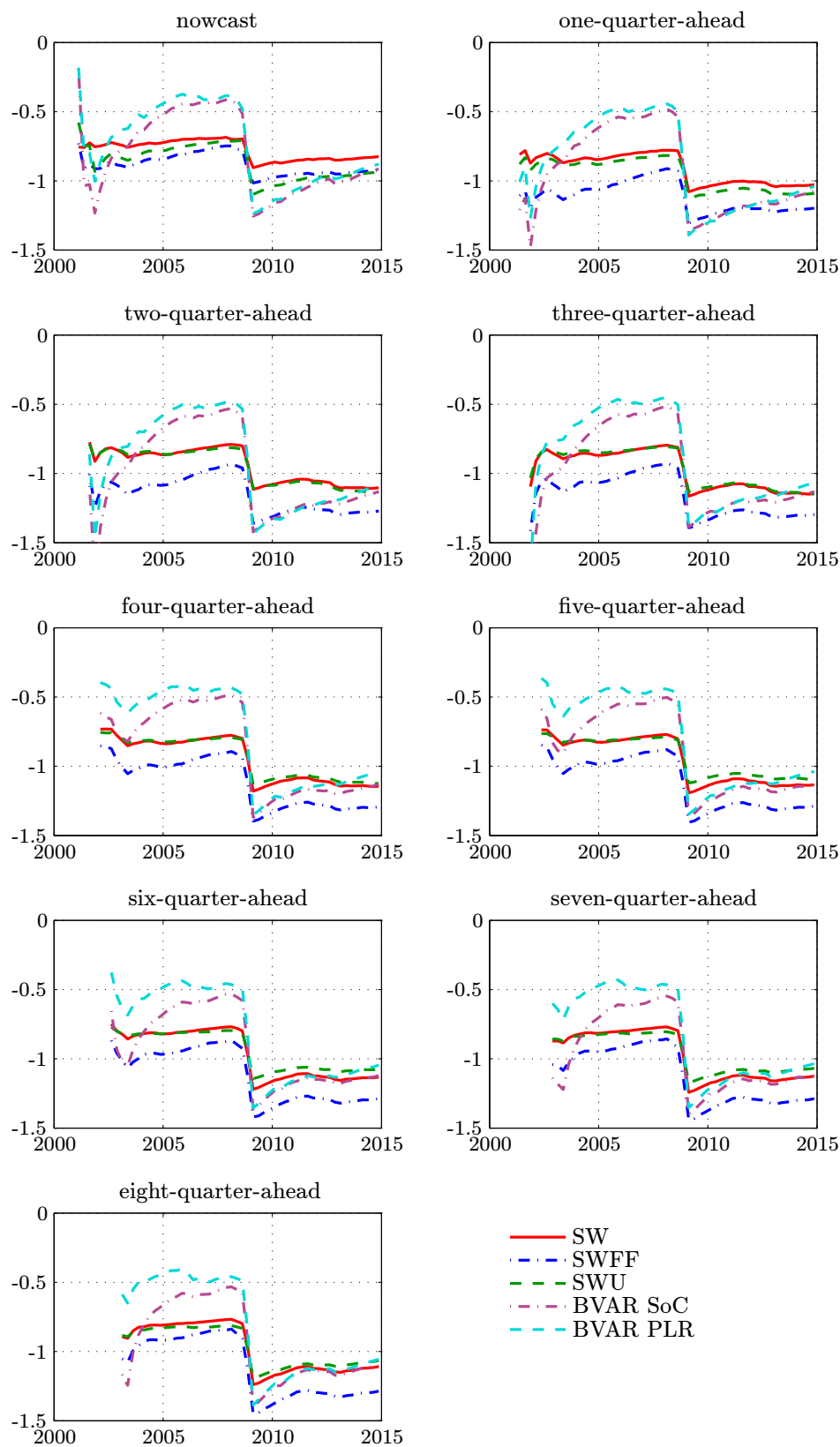
FIGURE 7: Recursive estimates of the average log predictive scores of GDP deflator inflation for the vintages 2001Q1–2014Q4.
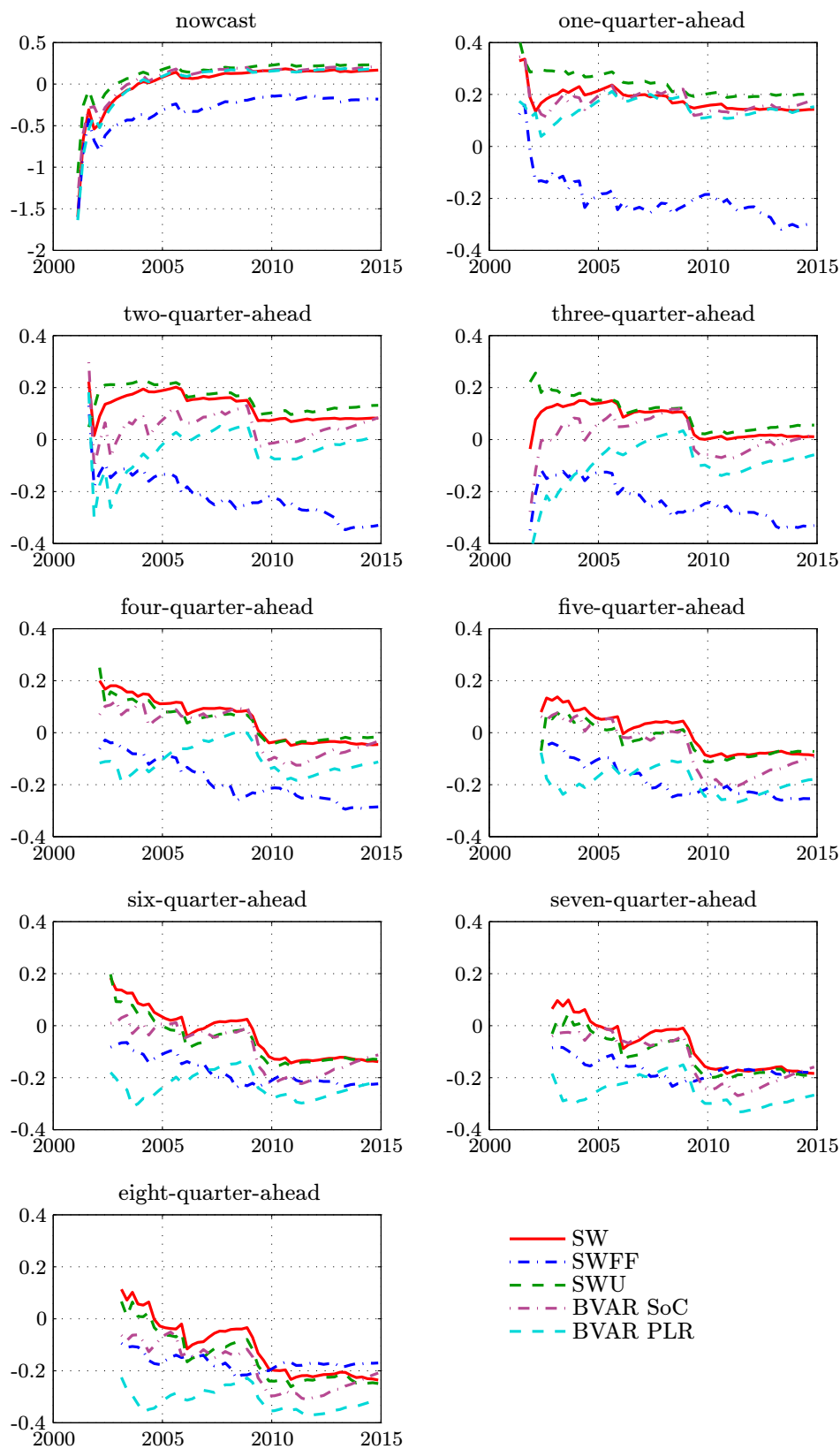
FIGURE 8: Log predictive scores for nowcasts and one-quarter-ahead to eight-quarter-ahead forecasts of DSGE models, BVAR models and combination methods in deviation from the log score of the dynamic prediction pool over the vintages 2001Q1–2014Q4.
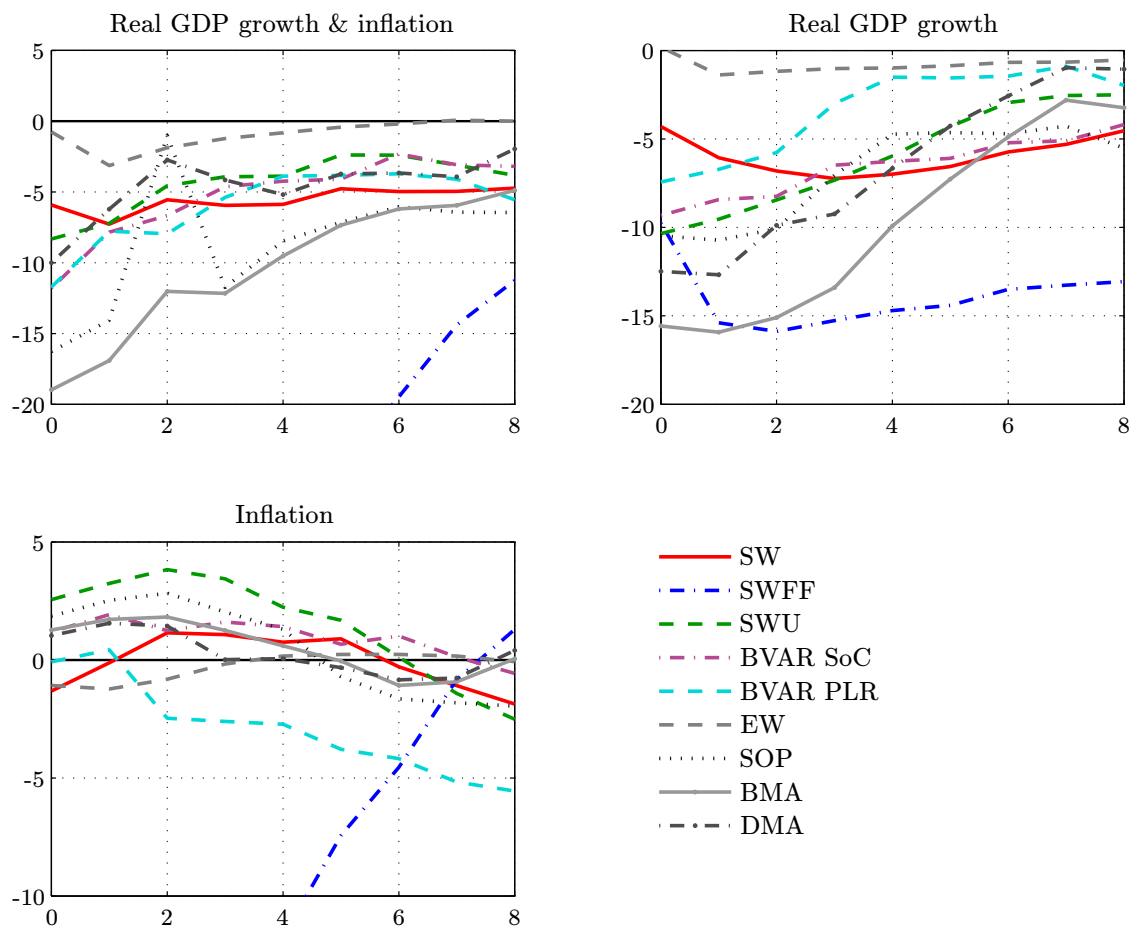
NOTES: All full sample log predictive scores are measured in deviation from the log score of the dynamic prediction pool (DP). The other density forecast combination methods are given by equal weight (EW), static optimal prediction pool (SOP), Bayesian model averaging (BMA) and dynamic model averaging (DMA). The DP, SOP, BMA and DMA combination methods are based on an information lag of four quarters.

FIGURE 9: Percentile values of the Amisano-Giacomini weighted likelihood ratio tests for the equality of the average log predictive scores of the dynamic prediction pool versus nine alternative forecast schemes for the sample 2001Q1–2014Q4.
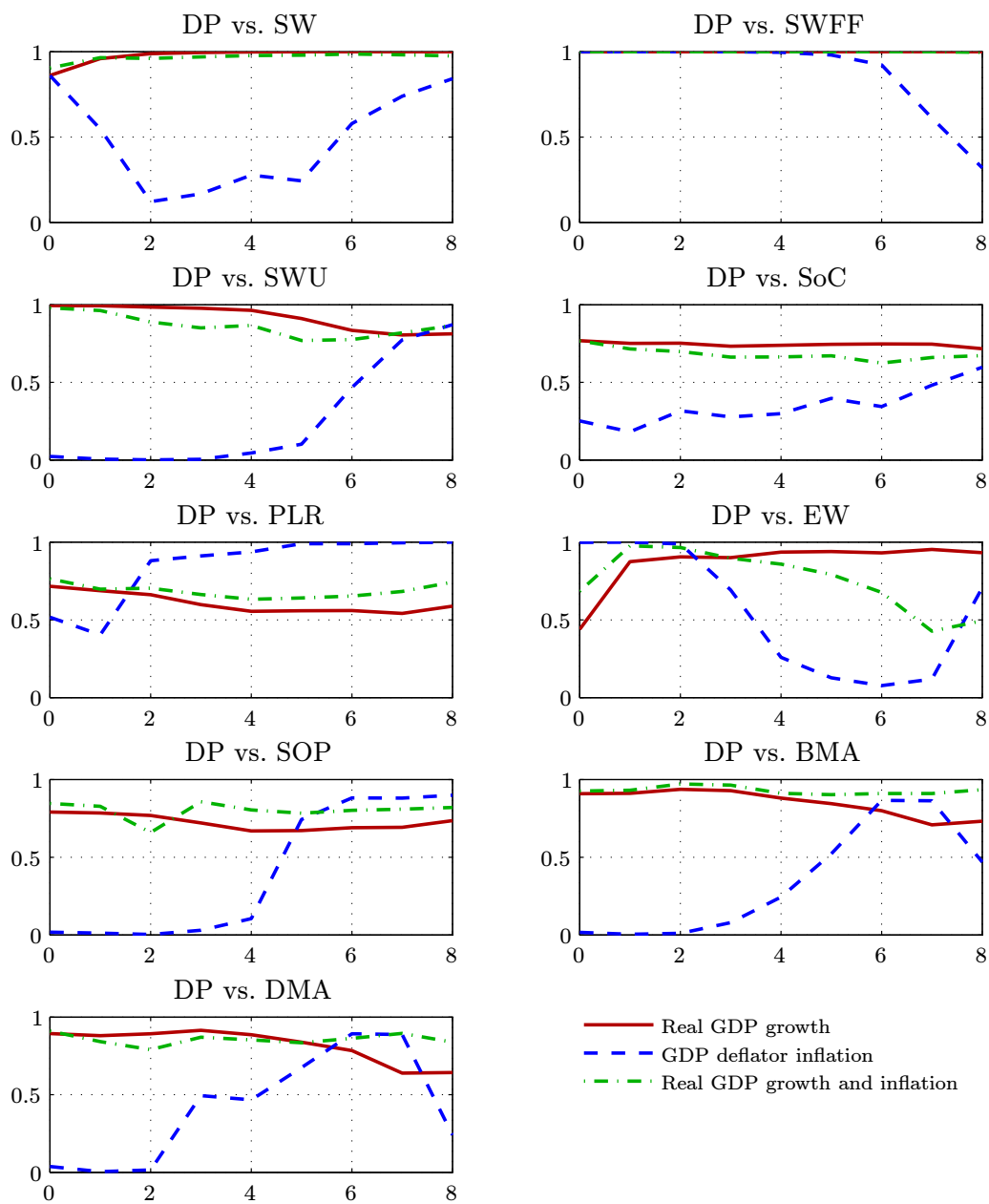
NOTES: See Figures 4 and 8 for details.

FIGURE 10: Recursive estimates of the average log predictive scores of joint real
GDP growth and GDP deflator inflation and in deviation from the
recursive estimates of the average log scores of the dynamic predic-
tion pool covering the vintages 2001Q1–2014Q4.
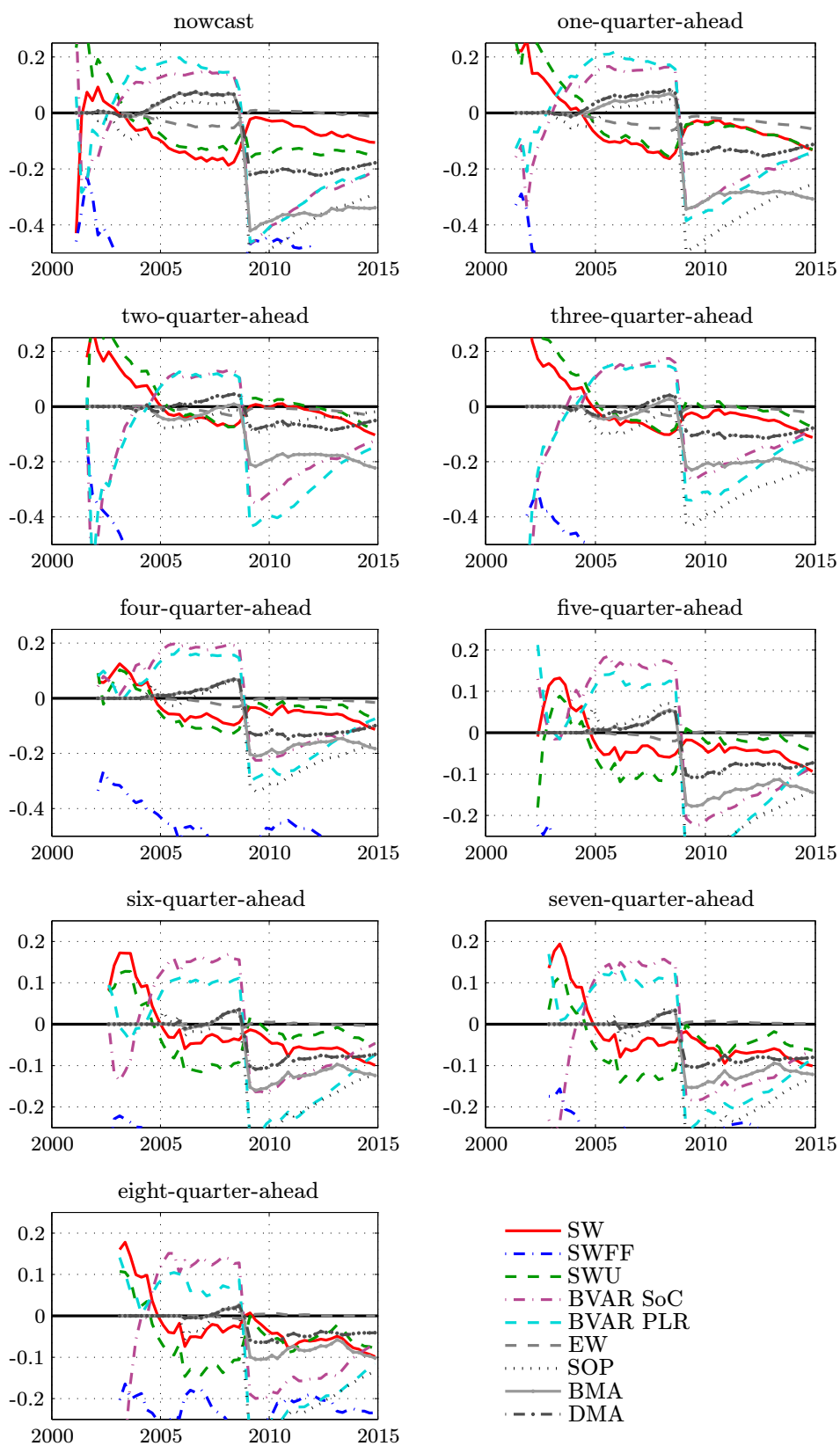
FIGURE 11: Posterior estimates of the model weights for the dynamic prediction
pool of joint real GDP growth and GDP deflator inflation covering
the vintages 2001Q1–2014Q4.
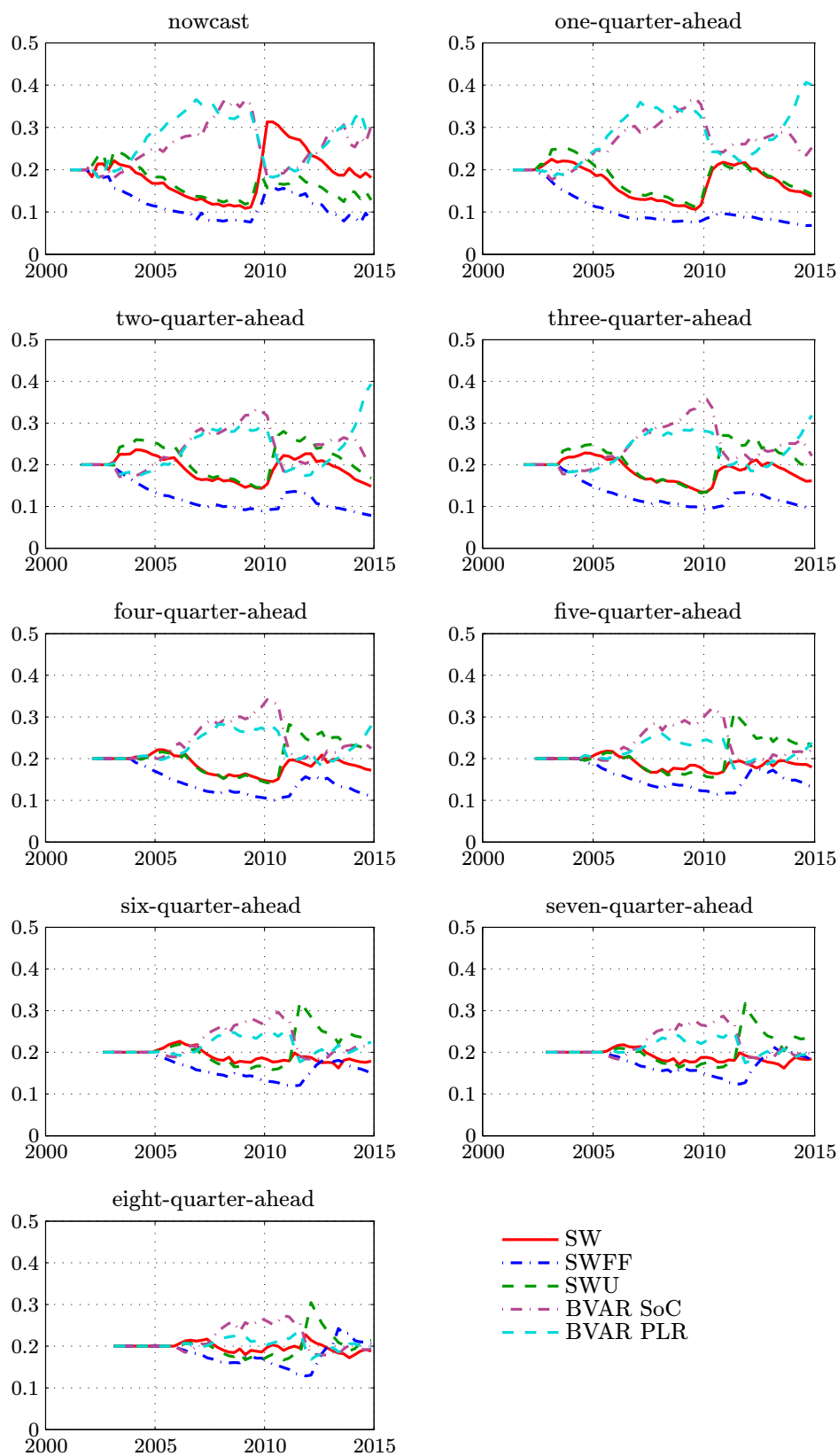
FIGURE 12: Recursive estimates of the average log predictive scores of joint real GDP growth and GDP deflator inflation for the combinations and in deviation from the recursive value of the upper bound covering the vintages 2001Q1–2014Q4.
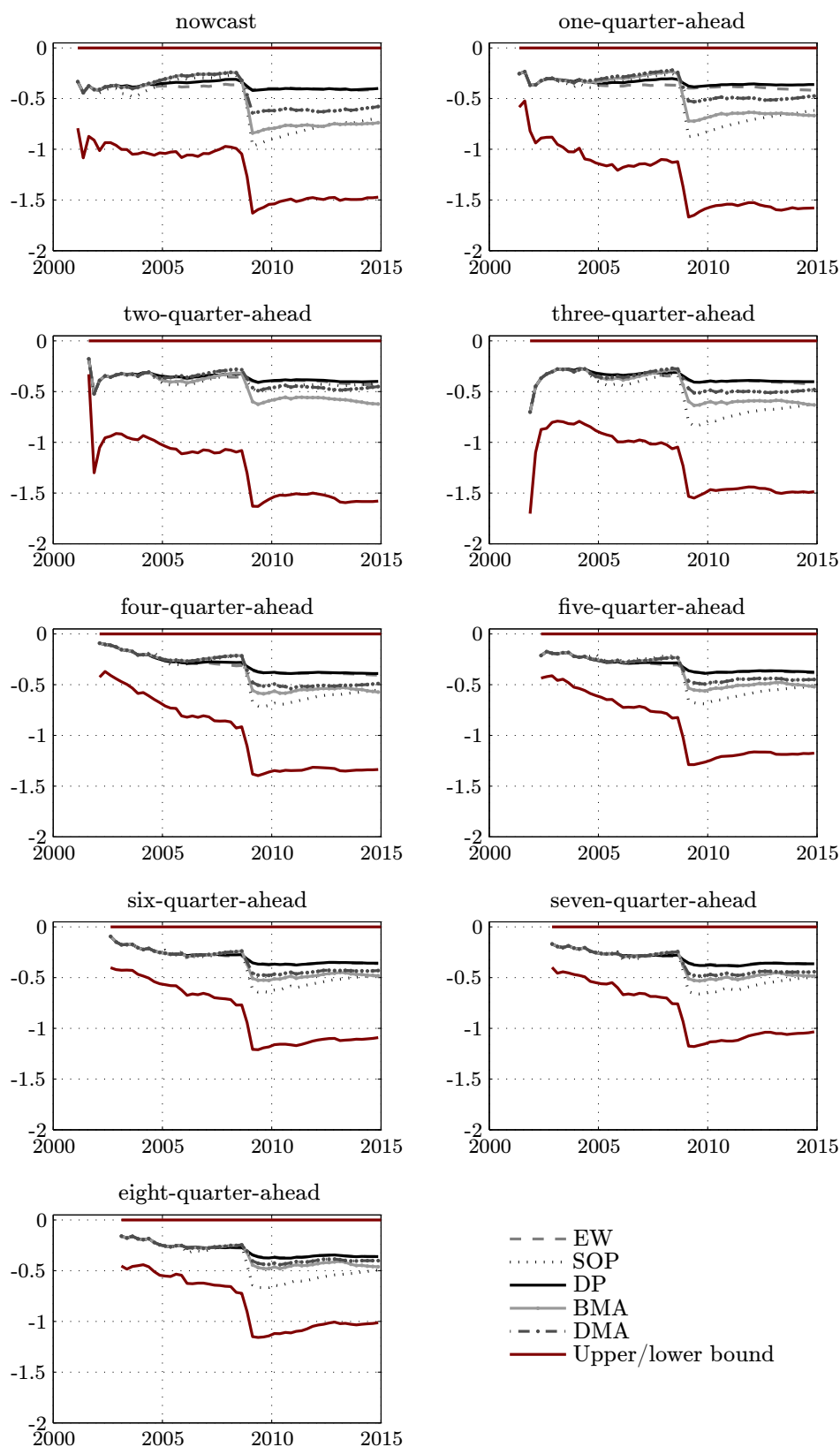
FIGURE 13: Recursive estimates of the differences of log predictive scores of joint real GDP growth and GDP deflator inflation for information lag 1 and 4 covering the vintages 2001Q1–2014Q4.

FIGURE 14: Recursive estimates of the differences of log predictive scores of joint real GDP growth and GDP deflator inflation for the SWFF zero initialization and the equal weights initialization covering the vintages 2001Q1–2014Q4.
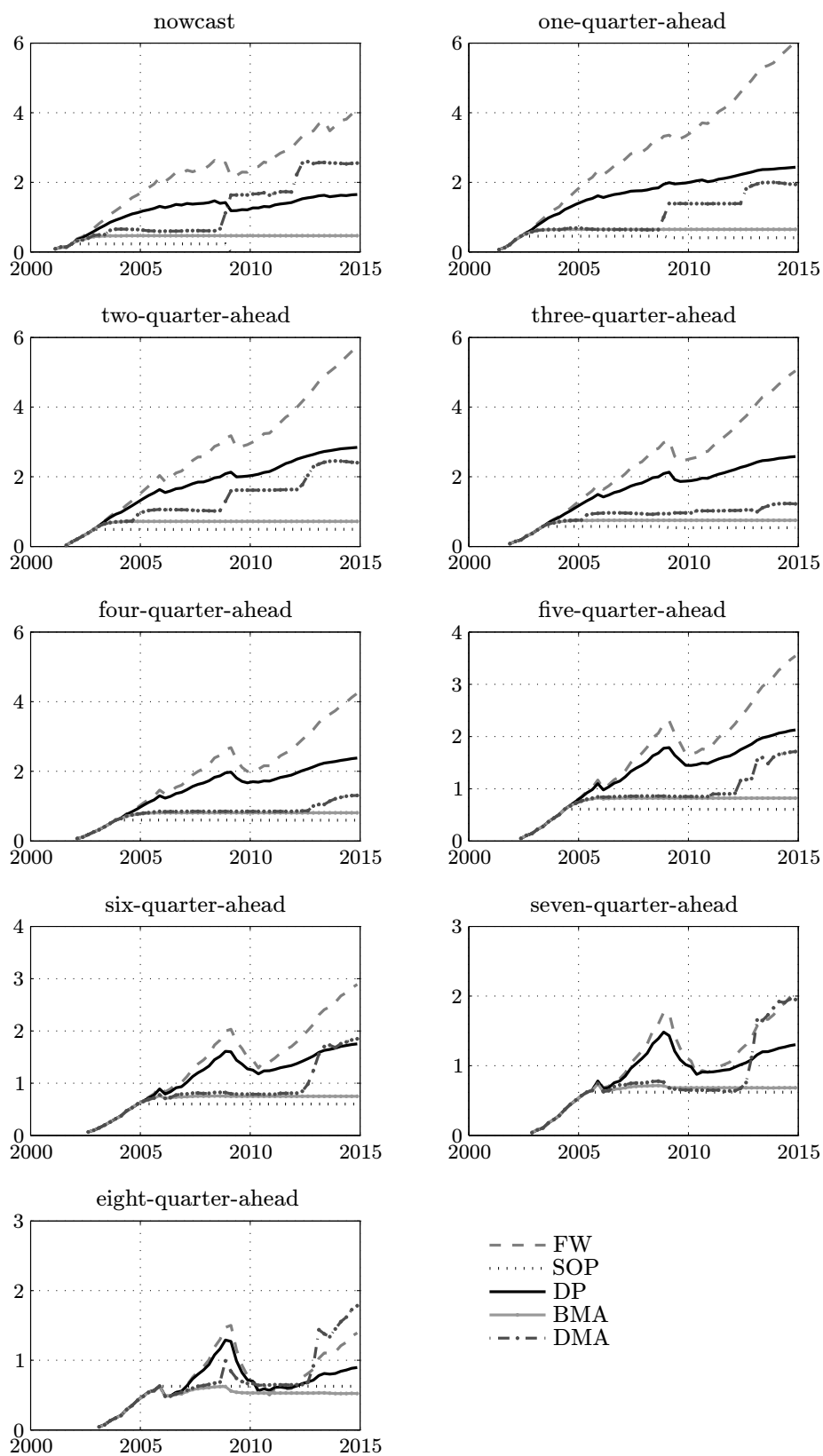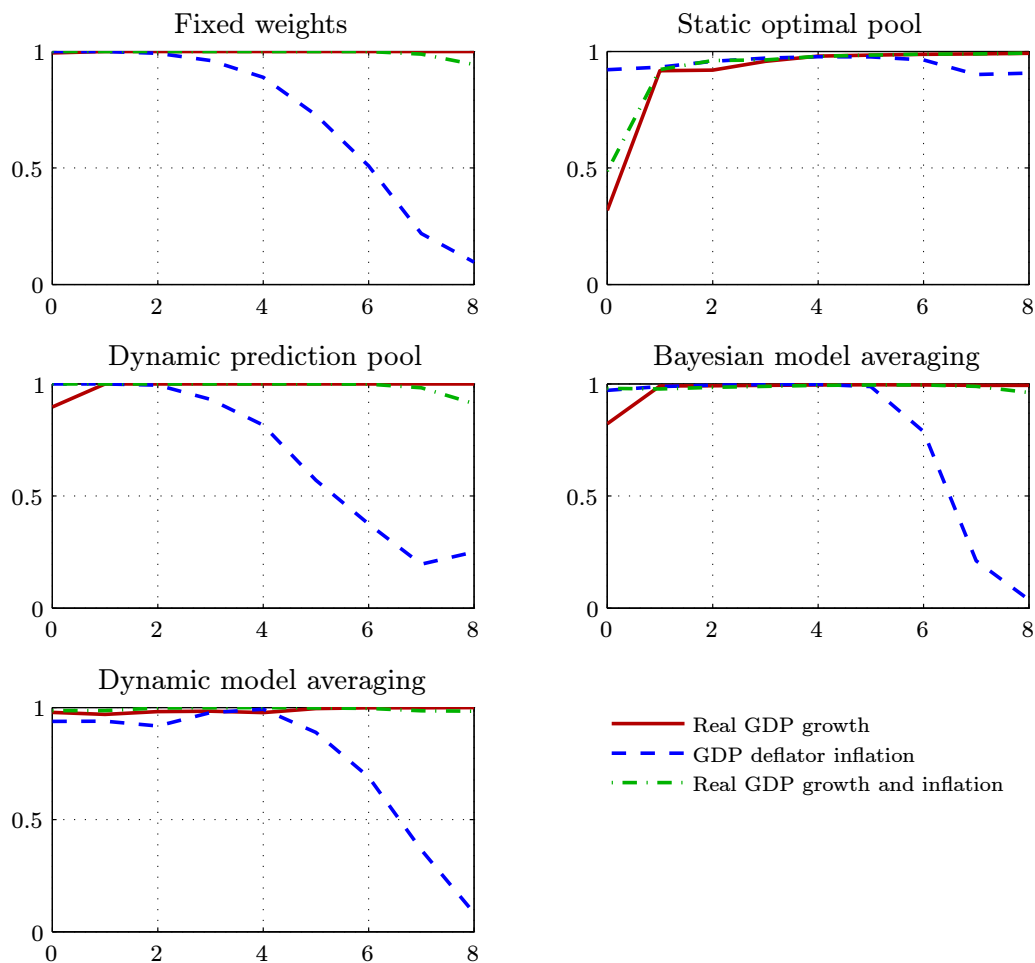
NOTES: See Figures 4 and 8 as well as Table 6 for details.

FIGURE 16: Posterior estimates of the model weights for the dynamic prediction pool of joint real GDP growth and GDP deflator inflation based on the SWFF zero initialization and covering the vintages 2001Q1– 2014Q4.
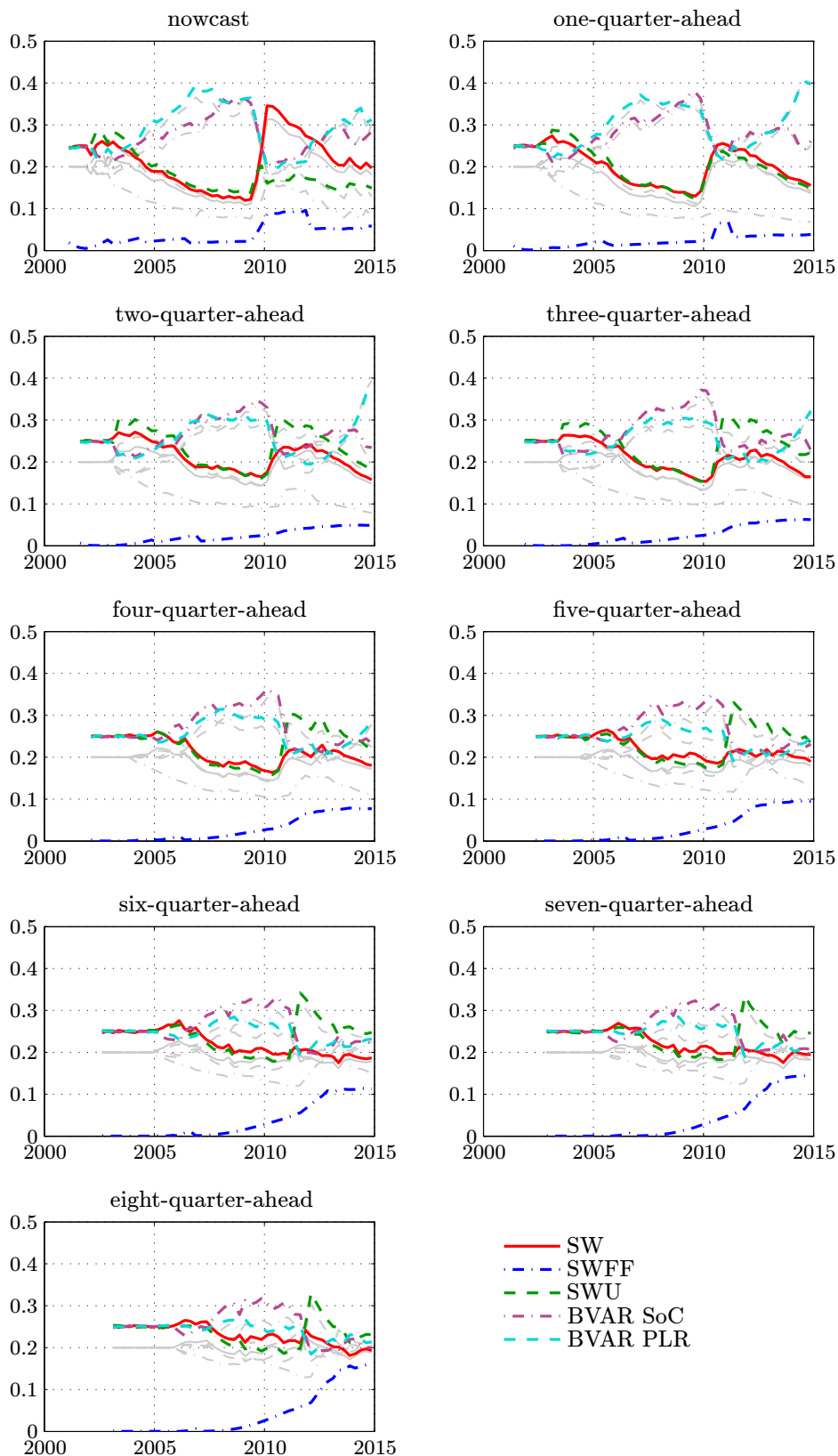
THE GENERAL NORMAL-INVERTED WISHART BVAR MODEL

Let y_t be an n-dimensional vector of observable variables such that its VAR representation is given by

$$y_t = \Phi_0 + \sum_{j=1}^{p} \Phi_j y_{t-j} + \epsilon_t, \quad t = 1, \ldots, T, \tag{A.1}$$

where $\epsilon_t \sim N_n(0, \Omega)$ and Φ_j are $n \times n$ matrices for $j \geq 1$ and an $n \times 1$ vector if $j = 0$. Let $X_t = [1\ y_t'\ \cdots\ y_{t-p+1}']'$ be an $(np + 1)$-dimensional vector, while the $n \times (np + 1)$ matrix $\Phi = [\Phi_0\ \Phi_1\ \cdots\ \Phi_p]$ such that the VAR can be expressed as:

$$y_t = \Phi X_{t-1} + \epsilon_t. \tag{A.2}$$

Stacking the VAR system as $y = [y_1\ \cdots\ y_T]$, $X = [X_0\ \cdots\ X_{T-1}]$ and $\epsilon = [\epsilon_1\ \cdots\ \epsilon_T]$, we can express this as

$$y = \Phi X + \epsilon, \tag{A.3}$$

with log-likelihood

$$\log p(y|X_0; \Phi, \Omega) = -\frac{nT}{2} \log(2\pi) - \frac{T}{2} \log|\Omega| - \frac{1}{2} \mathrm{tr}[\Omega^{-1} \epsilon\epsilon'], \tag{A.4}$$

where, for convenience, we use the same notation for the random variables as their realizations.

The normal-inverted Wishart prior for (Φ, Ω) is given by

$$\mathrm{vec}(\Phi)|\Omega, \alpha \sim N_{n(np+1)}(\mathrm{vec}(\mu_\Phi), [\Omega_\Phi \otimes \Omega]), \tag{A.5}$$

$$\Omega|\alpha \sim IW_n(A, v), \tag{A.6}$$

where the prior parameters $(\mu_\Phi, \Omega_\Phi, A, v)$ are determined through a vector of hyperparameters, denoted by α. This means that the sum of the log-likelihood and the log prior is given by

$$\begin{aligned}
\log p(y, \Phi, \Omega|X_0, \alpha) = &-\frac{n(T + np + 1)}{2} \log(2\pi) - \frac{nv}{2} \log(2) - \frac{n(n-1)}{4} \log(\pi) \\
&- \log \Gamma_n(v) - \frac{n}{2} \log|\Omega_\Phi| + \frac{v}{2} \log|A| \\
&- \frac{T + n(p+1) + v + 2}{2} \log|\Omega| \\
&- \frac{1}{2} \mathrm{tr}\left[\Omega^{-1}\left(\epsilon\epsilon' + A + (\Phi - \mu_\Phi)\Omega_\Phi^{-1}(\Phi - \mu_\Phi)'\right)\right].
\end{aligned} \tag{A.7}$$

Using standard "Zellner" algebra, it is straightforward to show that

$$\epsilon\epsilon' + A + (\Phi - \mu_\Phi)\Omega_\Phi^{-1}(\Phi - \mu_\Phi)') = (\Phi - \bar{\Phi})(XX' + \Omega_\Phi^{-1})(\Phi - \bar{\Phi})' + S, \tag{A.8}$$

where

$$\bar{\Phi} = (yX' + \mu_\Phi \Omega_\Phi^{-1})(XX' + \Omega_\Phi^{-1})^{-1},$$

$$S = yy' + A + \mu_\Phi \Omega_\Phi^{-1} \mu_\Phi' - \bar{\Phi}(XX' + \Omega_\Phi^{-1})\bar{\Phi}'.$$

Substituting for (A.8) in (A.7), we find that the conjugate normal-inverted Wishart prior gives us a normal posterior for $\Phi|\Omega, \alpha$ and an inverted Wishart posterior for $\Omega|\alpha$. Specifically,

$$\text{vec}(\Phi)|\Omega, y, X_0, \alpha \sim N_{n(np+1)}\big(\text{vec}(\bar{\Phi}), \big[(XX' + \Omega_\Phi^{-1})^{-1} \otimes \Omega\big]\big), \tag{A.9}$$

$$\Omega|y, X_0, \alpha \sim IW_n(S, T + v). \tag{A.10}$$

Combining these posterior results with equations (A.7) and (A.8) it follows that the log marginal likelihood conditional on α is given by

$$\begin{aligned}
\log p(y|X_0, \alpha) = &-\frac{nT}{2}\log(\pi) + \log \Gamma_n(T + v) - \log \Gamma_n(v) - \frac{n}{2}\log|\Omega_\Phi| \\
&+ \frac{v}{2}\log|A| - \frac{n}{2}\log|XX' + \Omega_\Phi^{-1}| - \frac{T+v}{2}\log|S|,
\end{aligned} \tag{A.11}$$

where $\Gamma_b(a) = \prod_{i=1}^{b}\Gamma([a - i + 1]/2)$ for positive integers a and b with $a \geq b$, while $\Gamma(\cdot)$ is the gamma function.

To allow for case of a diffuse and improper prior for the parameters on the constant term, Φ_0, let

$$X = \begin{bmatrix} \imath_T' \\ Y \end{bmatrix}, \qquad X_{(d)} = \begin{bmatrix} c_{(d)} \\ Y_{(d)} \end{bmatrix}, \qquad \Gamma = \begin{bmatrix} \Phi_1 & \cdots & \Phi_p \end{bmatrix}, \qquad \Omega_\Phi = \begin{bmatrix} \gamma^2 & 0_{1 \times np} \\ 0_{np \times 1} & \Omega_\Gamma \end{bmatrix},$$

where $\imath_T$ is a $T \times 1$ unit vector, and where $c_{(d)}$ is the first row of $X_{(d)}$ which is zero except for position $n(p+1) + 1$ being equal to γ^{-1}. The prior for the VAR parameters is now expressed as

$$\text{vec}(\Gamma)|\Omega \sim N_{n^2p}\big(\text{vec}(\mu_\Gamma), [\Omega_\Gamma \otimes \Omega]\big), \tag{A.12}$$

while $p(\Phi_0) \propto 1$ and the prior of Ω is given by (A.6). Let $Z = y - \Gamma Y$, $\bar{\Phi}_0 = T^{-1}Z\imath_T$, and let

$$D = I_T - T^{-1}\imath_T\imath_T',$$

a $T \times T$ symmetric and idempotent matrix. Through the usual Zellner algebra we have that

$$\epsilon\epsilon' = ZDZ' + (\Phi_0 - \bar{\Phi}_0)\imath_T'\imath_T(\Phi_0 - \bar{\Phi}_0)'.$$

Furthermore, with D being symmetric and idempotent we may define $\tilde{Z} = ZD$, such that $\tilde{y} = yD$, $\tilde{Y} = YD$ and $ZDZ' = \tilde{Z}\tilde{Z}'$. The Zellner algebra now provides us with

$$\tilde{Z}\tilde{Z}' + (\Gamma - \mu_\Gamma)\Omega_\Gamma^{-1}(\Gamma - \mu_\Gamma)' + A = (\Gamma - \bar{\Gamma})\left(\tilde{Y}\tilde{Y}' + \Omega_\Gamma^{-1}\right)(\Gamma - \bar{\Gamma})' + S,$$

where

$$\bar{\Gamma} = \left(\tilde{y}\tilde{Y}' + \mu_\Gamma\Omega_\Gamma^{-1}\right)\left(\tilde{Y}\tilde{Y}' + \Omega_\Gamma^{-1}\right)^{-1}$$

$$S = \tilde{y}\tilde{y}' + A + \mu_\Gamma\Omega_\Gamma^{-1}\mu_\Gamma' - \bar{\Gamma}\left(\tilde{Y}\tilde{Y}' + \Omega_\Gamma^{-1}\right)\bar{\Gamma}'.$$

It can therefore be shown that the normal-inverted Wishart posterior for the VAR parameters is given by

$$\Phi_0\big|\Gamma, \Omega, y, X_0, \alpha \sim N_n\big(\bar{\Phi}_0, T^{-1}\Omega\big), \tag{A.13}$$

$$\mathrm{vec}\big(\Gamma\big)\big|\Omega, y, X_0, \alpha \sim N_{n^2 p}\big(\mathrm{vec}(\bar{\Gamma}), \big[(\tilde{Y}\tilde{Y}' + \Omega_\Gamma^{-1})^{-1} \otimes \Omega\big]\big) \tag{A.14}$$

$$\Omega\big|y, X_0, \alpha \sim IW_n\big(S, T + v - 1\big). \tag{A.15}$$

Hence, the improper prior on Φ_0 results in a loss of degrees of freedom for the posterior of Ω.[36]

Furthermore, the log marginal likelihood is

$$\log p\big(y\big|X_0, \alpha\big) = -\frac{n(T-1)}{2}\log(\pi) + \log\Gamma_n(T+v-1) - \log\Gamma_n(v) - \frac{n}{2}\log\big|\Omega_\Gamma\big|$$
$$+ \frac{v}{2}\log\big|A\big| - \frac{n}{2}\log(T) - \frac{n}{2}\log\big|\tilde{Y}\tilde{Y}' + \Omega_\Gamma^{-1}\big| - \frac{T+v-1}{2}\log\big|S\big|, \tag{A.16}$$

where the term $\log(T)$ stems from $T = \iota_T' \iota_T$ and is obtained when integrating out Φ_0 from the joint posterior. The relationship between the dummy observations and the prior parameters is

$$\mu_\Gamma = y_{(d)} Y_{(d)}' \left(Y_{(d)} Y_{(d)}'\right)^{-1}, \qquad\qquad \Omega_\Gamma = \left(Y_{(d)} Y_{(d)}'\right)^{-1},$$
$$A = \left(y_{(d)} - \mu_\Gamma Y_{(d)}\right)\left(y_{(d)} - \mu_\Gamma Y_{(d)}\right)', \qquad\qquad v = T_d - (np+1).$$

Letting $\tilde{y}_\star = [y_{(d)}\ \tilde{y}]$ and $\tilde{Y}_\star = [Y_{(d)}\ \tilde{Y}]$, it follows that the posterior parameters

$$\bar{\Gamma} = \tilde{y}_\star \tilde{Y}_\star' \big(\tilde{Y}_\star \tilde{Y}_\star'\big)^{-1},$$
$$\tilde{Y}\tilde{Y}' + \Omega_\Gamma^{-1} = \tilde{Y}_\star \tilde{Y}_\star',$$
$$S = \big(\tilde{y}_\star - \bar{\Gamma}\tilde{Y}_\star\big)\big(\tilde{y}_\star - \bar{\Gamma}\tilde{Y}_\star\big)'.$$

---

[36] This loss of one degree of freedom is due to $(y_{(d)}, X_{(d)})$ having one observation less as $\gamma \to 0$, i.e., as the prior on Φ_0 becomes improper.

This Appendix first describes how the VAR model in equation (11) can be applied to backcast, nowcast and forecast when we have real-time data. To be specific, we shall assume that data on some variables are missing in periods $T-1$ and T, corresponding to the situation for the RTD of the euro area. The second part is concerned with the estimation of the marginal likelihood of the VAR model when taking the ragged edge of the real-time data into account.

In addition to being interested in the y_t variables, we are also interested in forecasting the first differences of some of these variables. To this end, let S be an $n \times s$ matrix with full column rank $s \leq n$ which selects unique elements of y_t such that

$$z_t = S'(y_t - y_{t-1}).$$

In other words, z_t is an s-dimensional vector whose elements are first differences of some of the elements in y_t. This means that

$$z_t = \Phi_0^* + \sum_{j=1}^{p} \Phi_j^* y_{t-j} + S'\epsilon_t,$$

where

$$\Phi_j^* = \begin{cases} S'(\Phi_1 - I_n), & \text{if } j = 1, \\ S'\Phi_j, & \text{otherwise.} \end{cases}$$

In order to derive a state-space system for the VAR model, including the first difference variables z_t, we stack these equations as follows:

$$
\begin{bmatrix} z_t \\ 1 \\ y_t \\ y_{t-1} \\ \vdots \\ y_{t-p+2} \\ y_{t-p+1} \end{bmatrix}
=
\begin{bmatrix}
0 & \Phi_0^* & \Phi_1^* & \Phi_2^* & \cdots & \Phi_{p-2}^* & \Phi_{p-1}^* & \Phi_p^* \\
0 & 1 & 0 & 0 & \cdots & 0 & 0 & 0 \\
0 & \Phi_0 & \Phi_1 & \Phi_2 & \cdots & \Phi_{p-2} & \Phi_{p-1} & \Phi_p \\
0 & 0 & I_n & 0 & \cdots & 0 & 0 & 0 \\
\vdots & \vdots & & \ddots & & & \vdots & \vdots \\
0 & 0 & 0 & 0 & & I_n & 0 & 0 \\
0 & 0 & 0 & 0 & \cdots & 0 & I_n & 0
\end{bmatrix}
\begin{bmatrix} z_{t-1} \\ 1 \\ y_{t-1} \\ y_{t-2} \\ \vdots \\ y_{t-p+1} \\ y_{t-p} \end{bmatrix}
+
\begin{bmatrix} S'\epsilon_t \\ 0 \\ \epsilon_t \\ 0 \\ \vdots \\ 0 \\ 0 \end{bmatrix}.
$$

This gives us the state equation of the system. More compactly, we express it as

$$\xi_t = F\xi_{t-1} + C\epsilon_t. \tag{B.1}$$

The measurement equation of the system is now given by

$$y_t = H'\xi_t, \quad t = 1, \ldots, T-2. \tag{B.2}$$

where

$$H' = \begin{bmatrix} 0_{n\times(s+1)} & I_n & 0_{n\times n(p-1)} \end{bmatrix}.$$

For $t = T - 1, T$, when some of the variables in y_t are unobserved, we introduce the matrices S_t, where $\tilde{y}_t = S_t' y_t$ includes all the observed values of y_t and none (NaN) of the unobserved. Accordingly, we have that for $\tilde{H}_t = HS_t$ the measurement equations are given by

$$\tilde{y}_t = \tilde{H}_t' \xi_t, \quad t = T - 1, T. \tag{B.3}$$

We are now equipped with the state-space system and can proceed to setup a suitable Kalman filter, updater and smoother; see, e.g., Durbin and Koopman (2012) for details.

To this end, note that for $t = 1, \ldots, T - 2$ the vector ξ_t is observed and determined as

$$\xi_t = KX_t,$$

where

$$K = \begin{bmatrix} 0 & S' & -S' & 0 \\ 1 & 0 & 0 & 0 \\ 0 & I_n & 0 & 0 \\ 0 & 0 & I_n & 0 \\ 0 & 0 & 0 & I_{n(p-2)} \end{bmatrix},$$

is an $(np + s + 1) \times (np + 1)$ matrix. Notice that the case $p = 1$ is treated as $p = 2$ with $\Phi_2 = 0$. Letting $\xi_{t|t-1}$ denote the standard Kalman filter projection of ξ_t based on the data up to period $t - 1$ and taking the parameters as fixed, it follows that

$$\xi_{t|t-1} = F\xi_{t-1}, \quad t = 1, \ldots, T - 2.$$

Similarly, let $P_{t|t-1}$ denote the covariance matrix of $\xi_{t|t-1}$ with the consequence that

$$P_{t|t-1} = C\Omega C', \quad t = 1, \ldots, T - 2.$$

Furthermore, it holds that $\xi_{t|t} = \xi_t$ and $P_{t|t} = 0$ for the same time periods. It can also be seen that the covariance matrix of y_t given the data up to period $t - 1$ is given by

$$\Sigma_{y,t|t-1} = H'C\Omega C'H = \Omega, \quad t = 1, \ldots, T - 2.$$

Unless one is interested in computing the likelihood function, there is no need to run this Kalman filter recursively. Rather, the above filter equations are merely used as input for the interesting time periods $t = T - 1, T, T + 1, \ldots, T + h$, where we shall perform backcasting, nowcasting and forecasting taking the ragged edge into account.

For $t = T-1, T$, it no longer holds that all elements of y_t are observed. As mentioned above, the observations are instead given by $\tilde{y}_t$. For $t = T-1$, the filtering equations are:

$$\xi_{T-1|T-2} = F\xi_{T-2|T-2} = F\xi_{T-2}, \tag{B.4}$$

$$P_{T-1|T-2} = C\Omega C', \tag{B.5}$$

$$\tilde{y}_{T-1|T-2} = \tilde{H}'_{T-1}\xi_{T-1|T-2}, \tag{B.6}$$

$$\Sigma_{\tilde{y},T-1|T-2} = \tilde{H}'_{T-1}P_{T-1|T-2}\tilde{H}_{T-1} = S'_{T-1}\Omega S_{T-1}, \tag{B.7}$$

where $\Sigma_{\tilde{y},t|t-1}$ denotes the one-step-ahead forecast error covariance matrix of $\tilde{y}_t$. Concerning the update equations, these are given by

$$\xi_{T-1|T-1} = \xi_{T-1|T-2} + P_{T-1|T-2}\tilde{H}_{T-1}\Sigma_{\tilde{y},T-1|T-2}^{-1}(\tilde{y}_{T-1} - \tilde{y}_{T-1|T-2}), \tag{B.8}$$

$$P_{T-1|T-1} = P_{T-1|T-2} - P_{T-1|T-2}\tilde{H}_{T-1}\Sigma_{\tilde{y},T-1|T-2}^{-1}\tilde{H}'_{T-1}P_{T-1|T-2}. \tag{B.9}$$

Notice that $P_{T-1|T-1}$ is not a zero matrix and that its rank is expected to be $n - \text{rank}(S_{T-1})$.

Turning to $t = T$, the filtering equations are:

$$\xi_{T|T-1} = F\xi_{T-1|T-1}, \tag{B.10}$$

$$P_{T|T-1} = FP_{T-1|T-1}F' + C\Omega C', \tag{B.11}$$

$$\tilde{y}_{T|T-1} = \tilde{H}'_T\xi_{T|T-1}, \tag{B.12}$$

$$\Sigma_{\tilde{y},T|T-1} = \tilde{H}'_T P_{T|T-1}\tilde{H}_T, \tag{B.13}$$

while the update equations are given by:

$$\xi_{T|T} = \xi_{T|T-1} + P_{T|T-1}\tilde{H}_T\Sigma_{\tilde{y},T|T-1}^{-1}(\tilde{y}_T - \tilde{y}_{T|T-1}) = \xi_{T|T-1} + P_{T|T-1}r_{T|T}, \tag{B.14}$$

$$P_{T|T} = P_{T|T-1} - P_{T|T-1}\tilde{H}_T\Sigma_{\tilde{y},T|T-1}^{-1}\tilde{H}'_T P_{T|T-1} = P_{T|T-1} - P_{T|T-1}N_{T|T}P_{T|T-1}. \tag{B.15}$$

These equations define the vector $r_{T|T}$ and the matrix $N_{T|T}$ which are used as input for Kalman smoothing.

While the smooth estimates for period T are equal to the update estimates for T, we are also interested in the smooth estimates of the state variables and the corresponding covariance matrix for period $T-1$. These are determined from

$$\xi_{T-1|T} = \xi_{T-1|T-2} + P_{T-1|T-2}r_{T-1|T}, \tag{B.16}$$

$$P_{T-1|T} = P_{T-1|T-2} - P_{T-1|T-2}N_{T-1|T}P_{T-1|T-2}, \tag{B.17}$$

where

$$r_{T-1|T} = \tilde{H}_{T-1}\Sigma_{\tilde{y},T-1|T-2}^{-1}(\tilde{y}_{T-1} - \tilde{y}_{T-1|T-2}) + (F - K_{T-1}\tilde{H}'_{T-1})'r_{T|T},$$

$$K_{T-1} = FP_{T-1|T-2}\tilde{H}_{T-1}\Sigma_{\tilde{y},T-1|T-2}^{-1},$$

$$N_{T-1|T} = \tilde{H}_{T-1}\Sigma_{\tilde{y},T-1|T-2}^{-1}\tilde{H}'_{T-1} + (F - K_{T-1}\tilde{H}'_{T-1})'N_{T|T}(F - K_{T-1}\tilde{H}'_{T-1}).$$

The smooth estimates for period T are used for the nowcasts, while the smooth estimates for period $T-1$ are similarly employed for the backcasts.

Define the $(np + s + 1) \times s$ matrix G such that

$$G' = \begin{bmatrix} I_s & 0_{s,np+1} \end{bmatrix},$$

with the consequence that $z_t = G'\xi_t$. The backcast $(T-1)$ and nowcast (T) of z_t are therefore given by

$$z_{t|T} = G'\xi_{t|T}, \quad t = T-1, T, \tag{B.18}$$

while the covariance matrices are

$$\Sigma_{z,t|T} = G'P_{t|T}G. \tag{B.19}$$

We can similarly compute the backcast and nowcast of y_t as

$$y_{t|T} = H'\xi_{t|T}, \tag{B.20}$$

and covariance matrices

$$\Sigma_{y,t|T} = H'P_{t|T}H. \tag{B.21}$$

Forecasting is also straightforward in this setup. Specifically, the forecasts of z_{T+h} and y_{T+h} for $h \geq 1$ are:

$$z_{T+h|T} = G'\xi_{T+h|T}, \tag{B.22}$$

$$y_{T+h|T} = H'\xi_{T+h|T}, \tag{B.23}$$

with covariance matrices

$$\Sigma_{z,T+h|T} = G'P_{T+h|T}G, \tag{B.24}$$

$$\Sigma_{y,T+h|T} = H'P_{T+h|T}H. \tag{B.25}$$

The required forecasts of the state variables and corresponding covariance matrices are determined from

$$\xi_{T+h|T} = F^h\xi_{T|T} = F\xi_{T+h-1|T}, \tag{B.26}$$

$$P_{T+h|T} = F^h P_{T|T}(F')^h + \sum_{j=0}^{h-1} F^j C\Omega C'(F')^j = FP_{T+h-1|T}F' + C\Omega C'. \tag{B.27}$$

To compute the projected value and the covariance matrix for a combination of variables in z_t and y_t, we simply construct a matrix D from the corresponding columns of G and H and use this matrix instead of G or H in the expressions above. We can thereafter proceed to compute the predictive likelihood of the combination of variables as in Warne et al. (2017) and McAdam and Warne (2019), using the actual values of the variables for the normal density with mean and covariance given by the values of these objects for a fixed posterior value of (Φ, Ω, α), and average these likelihoods conditional on the parameters over all the posterior draws.

Appendix C: Data and Transformations

Table C.1 lists the observable variables and expresses their different treatment across the DSGE and BVAR models. The SW model uses seven observables: real GDP, private consumption, total investment, real wages (real compensation per employee), total employment, the GDP deflator, and the short-term nominal interest rate (given by the three-month EURIBOR). For the SWU model there is the addition of the unemployment rate, and for SWFF there is the addition of the financial lending Spread. The BVARs, by contrast, use all nine observables (albeit mostly with a different transformation, see below).

For the DSGE models, the first five observables are transformed into quarterly growth rates by the first difference of their logarithm multiplied by 100, whilst the BVARs instead use the log level of the these variables multiplied by 100. The inflation time series is obtained as the first difference of the log of the GDP deflator times 100 and the same transformation is used in all models. The final three observables (r, u and s) are also defined in the same manner across the DSGEs and BVARs with the interest rate and spread being expressed in annualised percentage terms. As in Smets et al. (2014), we only consider data from 1979Q4, such that the growth rates are available from 1980Q1. All variables are available at quarterly frequency, except for the unemployment and the interest rate series which exist at a monthly frequency.

The euro area real-time database (RTD), on which these models are estimated and assessed, is described in Giannone et al. (2012). To extend the data back in time, we follow Smets et al. (2014) and McAdam and Warne (2019) and link the real-time data to various updates from the area-wide model (AWM) database; see Fagan, Henry, and Mestre (2005). The exception is the spread which is not included in the RTD vintages nor in the AWM updates.

The RTD covers vintages starting in January 2001 and has been available on a monthly basis until early 2015 when the vintage frequency changed from three to two per quarter. We consider the vintages from 2001Q1–2014Q4 for estimation and forecasting. For more detailed information, see McAdam and Warne (2019).

TABLE C.1: Observables used in the DSGE and BVAR models.

Variable	Symbol	DSGEs:	SW	SWU	SWFF	BVARS:
			Observed Variables			
real GDP (log)	y	$100 \times \Delta y_t$	$\checkmark$	$\checkmark$	$\checkmark$	$100 \times y_t$
real private consumption (log)	c	$100 \times \Delta c_t$	$\checkmark$	$\checkmark$	$\checkmark$	$100 \times c_t$
real total investment (log)	i	$100 \times \Delta i_t$	$\checkmark$	$\checkmark$	$\checkmark$	$100 \times i_t$
real wages (log)	w	$100 \times \Delta w_t$	$\checkmark$	$\checkmark$	$\checkmark$	$100 \times w_t$
total employment (log)	e	$100 \times \Delta e_t$	$\checkmark$	$\checkmark$	$\checkmark$	$100 \times e_t$
GDP deflator inflation (log, quarterly)	π	$100 \times \pi_t$	$\checkmark$	$\checkmark$	$\checkmark$	$100 \times \pi_t$
short-term nominal interest rate (%)	r	r_t	$\checkmark$	$\checkmark$	$\checkmark$	r_t
unemployment rate (%)	u	$100 \times u_t$		$\checkmark$		$100 \times u_t$
spread (%)	s	s_t			$\checkmark$	s_t

Table D.1: Amisano-Giacomini weighted likelihood ratio tests for the equality of the average log predictive scores of the BVAR SoC model versus the DSGE models and percentile values of the statistics for the sample 2001Q1–2014Q4.

	SoC vs. SW			SoC vs. SWFF			SoC vs. SWU		
h	Δy	π	Δy & π	Δy	π	Δy & π	Δy	π	Δy & π
0	-0.31	0.90	-0.29	0.03	3.69	0.98	0.09	-0.50	-0.23
	0.38	0.82	0.38	0.51	1.00	0.84	0.54	0.31	0.41
1	-0.15	0.70	-0.03	0.53	3.65	2.12	0.07	-0.45	-0.04
	0.44	0.75	0.49	0.70	1.00	0.98	0.53	0.33	0.48
2	-0.10	0.03	-0.07	0.64	3.05	2.20	0.01	-0.81	-0.13
	0.46	0.51	0.47	0.74	1.00	0.99	0.50	0.21	0.45
3	0.06	0.17	0.10	0.85	2.65	2.24	0.06	-0.56	-0.05
	0.52	0.57	0.54	0.80	1.00	0.99	0.52	0.29	0.48
4	0.06	0.21	0.14	0.90	2.09	2.03	-0.02	-0.26	-0.03
	0.52	0.58	0.55	0.82	0.98	0.98	0.49	0.40	0.49
5	0.04	-0.07	0.06	1.00	1.50	1.82	-0.15	-0.34	-0.14
	0.52	0.47	0.52	0.84	0.93	0.96	0.44	0.37	0.44
6	0.06	0.41	0.31	1.21	1.11	1.89	-0.21	0.29	0.01
	0.52	0.66	0.62	0.89	0.87	0.97	0.42	0.61	0.50
7	0.02	0.35	0.21	1.21	0.20	1.27	-0.24	0.44	0.00
	0.51	0.64	0.58	0.89	0.58	0.90	0.40	0.67	0.50
8	0.04	0.40	0.18	1.43	-0.44	1.02	-0.17	0.55	0.06
	0.52	0.65	0.57	0.92	0.33	0.85	0.43	0.71	0.52

Notes: Real GDP growth is denoted by Δy and inflation by π. The test statistics have been computed with equal weights and using the Bartlett kernel for the HAC estimator (Newey and West, 1987). Following Amisano and Giacomini (2007) we use a short truncation lag, but rather than using their selection of zero lags we use one lag. The percentile value of the test statistic, taken from a standard normal distribution, is shown below the test statistics, where large percentile values favor the first (SoC) model of the test and small percentile values the second model.

TABLE D.2: Amisano-Giacomini weighted likelihood ratio tests for the equality of the average log predictive scores of the BVAR PLR model versus the DSGE models and percentile values of the statistics for the sample 2001Q1–2014Q4.

h	PLR vs. SW			PLR vs. SWFF			PLR vs. SWU		
	Δy	π	Δy & π	Δy	π	Δy & π	Δy	π	Δy & π
0	−0.19	0.44	−0.29	0.15	3.26	0.96	0.25	−0.97	−0.22
	0.42	0.67	0.39	0.56	1.00	0.83	0.60	0.17	0.41
1	−0.04	0.22	−0.03	0.60	3.42	1.96	0.17	−1.11	−0.03
	0.48	0.59	0.49	0.72	1.00	0.98	0.57	0.13	0.49
2	0.06	−1.34	−0.14	0.73	2.76	1.90	0.16	−2.18	−0.19
	0.52	0.09	0.44	0.77	1.00	0.97	0.56	0.01	0.42
3	0.30	−1.39	0.04	1.00	2.38	1.97	0.28	−2.13	−0.09
	0.62	0.08	0.51	0.84	0.99	0.98	0.61	0.02	0.46
4	0.43	−1.34	0.15	1.22	1.74	1.86	0.32	−1.87	0.00
	0.67	0.09	0.56	0.89	0.96	0.97	0.62	0.03	0.50
5	0.43	−1.93	0.08	1.31	0.86	1.65	0.20	−2.27	−0.11
	0.67	0.03	0.53	0.90	0.81	0.95	0.58	0.01	0.46
6	0.42	−1.45	0.12	1.37	0.09	1.45	0.12	−1.62	−0.11
	0.66	0.07	0.55	0.91	0.54	0.93	0.55	0.05	0.46
7	0.48	−1.41	0.09	1.55	−1.10	1.04	0.15	−1.25	−0.09
	0.68	0.08	0.54	0.94	0.14	0.85	0.56	0.10	0.46
8	0.26	−1.38	−0.08	1.40	−1.85	0.63	0.05	−1.05	−0.16
	0.60	0.08	0.47	0.92	0.03	0.74	0.21	0.15	0.44

NOTES: See Table D.1.

TABLE D.3: Amisano-Giacomini weighted likelihood ratio tests for the equality of the average log predictive scores of the BVAR SoC model versus the PLR model and percentile values of the statistics for the sample 2001Q1–2014Q4.

h	SoC vs. PLR		
	Δy	π	Δy & π
0	-1.44	0.86	-0.05
	0.07	0.80	0.48
1	-0.97	0.94	-0.02
	0.17	0.83	0.49
2	-1.05	2.12	0.42
	0.15	0.98	0.66
3	-1.49	2.06	0.27
	0.07	0.98	0.61
4	-2.30	1.92	-0.14
	0.01	0.97	0.44
5	-2.10	2.19	-0.10
	0.02	0.98	0.46
6	-1.46	2.53	0.47
	0.07	0.99	0.68
7	-2.14	2.76	0.50
	0.02	1.00	0.69
8	-1.00	2.66	0.99
	0.16	1.00	0.84

TABLE D.4: Amisano-Giacomini weighted likelihood ratio tests for the equality of the average log predictive scores of two DSGE models and percentile values of the statistics for the sample 2001Q1–2014Q4.

	SW vs. SWFF			SW vs. SWU			SWFF vs. SWU		
h	Δy	π	Δy & π	Δy	π	Δy & π	Δy	π	Δy & π
0	2.74	4.02	4.36	1.07	-3.06	0.41	0.12	-4.05	-2.93
	1.00	1.00	1.00	0.86	0.00	0.66	0.55	0.00	0.00
1	3.07	4.03	4.61	4.06	-3.49	-0.08	-2.10	-4.12	-4.50
	1.00	1.00	1.00	1.00	0.00	0.47	0.02	0.00	0.00
2	2.83	3.71	4.47	1.56	-3.27	-0.92	-1.90	-3.84	-4.34
	1.00	1.00	1.00	0.94	0.00	0.18	0.03	0.00	0.00
3	2.78	3.20	4.10	0.08	-3.05	-1.64	-2.06	-3.39	-4.02
	1.00	1.00	1.00	0.53	0.00	0.05	0.02	0.00	0.00
4	2.75	2.52	3.63	-0.72	-1.96	-1.46	-2.13	-2.69	-3.53
	1.00	0.99	1.00	0.24	0.02	0.07	0.02	0.00	0.00
5	2.84	1.89	3.20	-1.10	-1.07	-1.28	-2.15	-2.00	-3.06
	1.00	0.97	1.00	0.14	0.14	0.10	0.02	0.02	0.00
6	3.00	1.03	2.64	-1.18	-0.59	-1.24	-2.20	-1.12	-2.64
	1.00	0.85	1.00	0.12	0.28	0.11	0.01	0.13	0.00
7	3.03	-0.06	1.82	-1.18	0.45	-0.90	-2.25	0.13	-1.85
	1.00	0.48	0.96	0.12	0.67	0.18	0.01	0.55	0.03
8	2.80	-0.74	1.25	-1.02	0.73	-0.49	-2.18	0.84	-1.21
	1.00	0.23	0.89	0.15	0.77	0.31	0.01	0.80	0.11

NOTES: See Table D.1.

TABLE D.5: Summary statistics of the weights on the DSGE and BVAR models for density forecast combination methods of real GDP growth over the vintages 2001Q1–2014Q4.

h	model	DP				SOP				BMA				DMA			
		mean	std	min	max	mean	std	min	max	mean	std	min	max	mean	std	min	max
0	SW	0.189	0.044	0.112	0.299	0.198	0.227	0.000	1.000	0.426	0.429	0.000	0.988	0.232	0.245	0.000	0.805
	SWFF	0.156	0.032	0.106	0.211	0.014	0.052	0.000	0.200	0.043	0.067	0.000	0.209	0.108	0.096	0.000	0.316
	SWU	0.158	0.027	0.114	0.212	0.014	0.052	0.000	0.200	0.049	0.079	0.000	0.249	0.092	0.087	0.000	0.304
	SoC	0.232	0.036	0.168	0.304	0.014	0.052	0.000	0.200	0.132	0.116	0.000	0.371	0.194	0.127	0.000	0.509
	PLR	0.265	0.060	0.170	0.380	0.759	0.275	0.000	1.000	0.350	0.322	0.000	0.801	0.375	0.262	0.000	0.767
1	SW	0.176	0.039	0.111	0.248	0.213	0.274	0.000	1.000	0.384	0.382	0.000	0.931	0.285	0.307	0.000	0.798
	SWFF	0.135	0.033	0.098	0.200	0.018	0.058	0.000	0.200	0.034	0.066	0.000	0.200	0.045	0.065	0.000	0.200
	SWU	0.166	0.035	0.110	0.235	0.018	0.058	0.000	0.200	0.100	0.091	0.000	0.318	0.129	0.107	0.000	0.340
	SoC	0.237	0.038	0.174	0.307	0.018	0.058	0.000	0.200	0.132	0.103	0.000	0.258	0.168	0.113	0.000	0.312
	PLR	0.285	0.066	0.187	0.394	0.733	0.322	0.000	1.000	0.351	0.326	0.000	0.789	0.373	0.297	0.000	0.760
4	SW	0.173	0.020	0.143	0.201	0.031	0.072	0.000	0.200	0.134	0.110	0.000	0.314	0.160	0.131	0.003	0.409
	SWFF	0.152	0.026	0.126	0.200	0.031	0.072	0.000	0.200	0.043	0.075	0.000	0.200	0.054	0.071	0.001	0.200
	SWU	0.194	0.036	0.138	0.290	0.098	0.103	0.000	0.257	0.271	0.294	0.000	0.787	0.245	0.249	0.002	0.780
	SoC	0.218	0.022	0.186	0.271	0.031	0.072	0.000	0.200	0.128	0.082	0.001	0.214	0.176	0.117	0.000	0.392
	PLR	0.265	0.046	0.200	0.340	0.810	0.276	0.200	1.000	0.424	0.336	0.001	0.850	0.365	0.276	0.000	0.747
8	SW	0.188	0.011	0.169	0.206	0.050	0.087	0.000	0.200	0.137	0.101	0.001	0.278	0.162	0.098	0.029	0.361
	SWFF	0.170	0.022	0.132	0.200	0.050	0.087	0.000	0.200	0.065	0.086	0.000	0.200	0.080	0.078	0.005	0.200
	SWU	0.199	0.034	0.160	0.312	0.110	0.107	0.000	0.276	0.234	0.253	0.000	0.763	0.248	0.243	0.017	0.817
	SoC	0.211	0.018	0.173	0.251	0.050	0.087	0.000	0.200	0.130	0.061	0.005	0.200	0.194	0.117	0.000	0.423
	PLR	0.233	0.027	0.189	0.277	0.740	0.326	0.200	1.000	0.434	0.331	0.006	0.883	0.317	0.231	0.000	0.685

NOTES: See Table 4.

TABLE D.6: Summary statistics of the weights on the DSGE and BVAR models for density forecast combination methods of GDP deflator inflation over the vintages 2001Q1–2014Q4.

h	model	DP mean	DP std	DP min	DP max	SOP mean	SOP std	SOP min	SOP max	BMA mean	BMA std	BMA min	BMA max	DMA mean	DMA std	DMA min	DMA max
0	SW	0.191	0.009	0.170	0.204	0.014	0.052	0.000	0.200	0.093	0.050	0.019	0.200	0.120	0.038	0.043	0.200
	SWFF	0.122	0.034	0.086	0.200	0.014	0.052	0.000	0.200	0.025	0.059	0.000	0.200	0.025	0.059	0.000	0.200
	SWU	0.262	0.029	0.194	0.316	0.788	0.224	0.200	1.000	0.557	0.185	0.200	0.858	0.471	0.170	0.200	0.792
	SoC	0.217	0.013	0.196	0.245	0.140	0.153	0.000	0.521	0.198	0.081	0.046	0.388	0.221	0.080	0.058	0.396
	PLR	0.208	0.014	0.179	0.241	0.043	0.084	0.000	0.297	0.127	0.062	0.028	0.257	0.163	0.075	0.041	0.339
1	SW	0.207	0.009	0.188	0.223	0.018	0.058	0.000	0.200	0.164	0.057	0.047	0.244	0.181	0.044	0.071	0.250
	SWFF	0.131	0.033	0.087	0.200	0.018	0.058	0.000	0.200	0.030	0.064	0.000	0.200	0.031	0.064	0.000	0.200
	SWU	0.247	0.024	0.200	0.285	0.850	0.272	0.000	1.000	0.542	0.191	0.200	0.818	0.470	0.167	0.192	0.739
	SoC	0.216	0.015	0.196	0.258	0.096	0.181	0.000	1.000	0.160	0.076	0.045	0.392	0.184	0.080	0.060	0.430
	PLR	0.199	0.011	0.178	0.221	0.018	0.058	0.000	0.200	0.104	0.054	0.018	0.200	0.133	0.060	0.028	0.274
4	SW	0.214	0.014	0.183	0.241	0.584	0.401	0.000	1.000	0.376	0.100	0.200	0.526	0.276	0.076	0.133	0.420
	SWFF	0.183	0.034	0.125	0.282	0.031	0.072	0.000	0.200	0.054	0.076	0.000	0.200	0.125	0.127	0.000	0.563
	SWU	0.210	0.009	0.189	0.230	0.198	0.338	0.000	1.000	0.316	0.119	0.200	0.558	0.247	0.047	0.153	0.371
	SoC	0.208	0.019	0.168	0.250	0.156	0.172	0.000	0.658	0.195	0.110	0.017	0.452	0.233	0.090	0.053	0.439
	PLR	0.185	0.011	0.165	0.200	0.031	0.072	0.000	0.200	0.059	0.068	0.002	0.200	0.119	0.051	0.038	0.204
8	SW	0.209	0.018	0.173	0.242	0.622	0.314	0.200	1.000	0.355	0.175	0.103	0.686	0.253	0.113	0.039	0.476
	SWFF	0.214	0.043	0.161	0.318	0.170	0.220	0.000	0.682	0.237	0.221	0.008	0.835	0.272	0.213	0.033	0.852
	SWU	0.201	0.012	0.167	0.224	0.050	0.087	0.000	0.200	0.195	0.064	0.042	0.323	0.201	0.062	0.039	0.308
	SoC	0.194	0.013	0.164	0.213	0.108	0.114	0.000	0.421	0.145	0.082	0.006	0.288	0.167	0.068	0.034	0.302
	PLR	0.182	0.012	0.158	0.200	0.050	0.087	0.000	0.200	0.069	0.082	0.000	0.200	0.108	0.058	0.023	0.200

NOTES: See Table 4.

Table D.7: Log predictive scores for nowcasts and one-to eight-quarter-ahead forecasts of four combination methods based on different information lags over the vintages 2001Q1–2014Q4.

h	l	Real GDP growth				Inflation			
		SOP	DP	BMA	DMA	SOP	DP	BMA	DMA
0	1	−39.97	−40.36	−47.74	−39.84	12.30	10.76	11.99	11.78
	4	−52.36	−41.88	−57.45	−54.37	12.61	10.74	12.01	11.78
1	1	−59.59	−49.88	−65.64	−61.16	10.14	8.06	9.50	9.20
	4	−61.19	−50.46	−66.39	−63.14	10.49	7.97	9.69	9.52
2	1	−61.56	−52.29	−67.87	−61.51	6.47	3.40	5.41	4.77
	4	−62.83	−52.75	−67.85	−62.64	6.11	3.28	5.10	4.71
3	1	−58.85	−53.01	−65.75	−61.24	1.62	0.49	1.09	0.04
	4	−60.48	−53.44	−66.84	−62.68	1.52	−0.50	0.74	−0.49
4	1	−56.32	−52.24	−62.04	−58.36	−2.13	−3.10	−2.53	−3.13
	4	−57.25	−52.52	−62.43	−59.18	−1.83	−3.13	−2.54	−3.07
5	1	−55.33	−51.20	−59.86	−55.71	−5.41	−5.32	−5.12	−5.47
	4	−55.98	−51.33	−58.61	−55.60	−6.10	−5.39	−5.44	−5.71
6	1	−54.81	−50.88	−57.05	−54.12	−7.78	−6.59	−7.58	−7.49
	4	−55.57	−50.86	−55.75	−53.44	−8.28	−6.63	−7.72	−7.47
7	1	−53.40	−49.86	−53.87	−51.40	−10.13	−8.09	−9.52	−9.14
	4	−54.11	−49.82	−52.63	−50.80	−9.74	−7.92	−8.85	−8.69
8	1	−53.53	−48.63	−52.36	−49.56	−11.02	−9.62	−10.49	−10.28
	4	−54.19	−48.68	−51.91	−49.73	−11.40	−9.45	−9.40	−9.04

TABLE D.8: Log predictive scores of real GDP growth for nowcasts and one-to eight-quarter-ahead forecasts of five combination methods based on different initializations over the vintages 2001Q1–2014Q4.

h	Initial weights	FW	SOP	DP	BMA	DMA
0	SWFF zero	−39.99	−52.41	−41.20	−57.25	−51.76
	Equal	−41.69	−52.36	−41.88	−57.45	−54.37
1	SWFF zero	−49.01	−61.02	−48.84	−65.93	−61.68
	Equal	−51.85	−61.19	−50.46	−66.39	−63.14
2	SWFF zero	−51.04	−62.60	−50.94	−67.31	−60.58
	Equal	−53.93	−62.83	−52.75	−67.85	−62.64
3	SWFF zero	−51.63	−60.15	−51.66	−66.24	−60.84
	Equal	−54.46	−60.48	−53.44	−66.84	−62.68
4	SWFF zero	−50.77	−56.82	−50.77	−61.78	−57.64
	Equal	−53.51	−57.25	−52.52	−62.43	−59.18
5	SWFF zero	−49.53	−55.54	−49.56	−57.94	−54.10
	Equal	−52.19	−55.98	−51.33	−58.61	−55.60
6	SWFF zero	−49.05	−55.09	−49.19	−55.10	−52.26
	Equal	−51.54	−55.58	−50.86	−55.75	−53.44
7	SWFF zero	−48.03	−53.57	−48.18	−52.01	−49.75
	Equal	−50.49	−54.11	−49.82	−52.63	−50.80
8	SWFF zero	−46.80	−53.62	−47.06	−51.31	−48.77
	Equal	−49.20	−54.19	−48.67	−51.91	−49.73

NOTES: See Table 6 for details.

Table D.9: Log predictive scores of GDP deflator inflation for nowcasts and one-to eight-quarter-ahead forecasts of five combination methods based on different initializations over the vintages 2001Q1–2014Q4.

h	Initial weights	FW	SOP	DP	BMA	DMA
0	SWFF zero	12.45	12.82	12.15	12.45	12.17
	Equal	9.66	12.61	10.74	12.01	11.78
1	SWFF zero	10.12	10.75	9.68	10.15	10.01
	Equal	6.74	10.49	7.97	9.69	9.52
2	SWFF zero	5.22	6.32	4.77	5.56	5.45
	Equal	2.47	6.11	3.28	5.10	4.71
3	SWFF zero	1.39	1.75	0.44	1.19	0.92
	Equal	-0.68	1.52	-0.50	0.74	-0.49
4	SWFF zero	-1.66	-1.61	-2.56	-2.10	-1.77
	Equal	-2.97	-1.83	-3.13	-2.54	-3.07
5	SWFF zero	-4.55	-5.88	-5.27	-5.05	-4.88
	Equal	-5.16	-6.10	-5.39	-5.44	-5.71
6	SWFF zero	-6.38	-8.13	-6.88	-7.52	-7.14
	Equal	-6.40	-8.28	-6.63	-7.72	-7.47
7	SWFF zero	-8.62	-9.63	-8.72	-9.45	-9.06
	Equal	-7.76	-9.74	-7.92	-8.85	-8.69
8	SWFF zero	-10.92	-11.32	-9.75	-11.93	-11.13
	Equal	-9.52	-11.40	-9.45	-9.40	-9.04

NOTES: See Table 6 for details.

FIGURE D.1: Recursive estimates of the average log predictive scores of real GDP growth in deviation from the recursive estimates of the average log scores of the dynamic prediction pool covering the vintages 2001Q1–2014Q4.
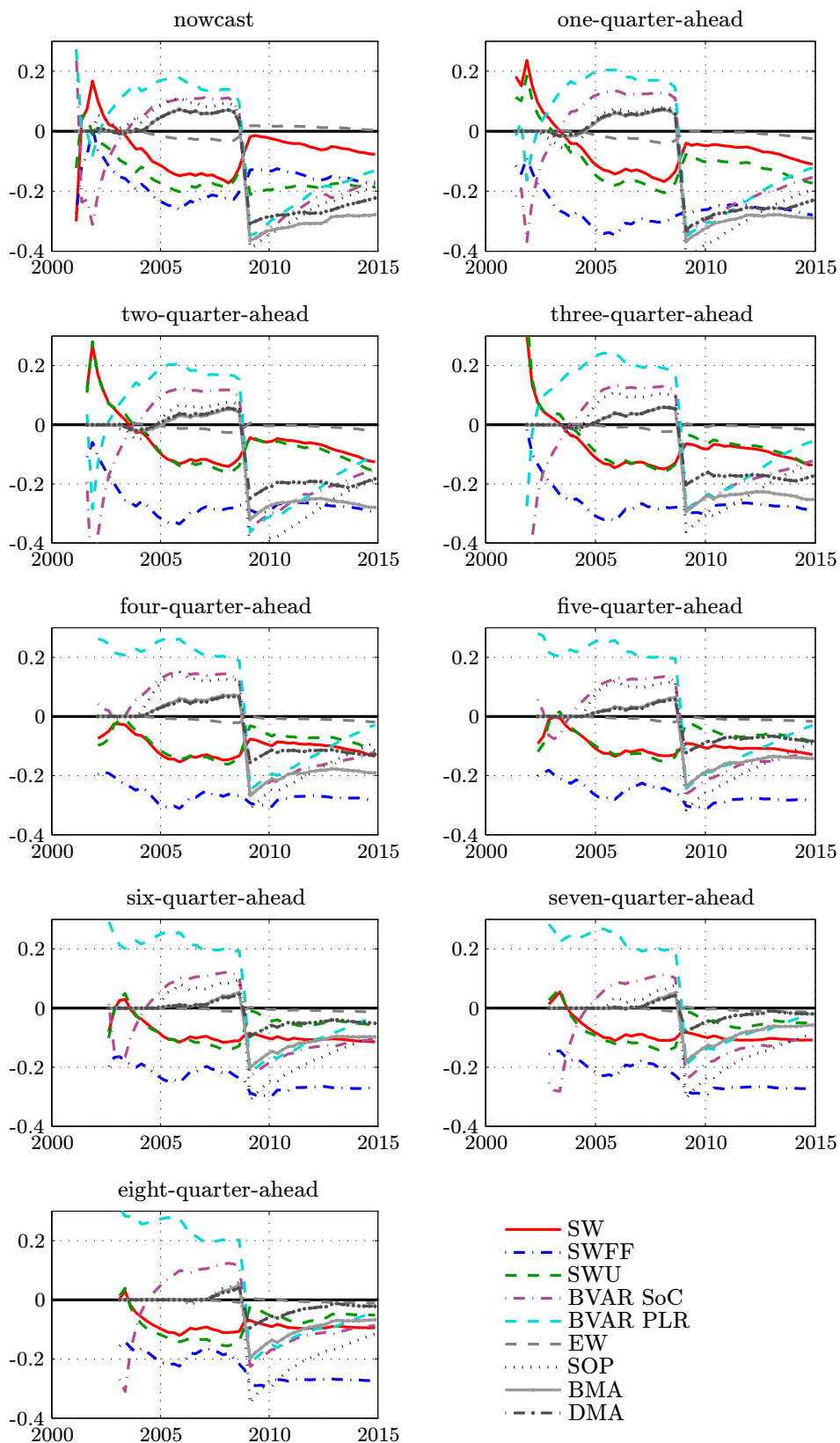
FIGURE D.2: Recursive estimates of the average log predictive scores of GDP deflator inflation in deviation from the recursive estimates of the average log scores of the dynamic prediction pool covering the vintages 2001Q1–2014Q4.
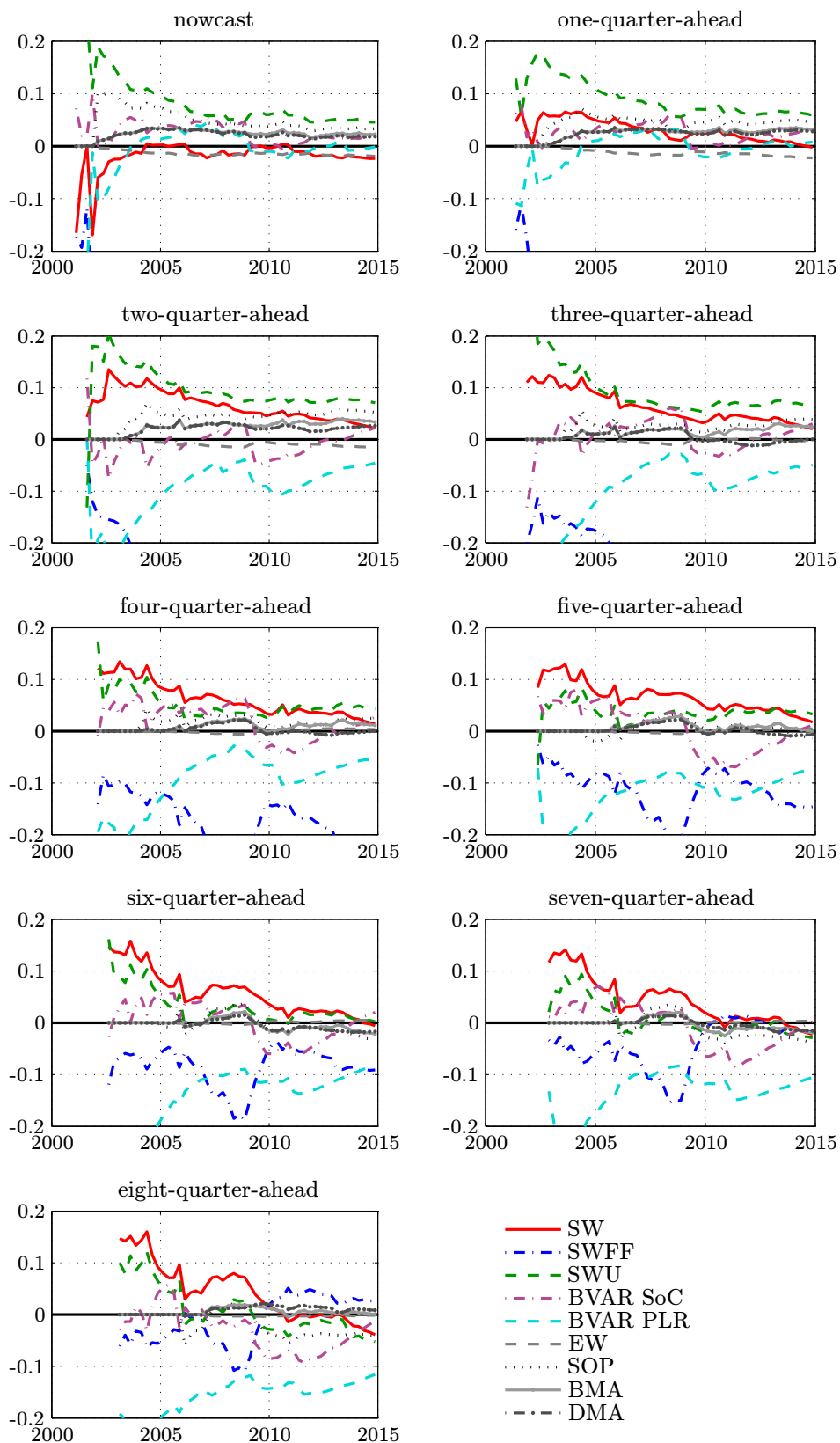
FIGURE D.3: Posterior estimates of the model weights for the dynamic prediction pool of real GDP growth covering the vintages 2001Q1–2014Q4.
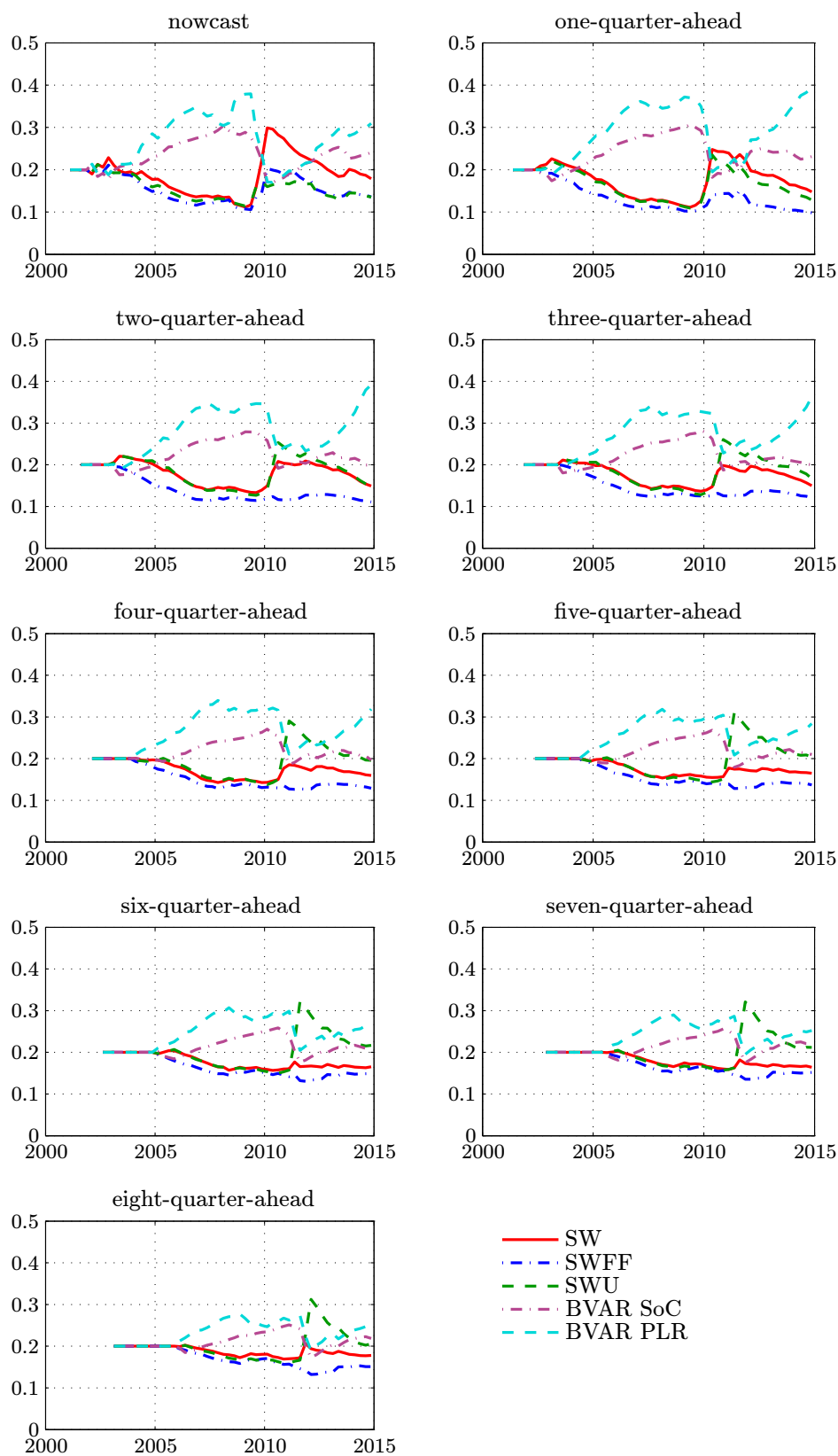
FIGURE D.4: Posterior estimates of the model weights for the dynamic prediction pool of GDP deflator inflation covering the vintages 2001Q1–2014Q4.
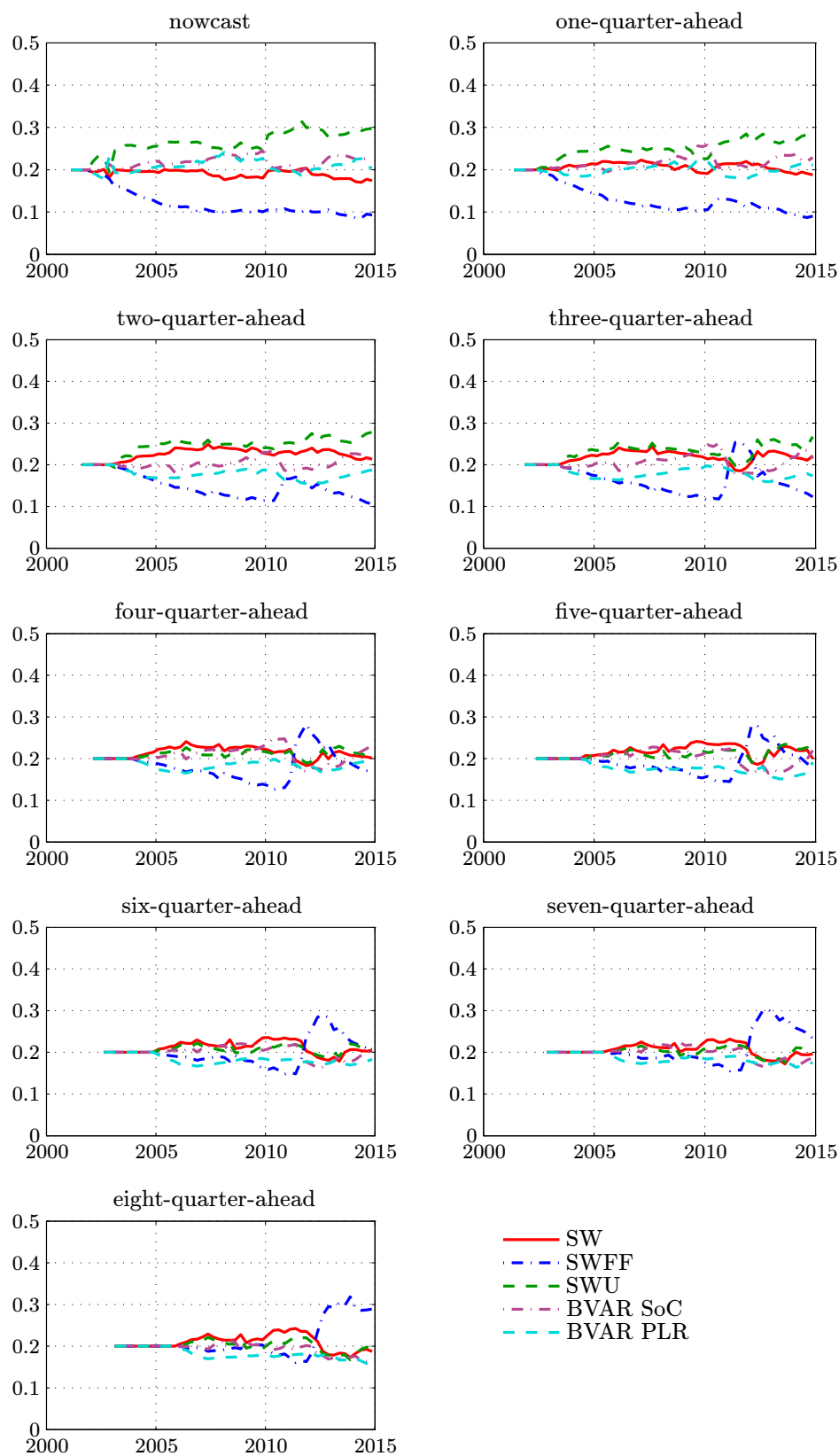
FIGURE D.5: Recursive estimates of the model weights for the static prediction pool of joint real GDP growth and GDP deflator inflation covering the vintages 2001Q1–2014Q4.
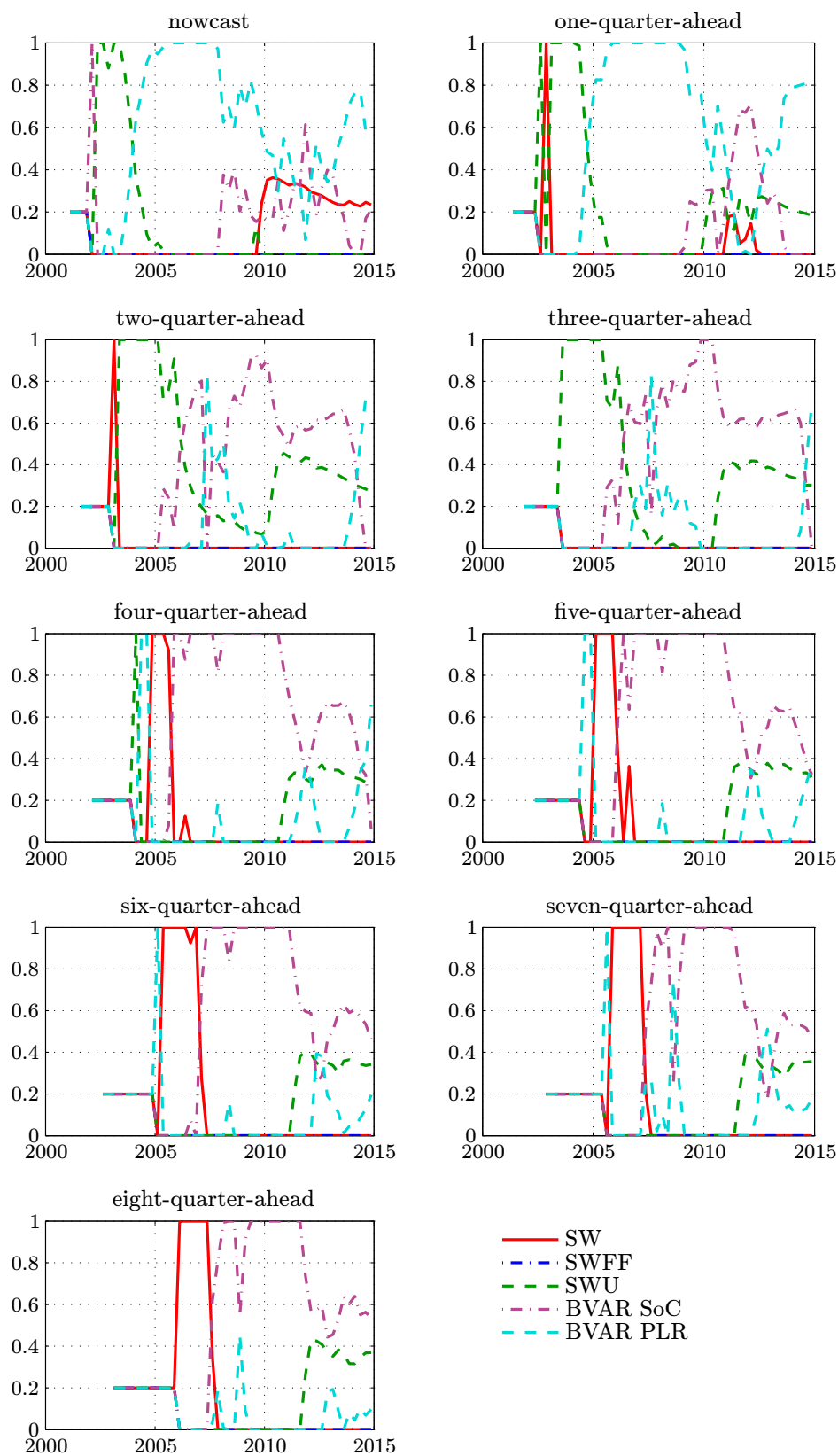
FIGURE D.6: Recursive estimates of the model weights for the static prediction pool of real GDP growth covering the vintages 2001Q1–2014Q4.
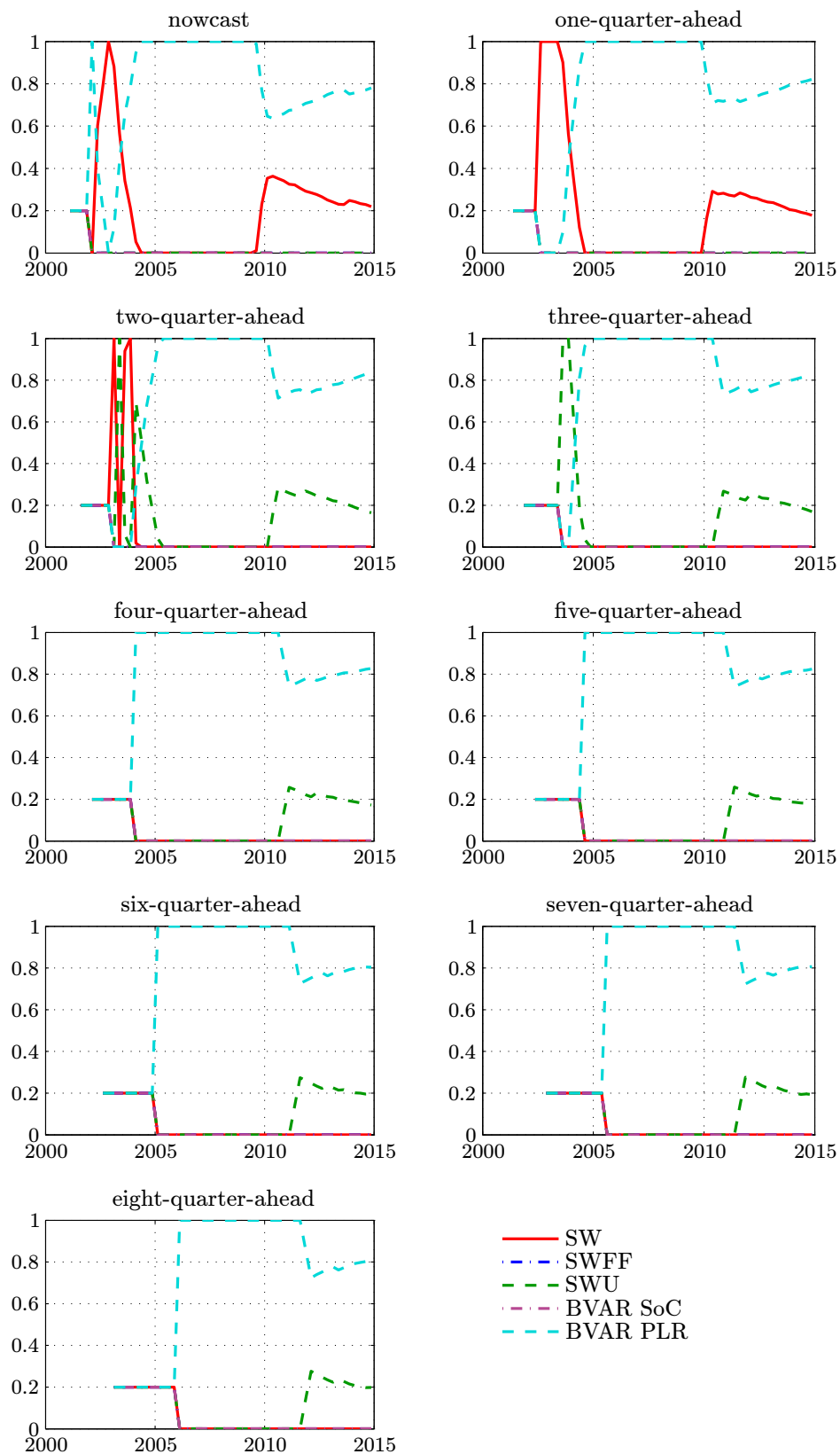
FIGURE D.7: Recursive estimates of the model weights for the static prediction pool of GDP deflator inflation covering the vintages 2001Q1–2014Q4.
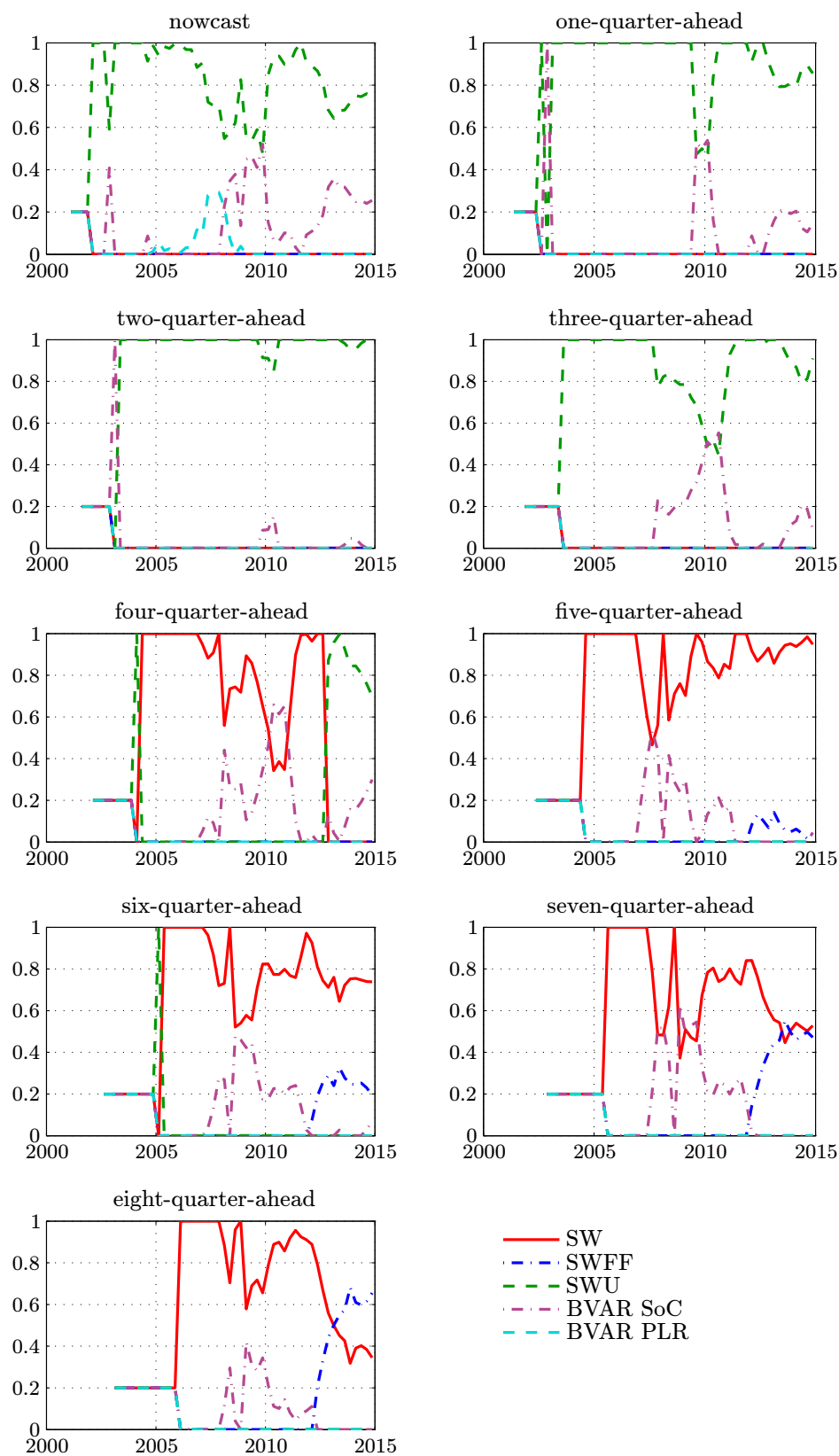
FIGURE D.8: Estimates of the model weights for Bayesian model averaging of joint real GDP growth and GDP deflator inflation covering the vintages 2001Q1–2014Q4.
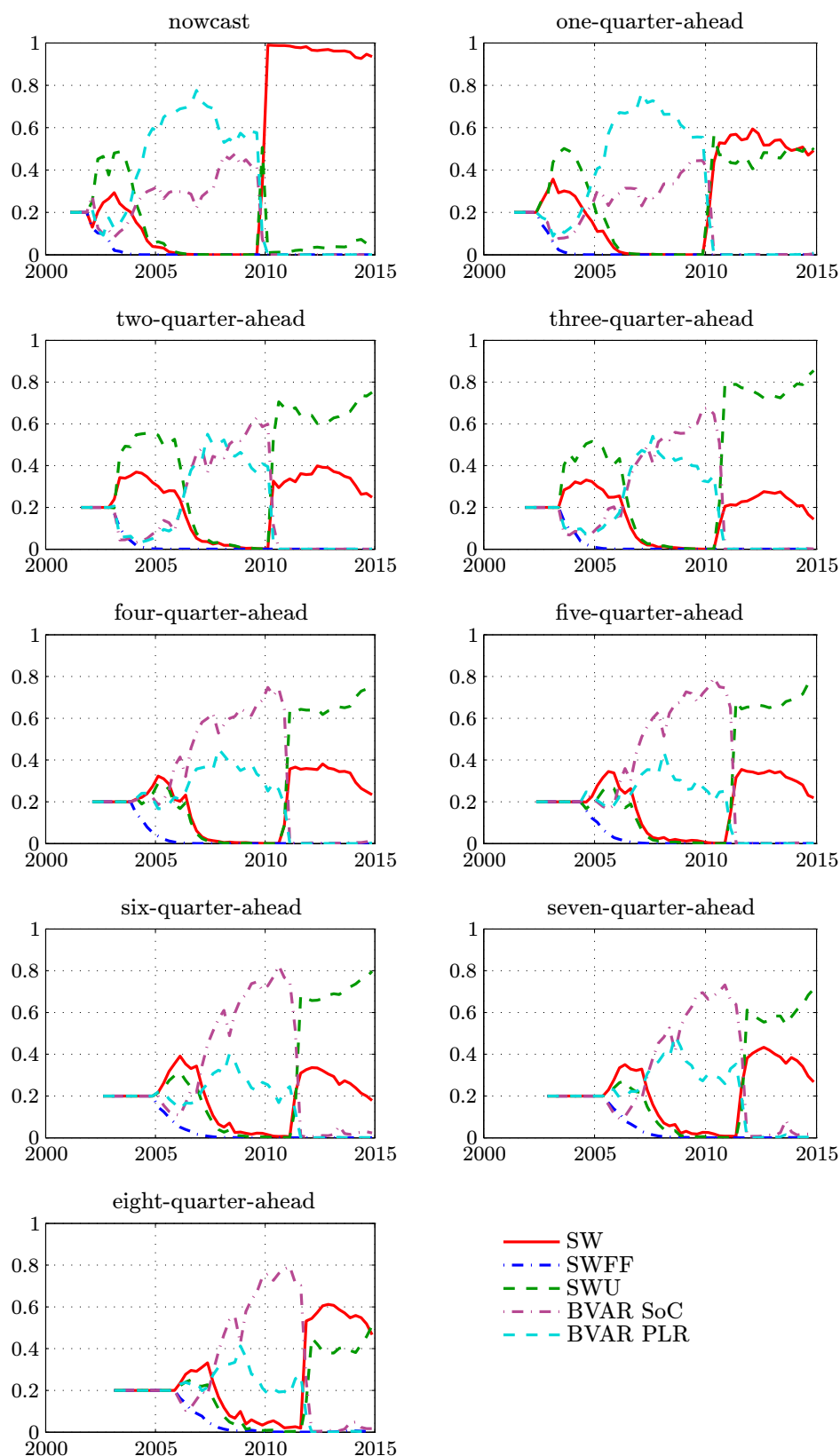
FIGURE D.9: Estimates of the model weights for Bayesian model averaging of real GDP growth covering the vintages 2001Q1–2014Q4.
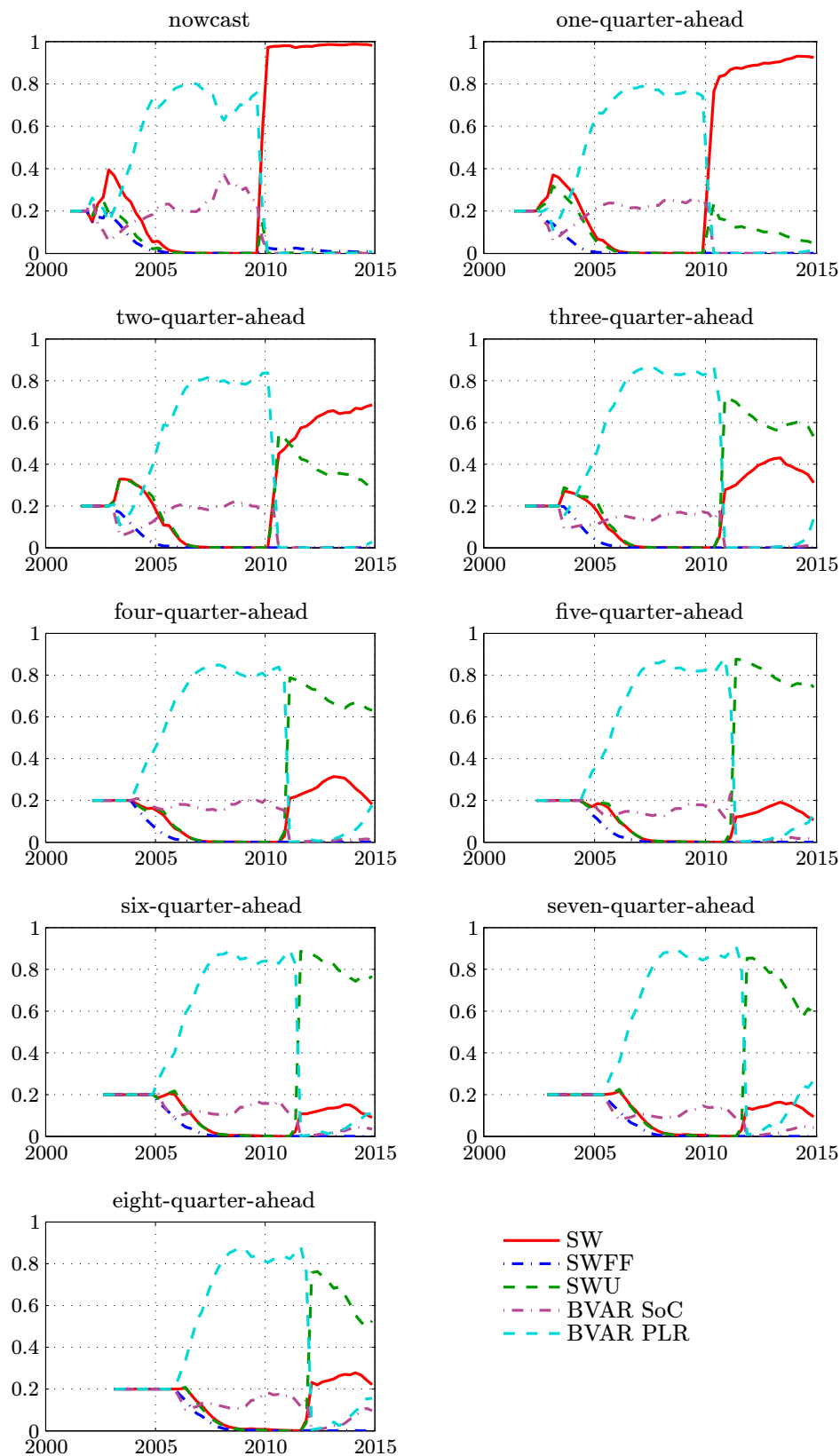
FIGURE D.10: Estimates of the model weights for Bayesian model averaging of GDP deflator inflation covering the vintages 2001Q1–2014Q4.
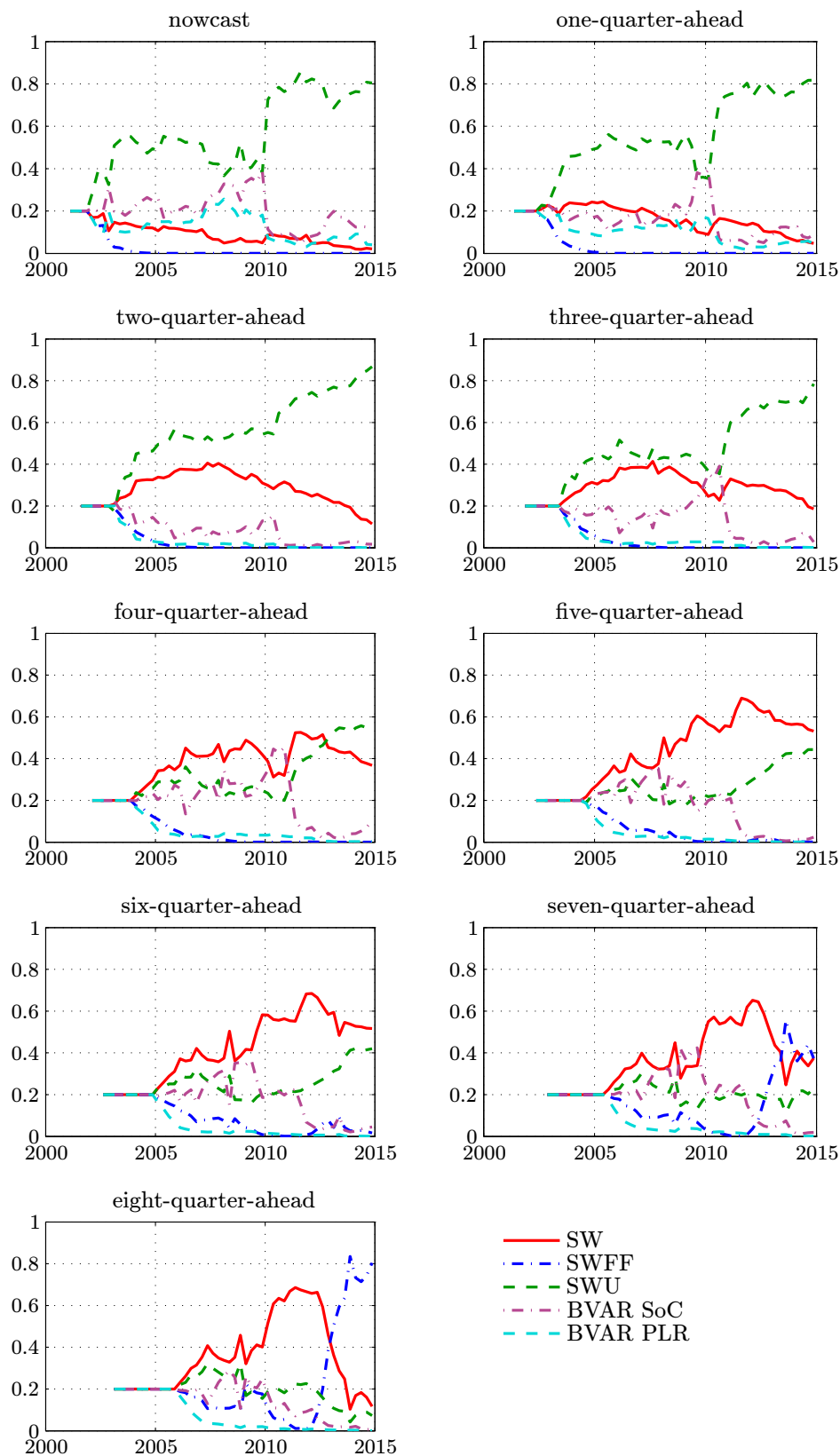
FIGURE D.11: Posterior estimates of the model weights for dynamic model averaging of joint real GDP growth and GDP deflator inflation covering the vintages 2001Q1–2014Q4.
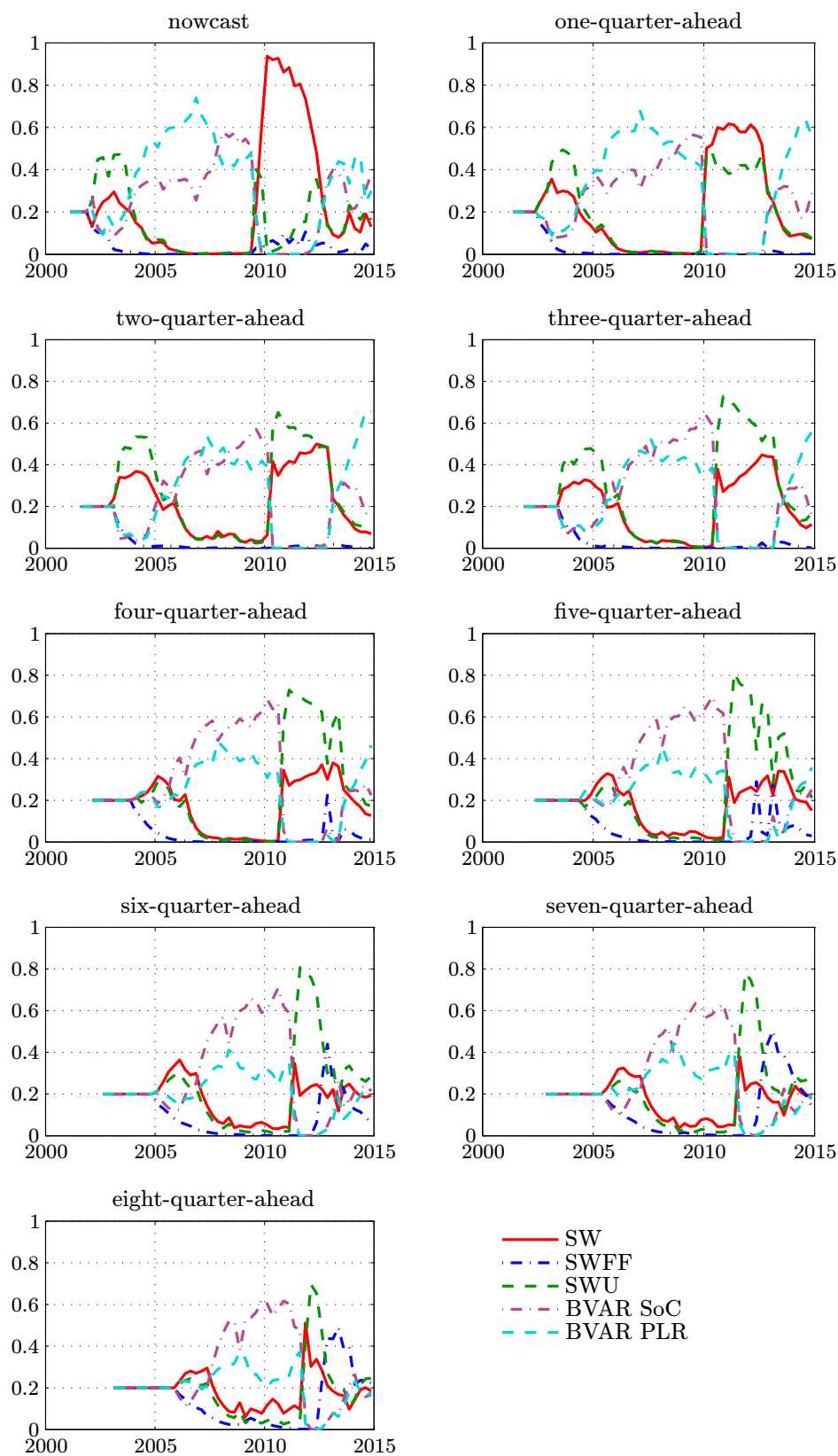
FIGURE D.12: Posterior estimates of the model weights for dynamic model averaging of real GDP growth covering the vintages 2001Q1–2014Q4.
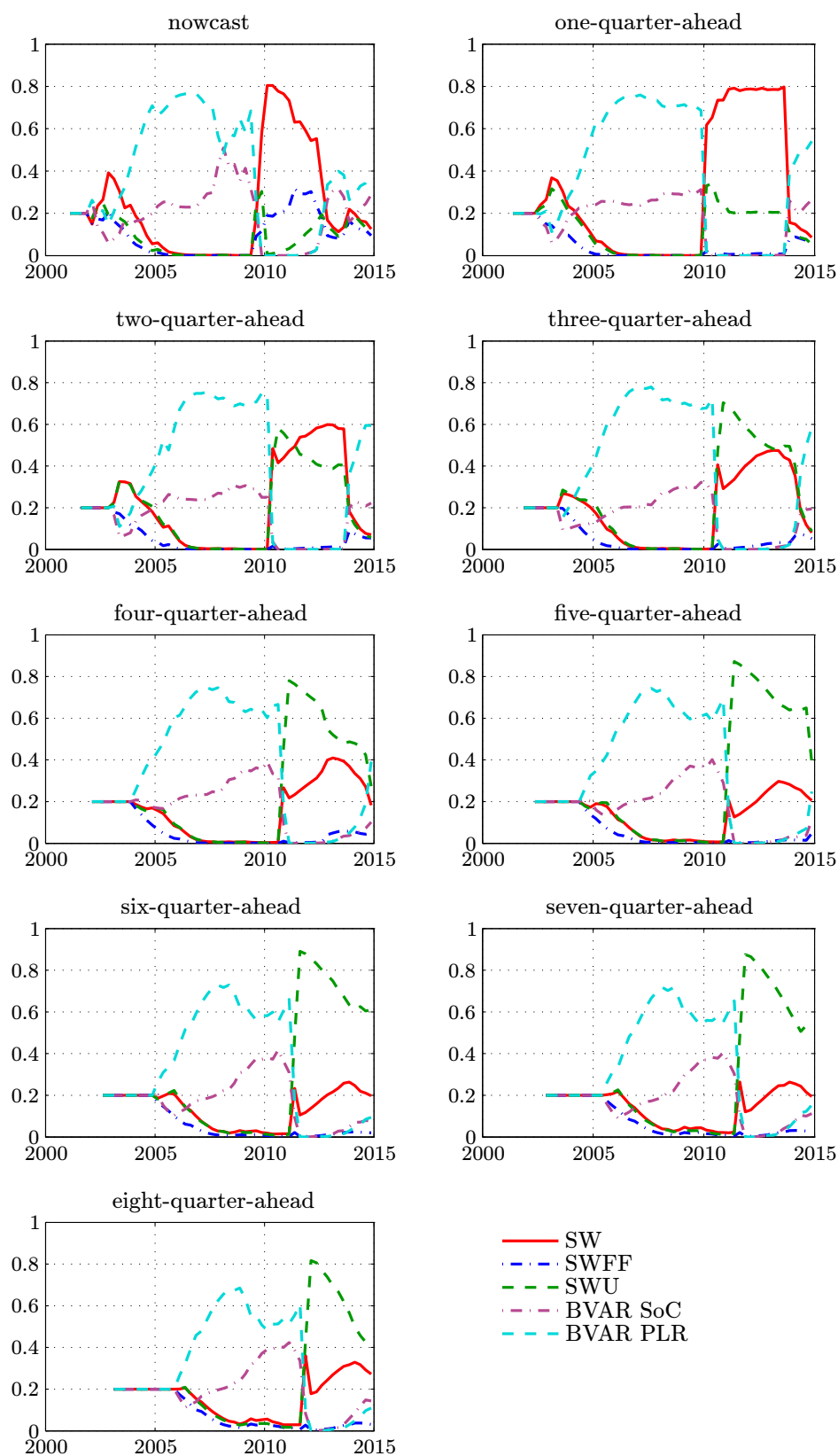
FIGURE D.13: Posterior estimates of the model weights for dynamic model averaging of GDP deflator inflation covering the vintages 2001Q1–2014Q4.
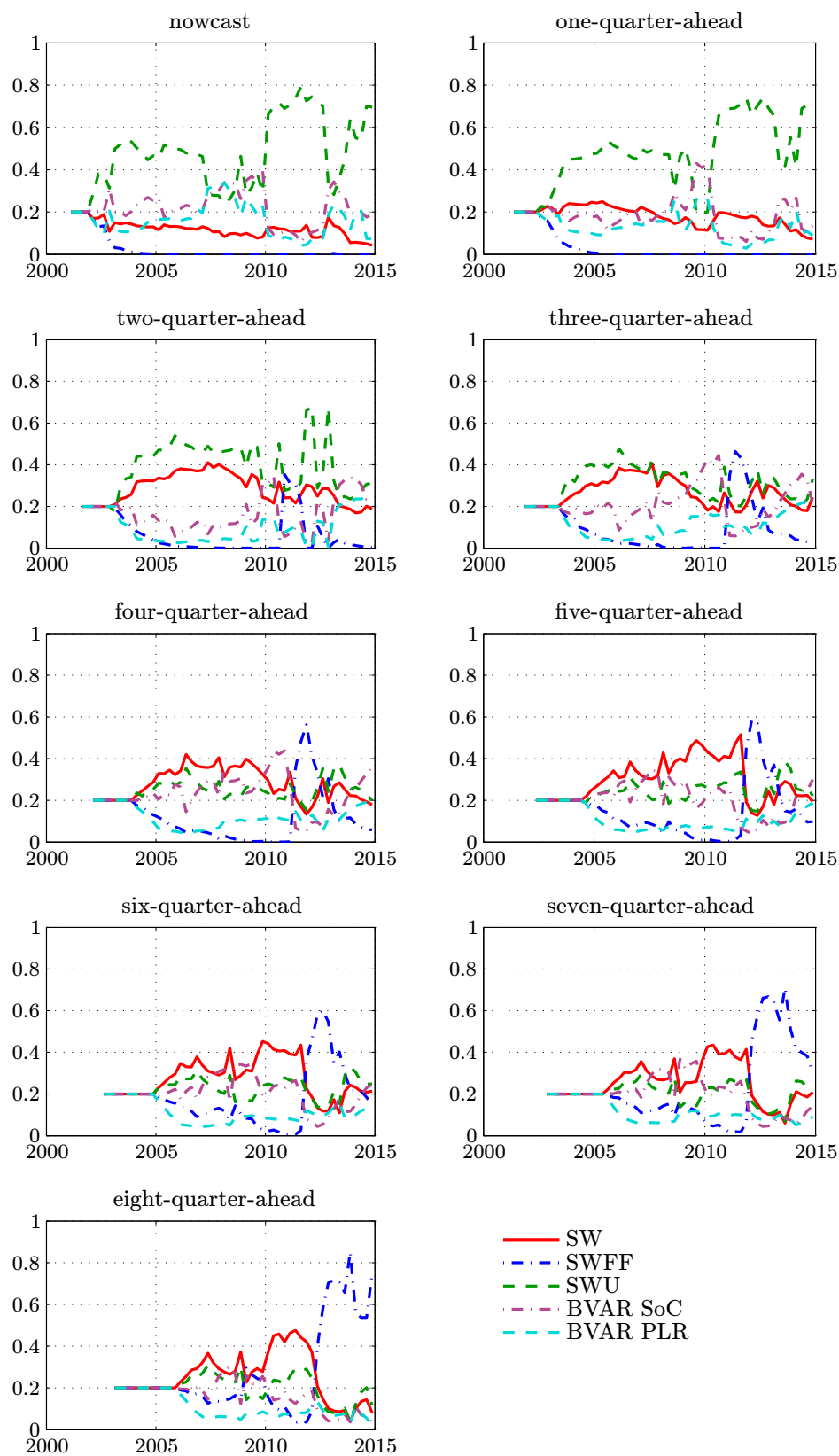
FIGURE D.14: Recursive posterior estimates of ρ for the dynamic prediction pool of joint real GDP growth and GDP deflator inflation covering the vintages 2001Q1–2014Q4.
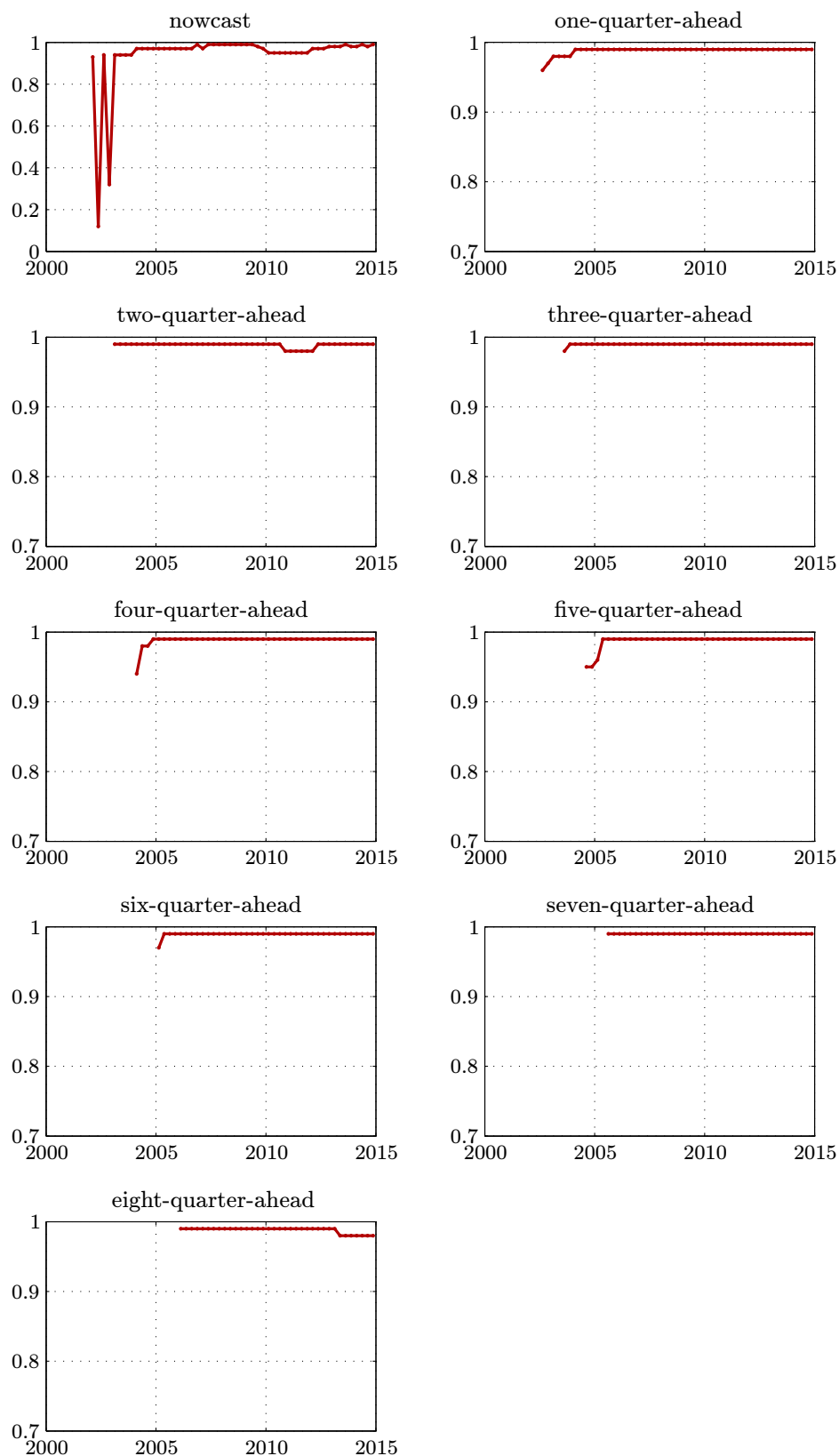
FIGURE D.15: Recursive posterior estimates of ρ for the dynamic prediction pool of real GDP growth covering the vintages 2001Q1–2014Q4.
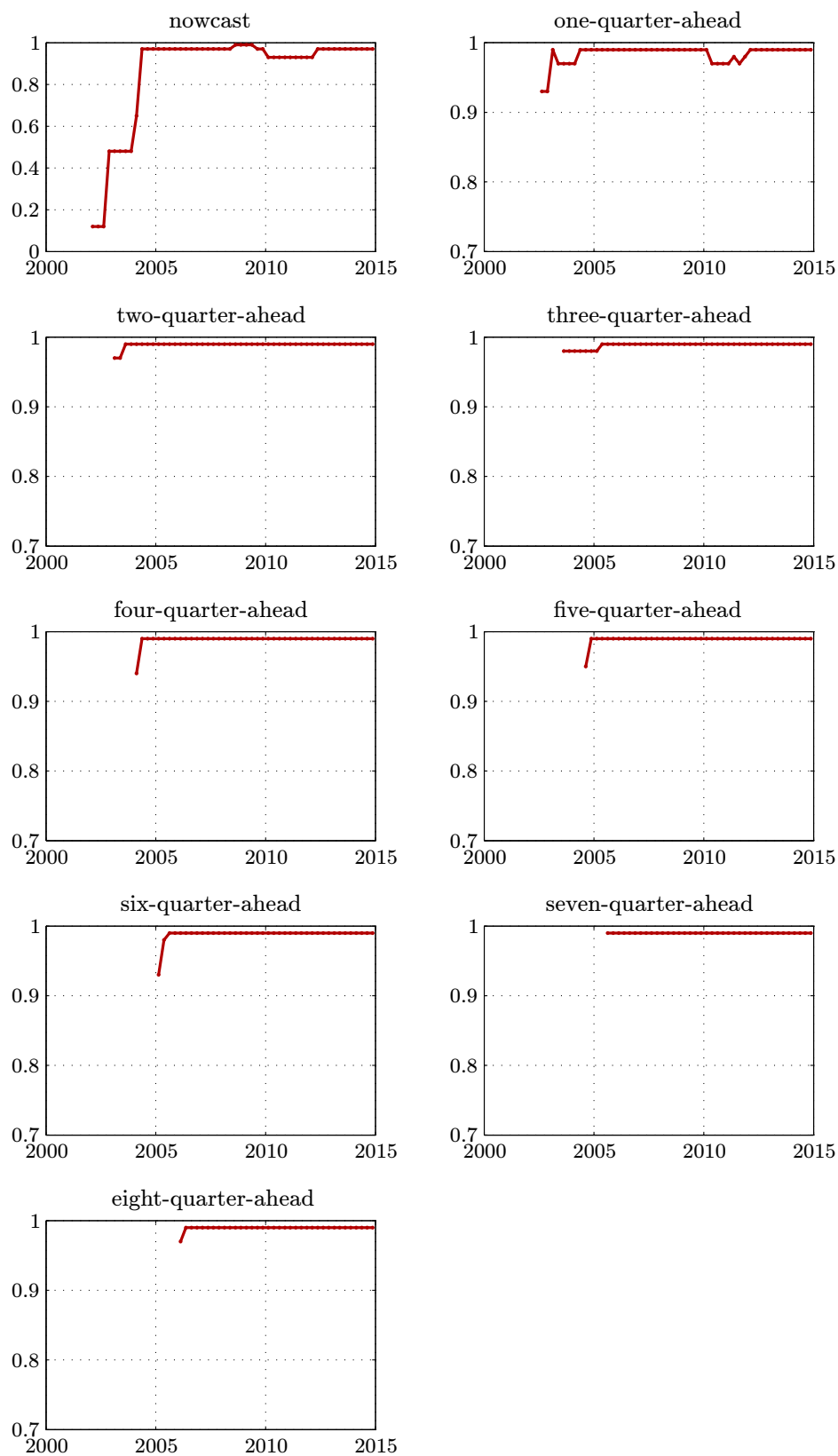
FIGURE D.16: Recursive posterior estimates of ρ for the dynamic prediction pool of GDP deflator inflation covering the vintages 2001Q1–2014Q4.
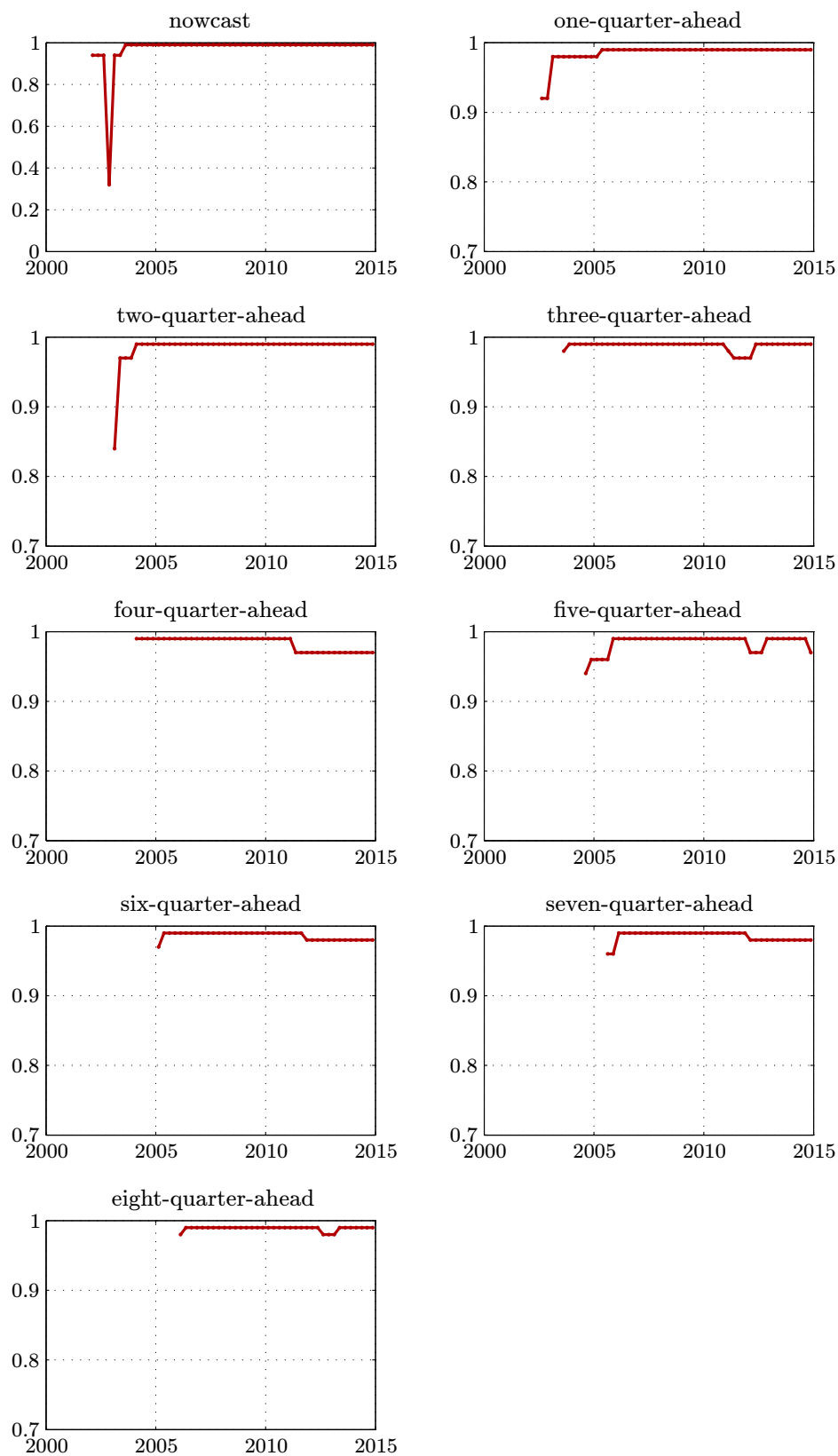
FIGURE D.17: Recursive posterior estimates of φ for dynamic model averaging of joint real GDP growth and GDP deflator inflation covering the vintages 2001Q1–2014Q4.
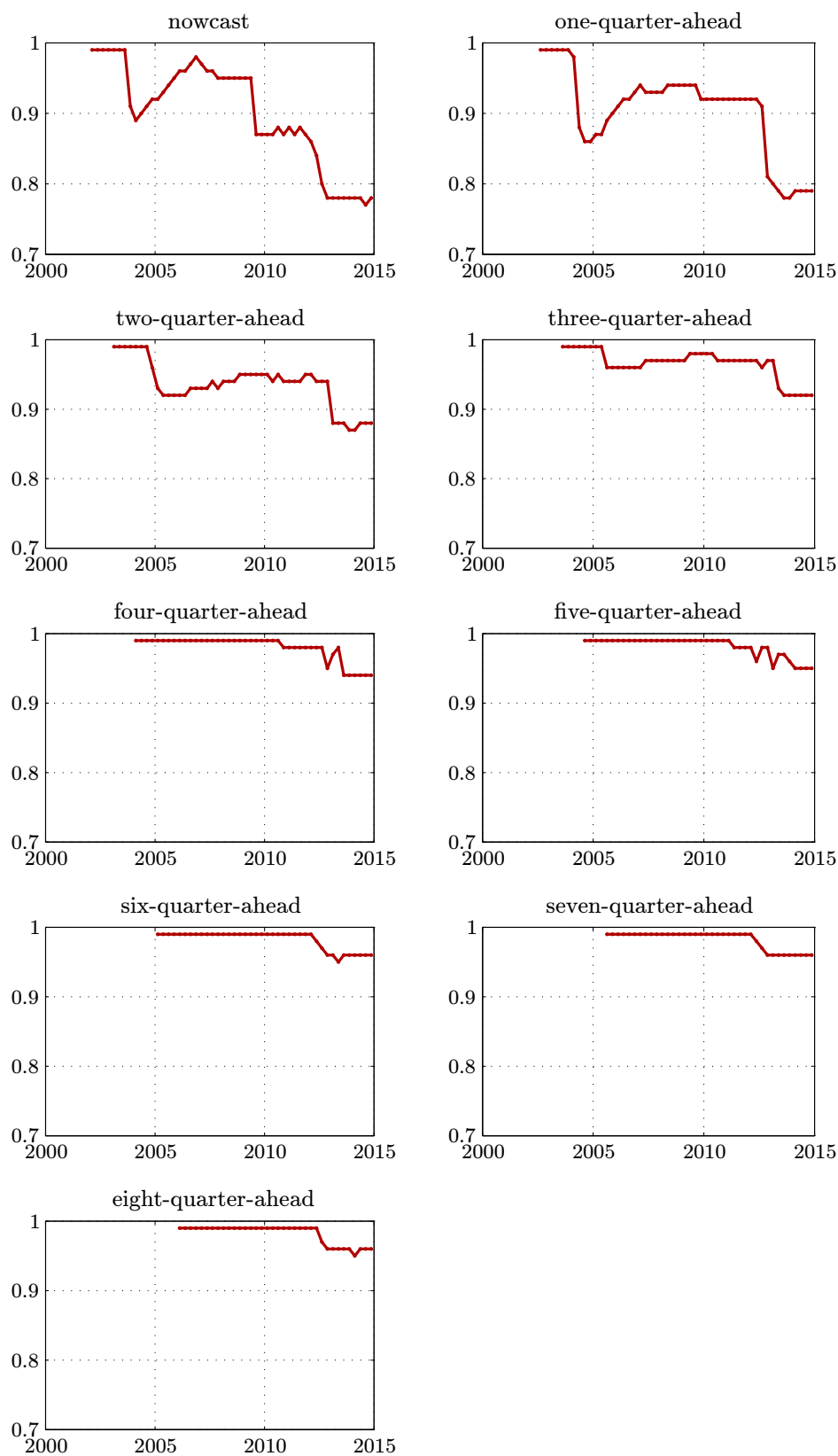
FIGURE D.18: Recursive posterior estimates of φ for dynamic model averaging of real GDP growth covering the vintages 2001Q1–2014Q4.
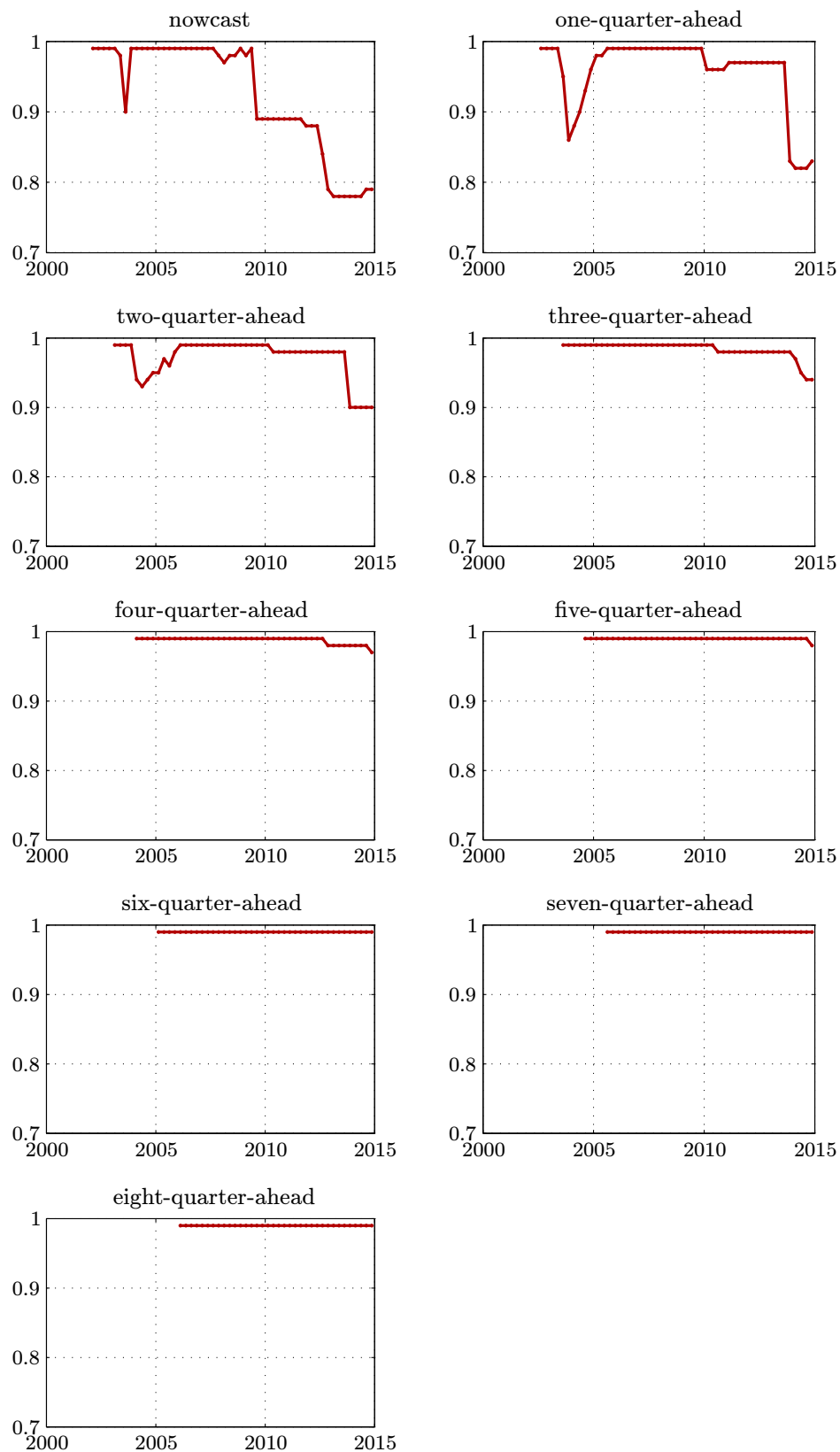
FIGURE D.19: Recursive posterior estimates of φ for dynamic model averaging of GDP deflator inflation covering the vintages 2001Q1–2014Q4.
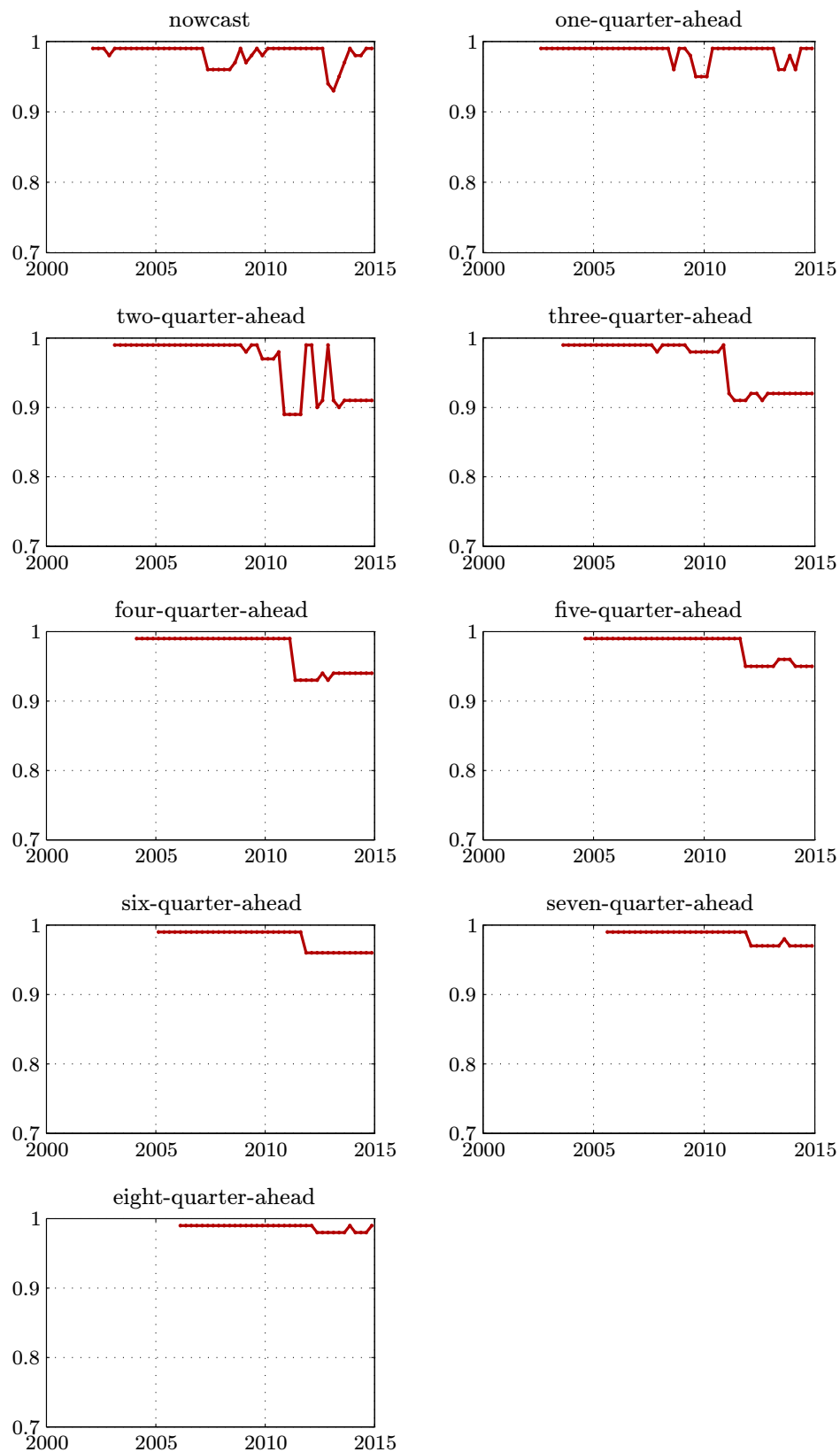
FIGURE D.20: Recursive estimates of the average log predictive scores of real GDP growth for the combinations and in deviation from the recursive value of the upper bound covering the vintages 2001Q1–2014Q4.
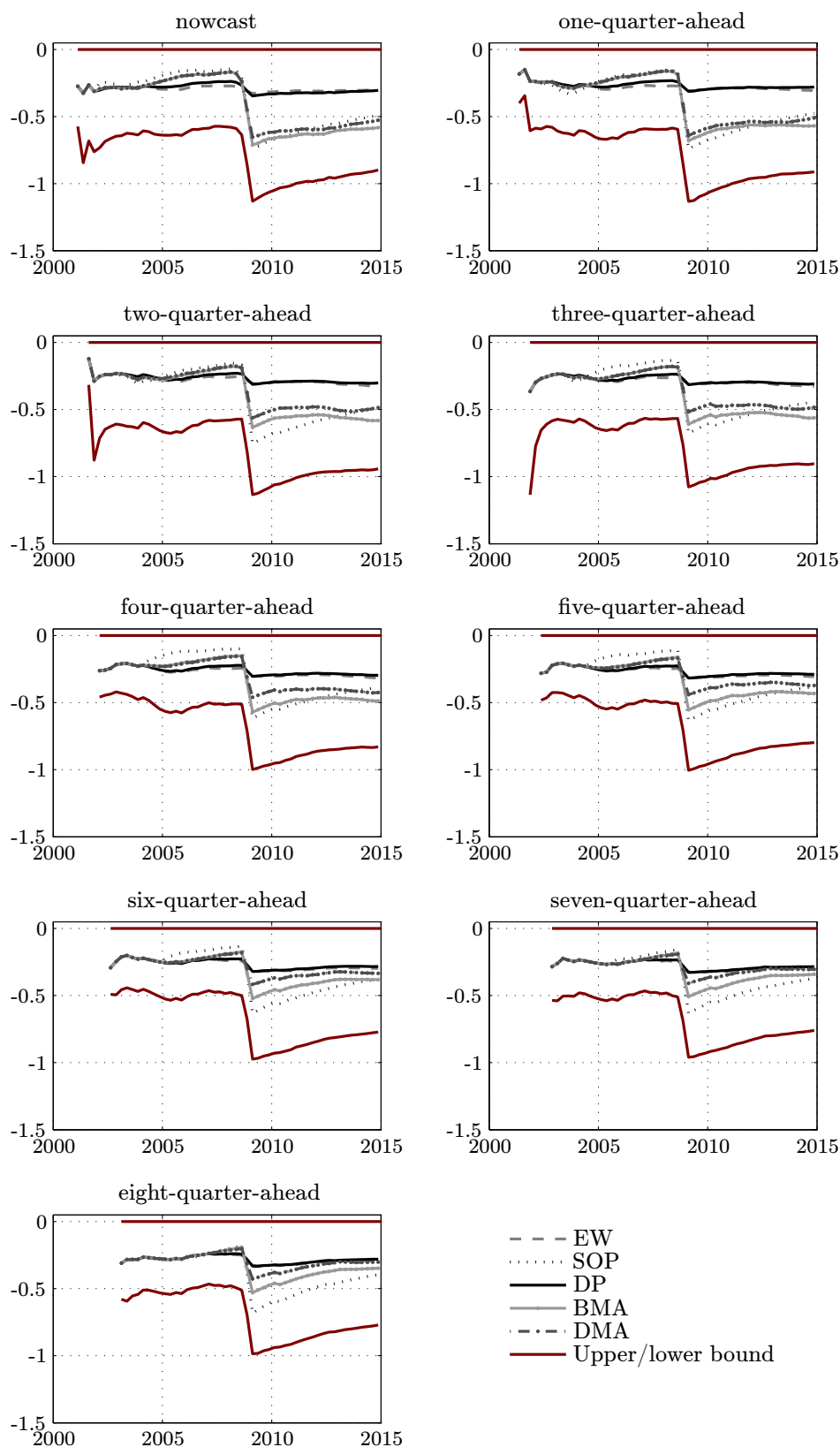
FIGURE D.21: Recursive estimates of the average log predictive scores of GDP
deflator inflation for the combinations and in deviation from the
recursive value of the upper bound covering the vintages 2001Q1–
2014Q4.
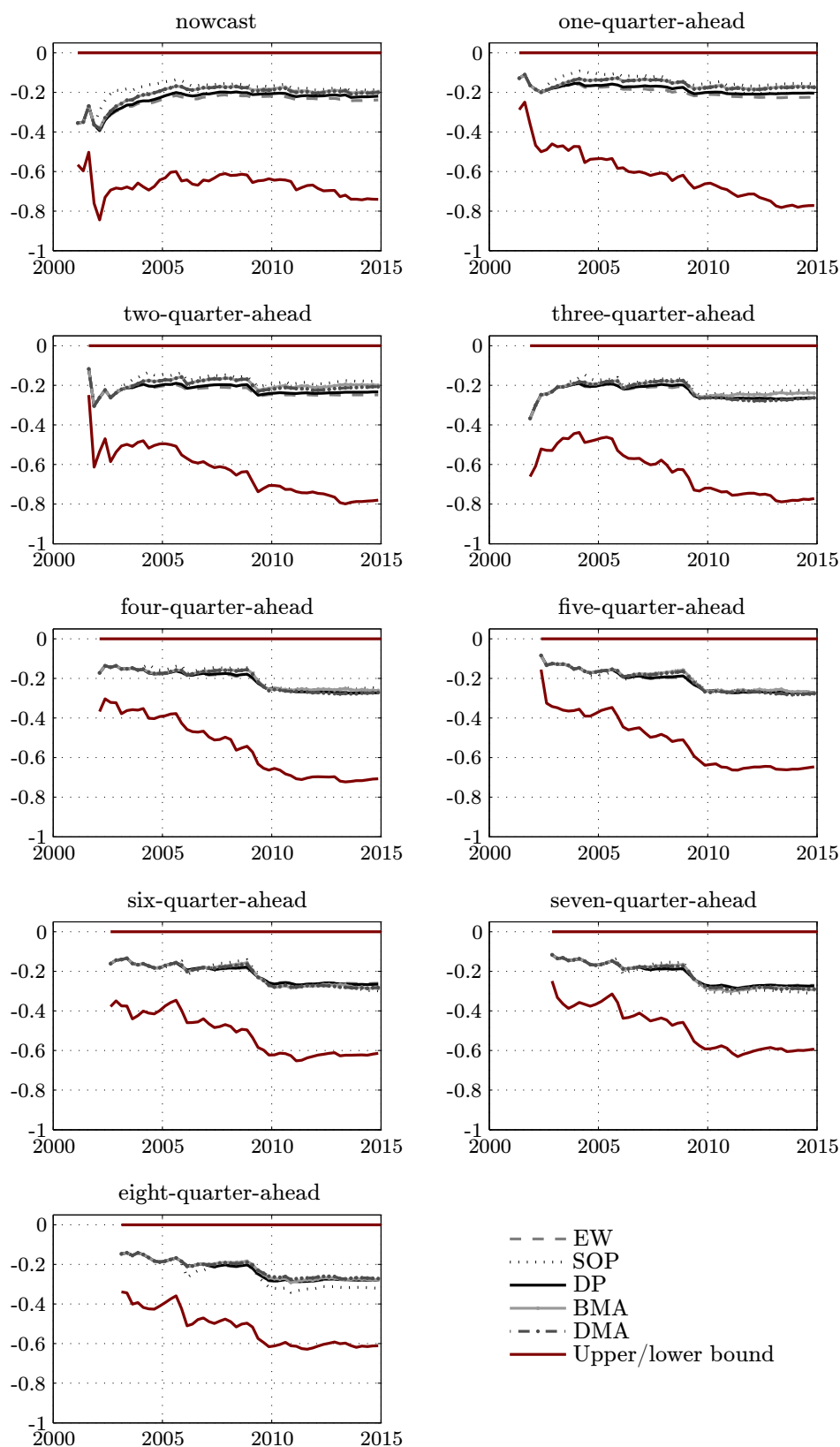
FIGURE D.22: Recursive estimates of the average log predictive scores of joint real GDP growth and GDP deflator inflation for the models and in deviation from the recursive value of the upper bound covering the vintages 2001Q1–2014Q4.
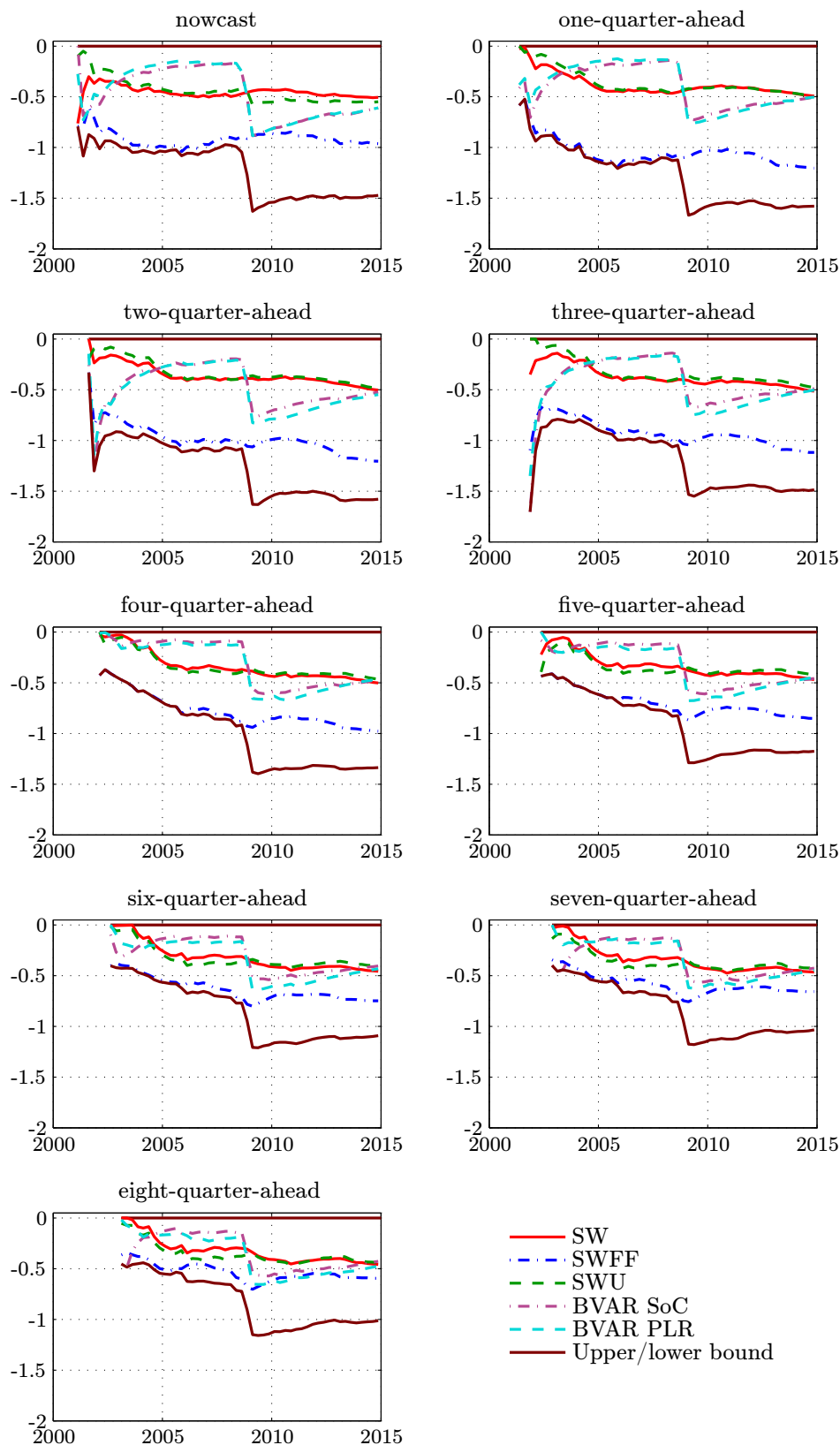
FIGURE D.23: Recursive estimates of the average log predictive scores of real
GDP growth for the models and in deviation from the recursive
value of the upper bound covering the vintages 2001Q1–2014Q4.
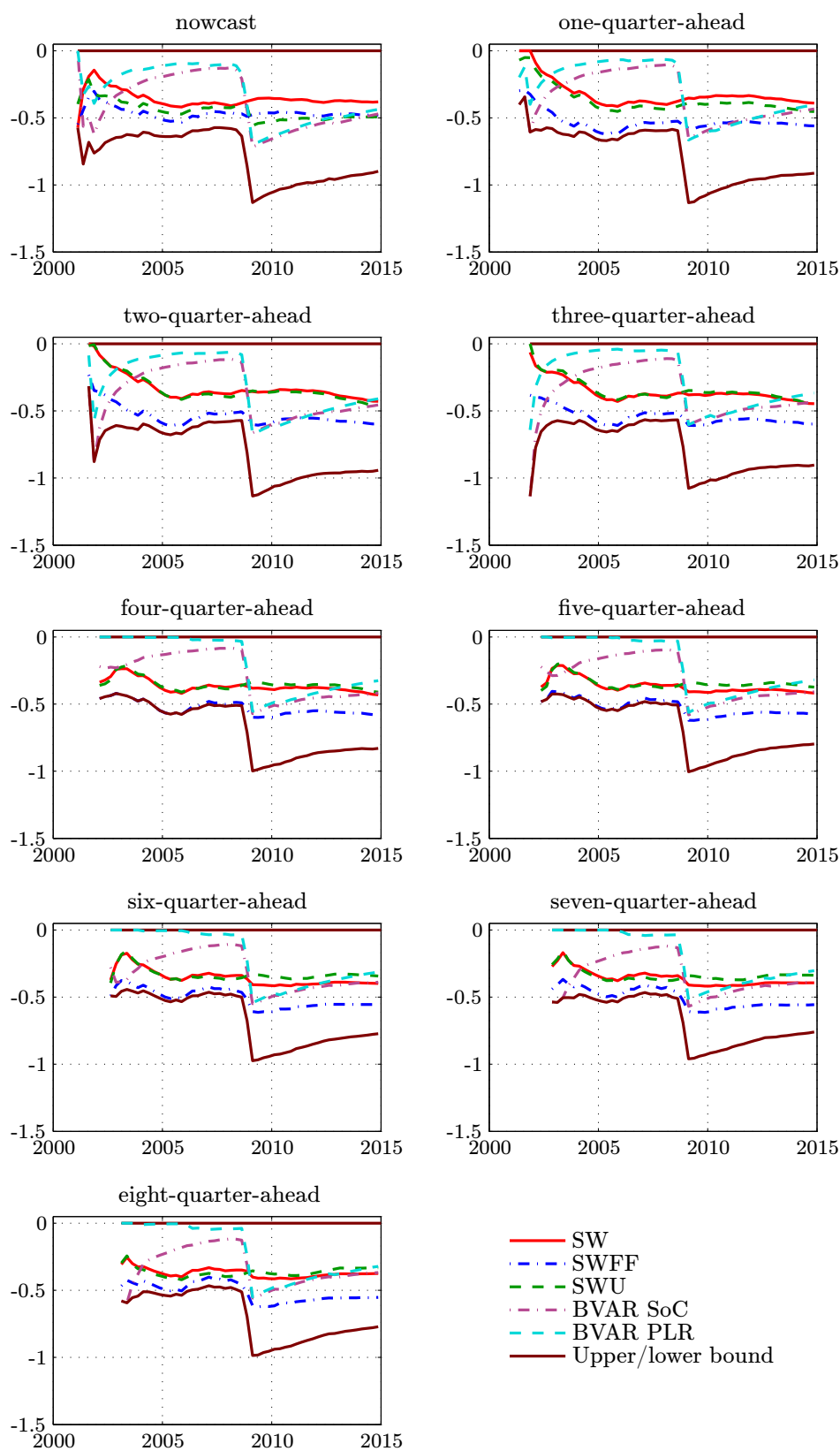
FIGURE D.24: Recursive estimates of the average log predictive scores of GDP deflator inflation for the models and in deviation from the recursive value of the upper bound covering the vintages 2001Q1–2014Q4.
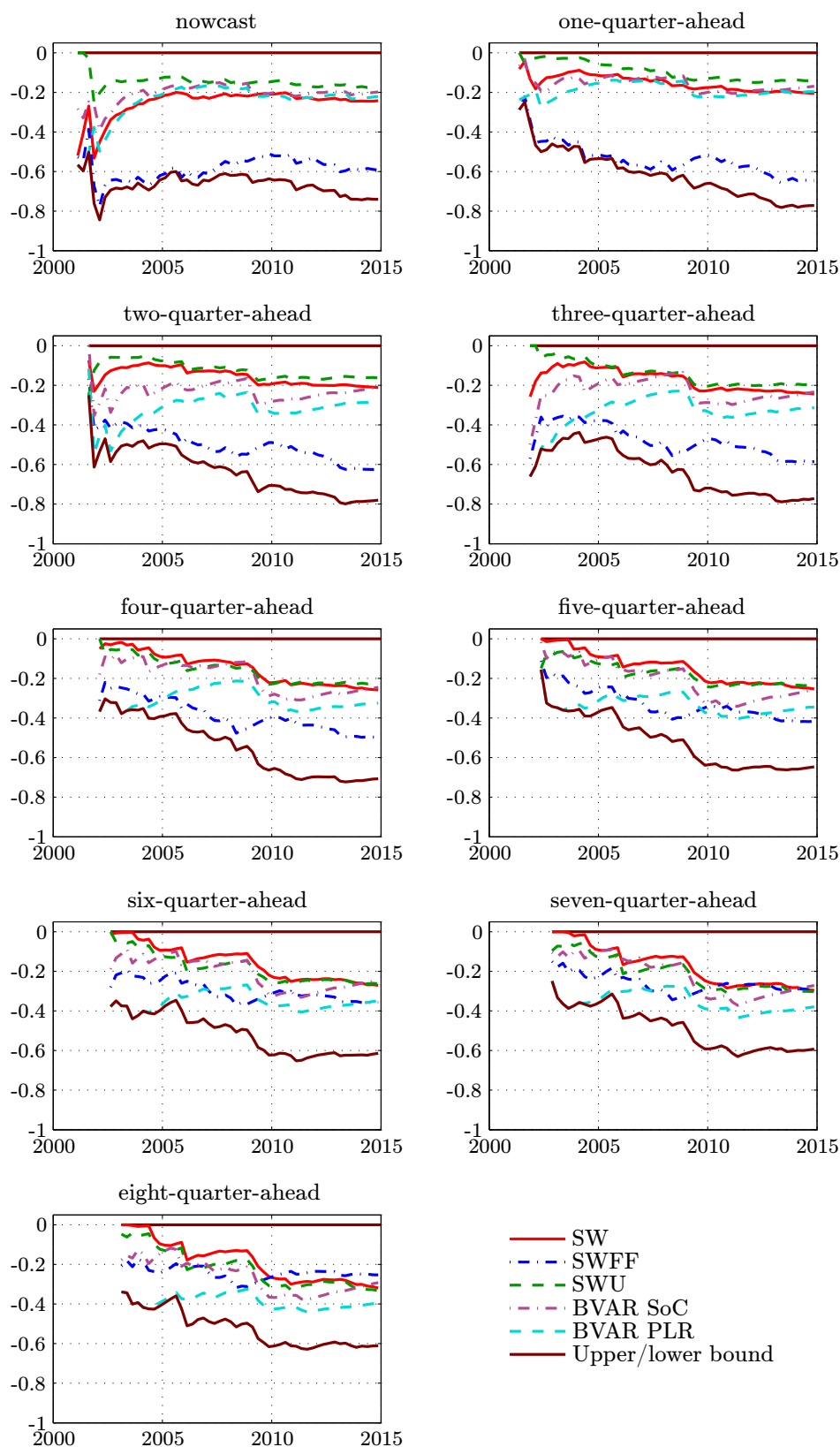
FIGURE D.25: Recursive estimates of the differences of log predictive scores of real GDP growth for information lag 1 and 4 covering the vintages 2001Q1–2014Q4.
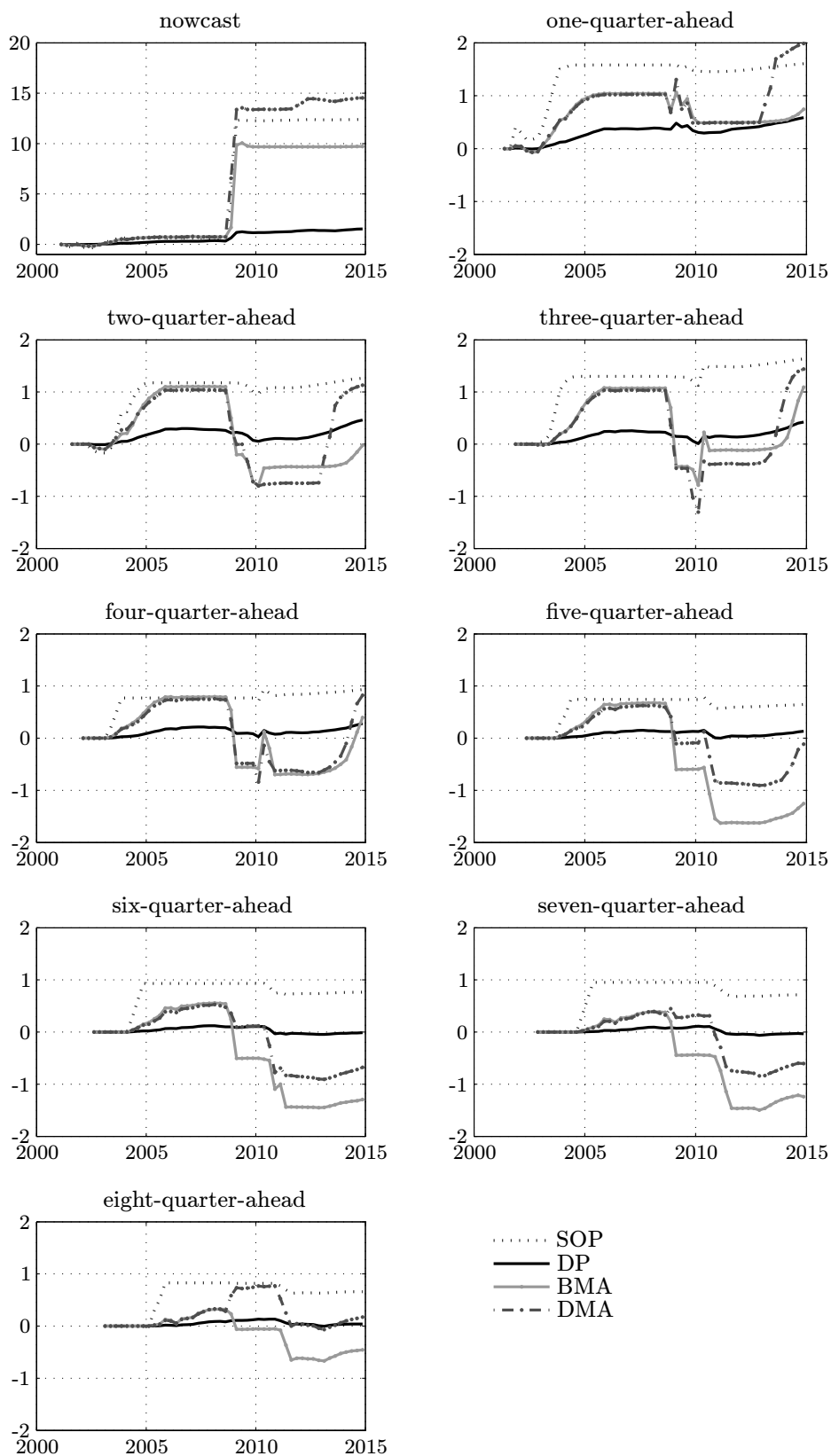
FIGURE D.26: Recursive estimates of the differences of log predictive scores of GDP deflator inflation for information lag 1 and 4 covering the vintages 2001Q1–2014Q4.
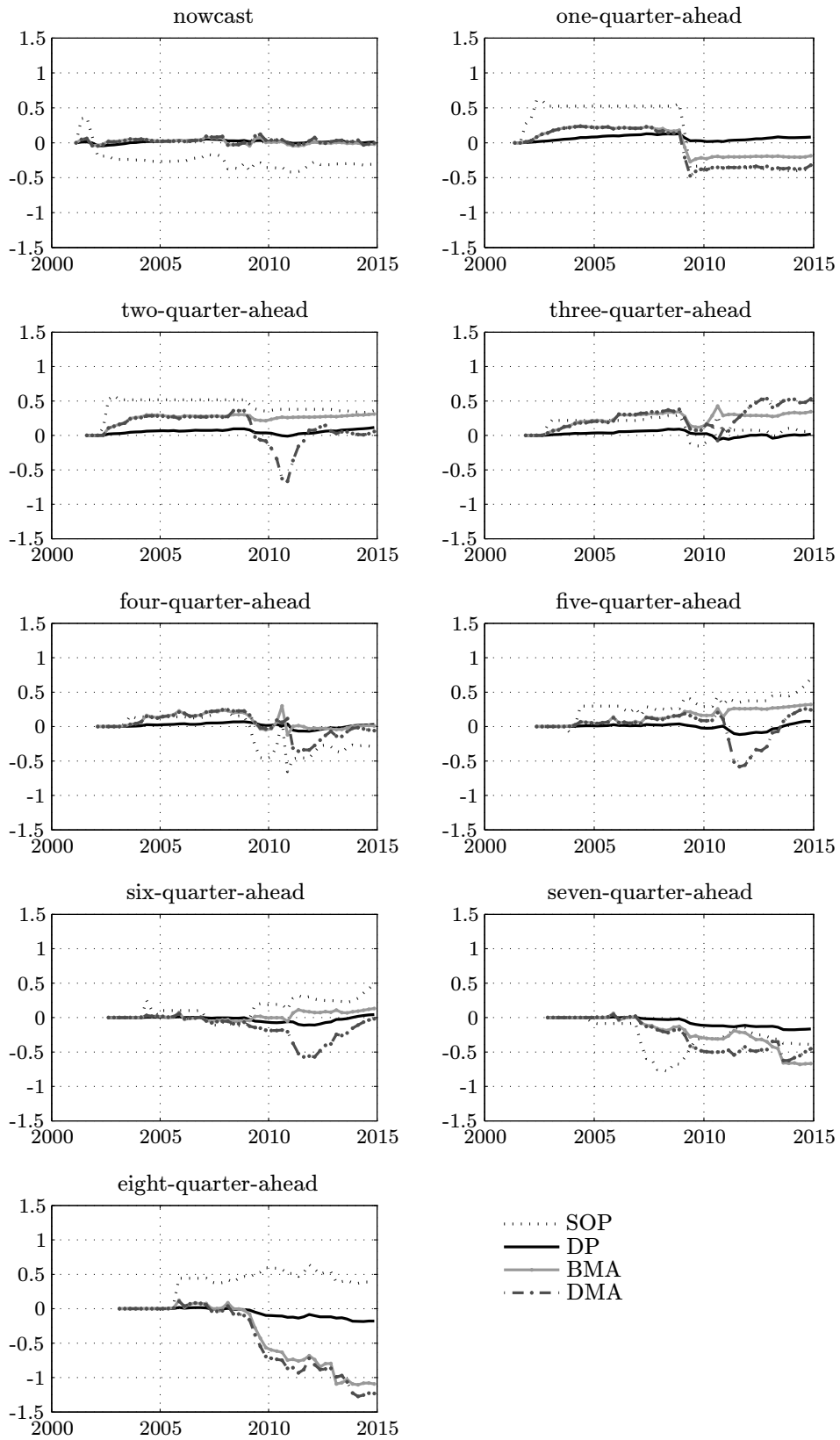
FIGURE D.27: Recursive estimates of the differences of log predictive scores of real GDP growth for the SWFF zero initialization and the equal weights initialization covering the vintages 2001Q1–2014Q4.
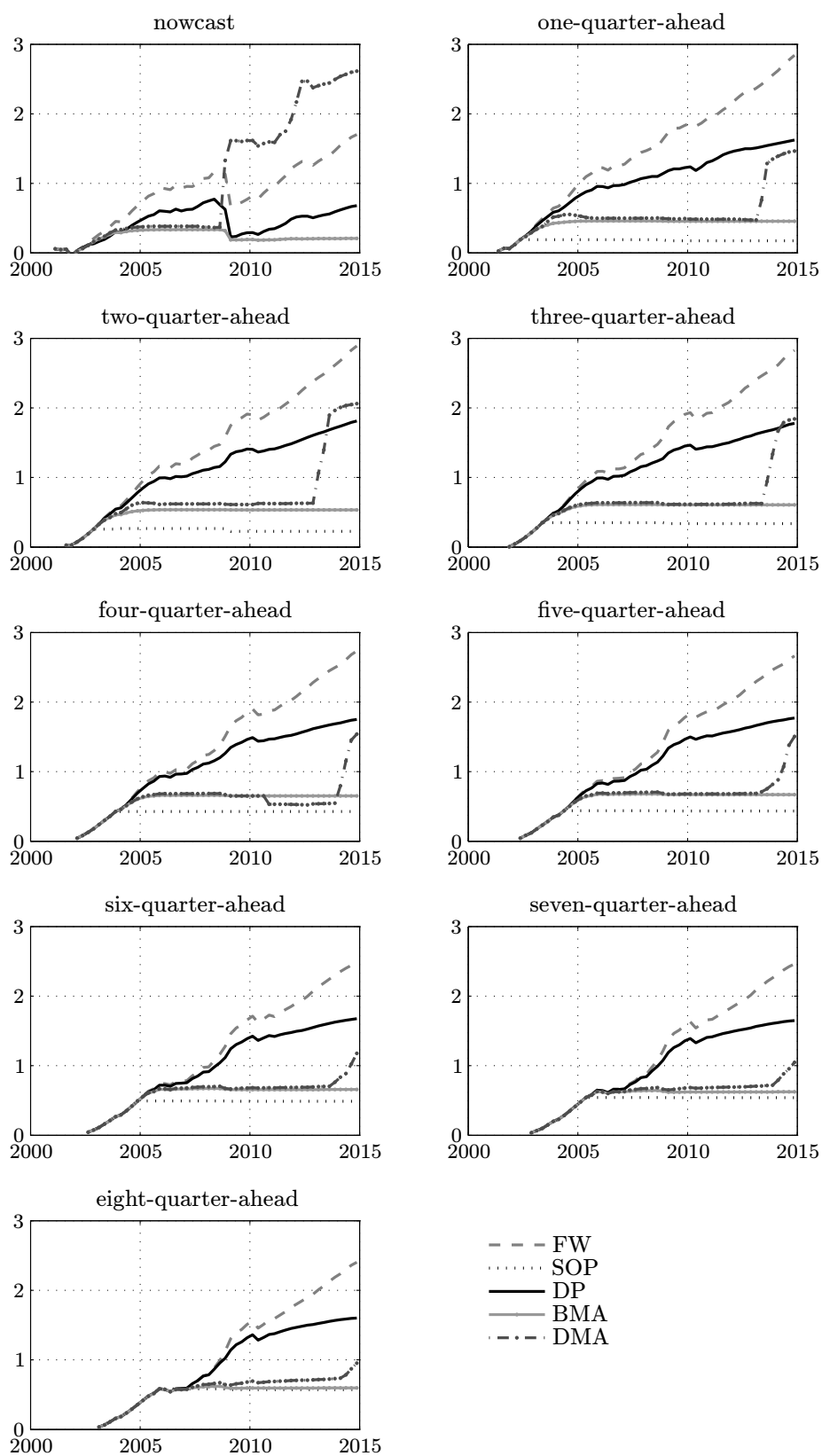
FIGURE D.28: Recursive estimates of the differences of log predictive scores of GDP deflator inflation for the SWFF zero initialization and the equal weights initialization covering the vintages 2001Q1–2014Q4.
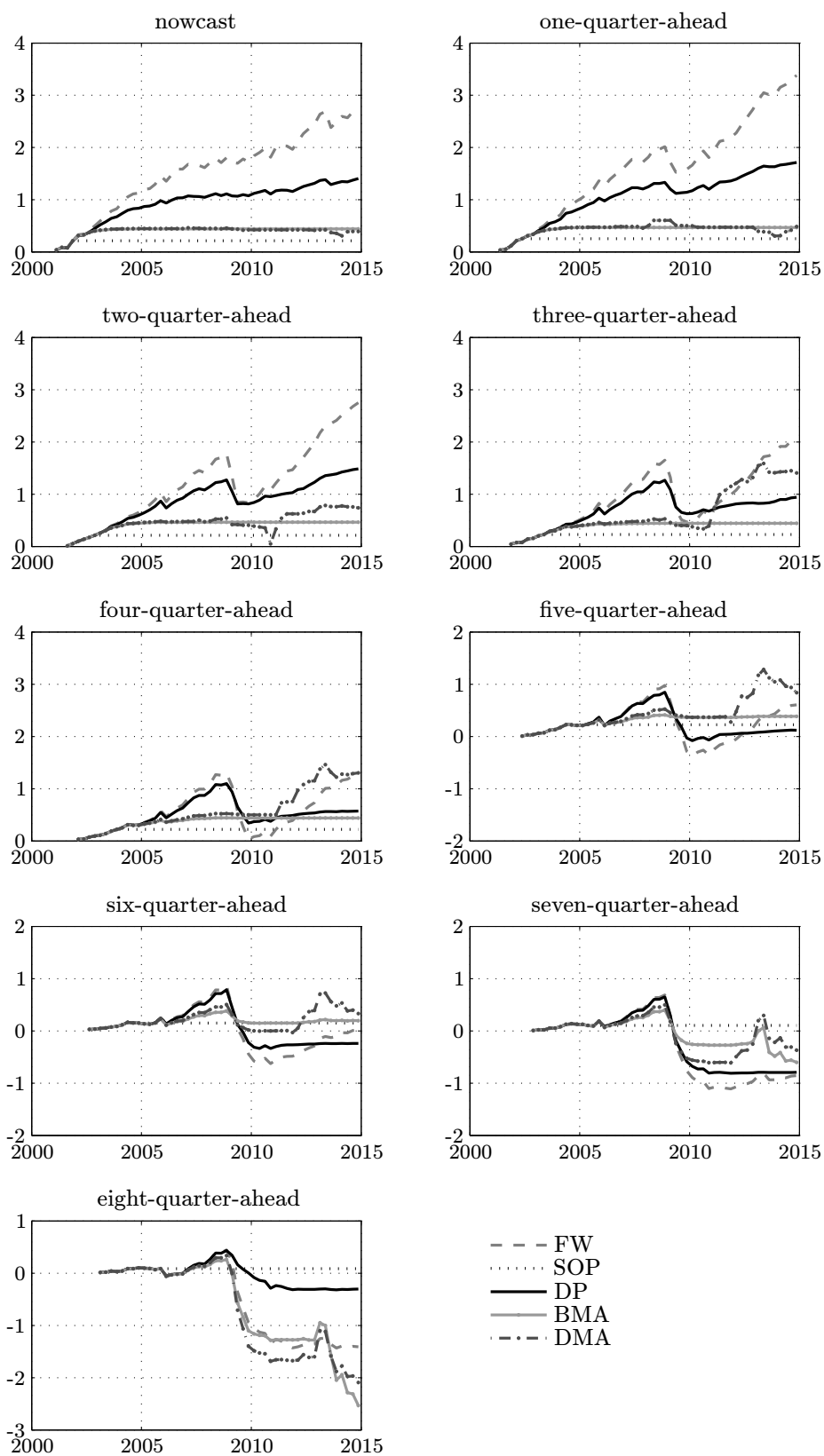
FIGURE D.29: Posterior estimates of the model weights for the dynamic prediction pool of real GDP growth based on the SWFF zero initialization and covering the vintages 2001Q1–2014Q4.
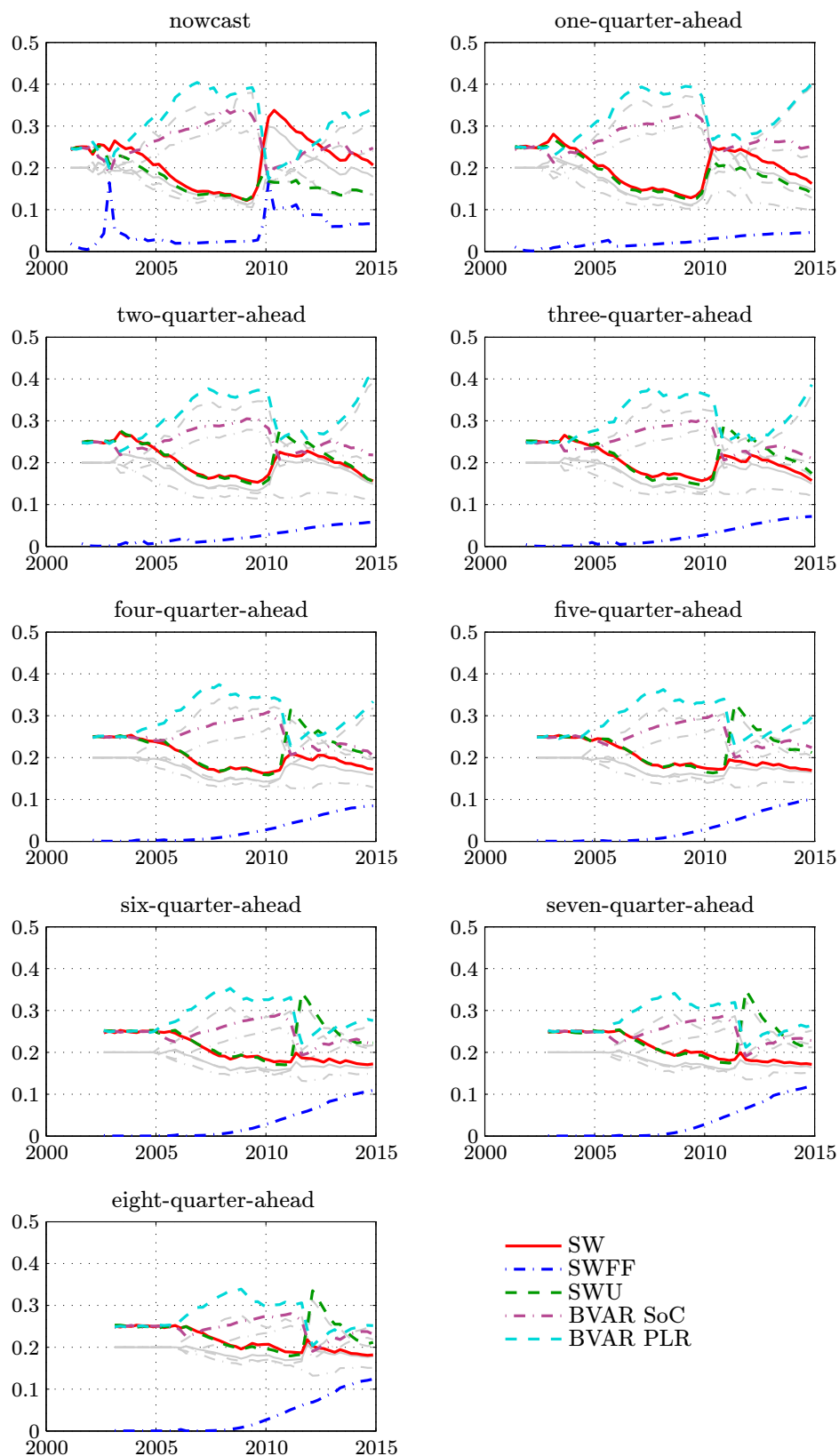
FIGURE D.30: Posterior estimates of the model weights for the dynamic pre-
diction pool of GDP deflator inflation based on the SWFF zero
initialization and covering the vintages 2001Q1–2014Q4.
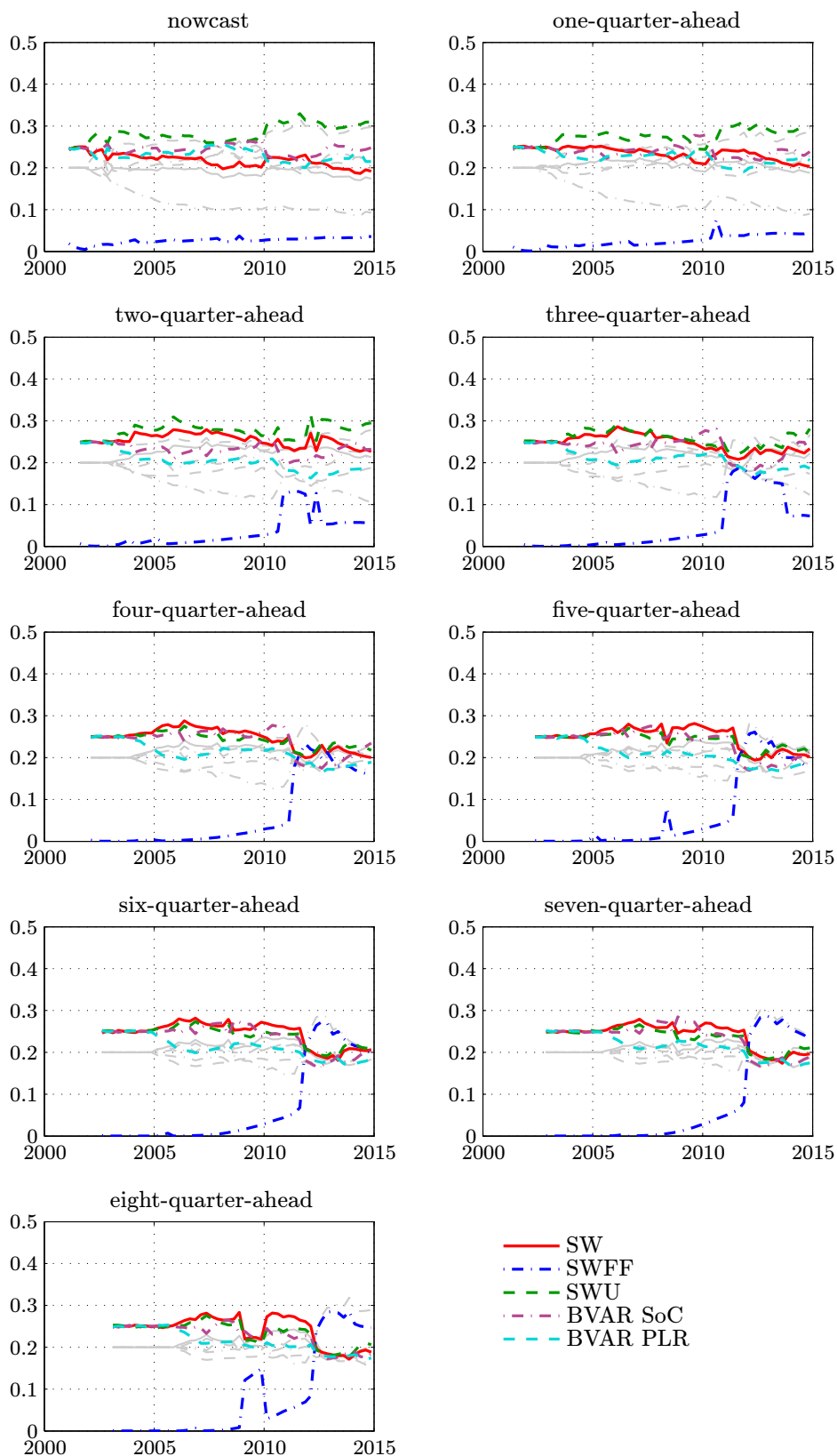
<center>REFERENCES</center>

Aastveit, K. A., Mitchell, J., Ravazzolo, F., and van Dijk, H. K. (2019), "The Evolution of Forecast Density Combinations in Economics," *Oxford Research Encyclopedia, Economics and Finance*, April, DOI: `10.1093/acrefore/9780190625979.013.381`.

Amisano, G. and Geweke, J. (2017), "Prediction Using Several Macroeconomic Models," *The Review of Economics and Statistics*, 99(5), 912–925.

Amisano, G. and Giacomini, R. (2007), "Comparing Density Forecasts via Weighted Likelihood Ratio Tests," *Journal of Business & Economic Statistics*, 25(2), 177–190.

Bańbura, M., Giannone, D., and Lenza, M. (2015), "Conditional Forecasts and Scenario Analysis with Vector Autoregressions for Large Cross-Sections," *International Journal of Forecasting*, 31(3), 739–756.

Bańbura, M., Giannone, D., and Reichlin, L. (2010), "Large Bayesian Vector Auto Regressions," *Journal of Applied Econometrics*, 25, 71–92.

Bernanke, B. S., Gertler, M., and Gilchrist, S. (1999), "The Financial Accelerator in a Quantitative Business Cycle Framework," in J. B. Taylor and M. Woodford (Editors), *Handbook of Macroeconomics*, volume 1C, 1341–1393, North Holland, Amsterdam.

Bernardo, J. M. (1979), "Expected Information as Expected Utility," *The Annals of Statistics*, 7(3), 686–690.

Billio, M., Casarin, R., Ravazzolo, F., and van Dijk, H. K. (2013), "Time-Varying Combinations of Predictive Densities using Nonlinear Filtering," *Journal of Econometrics*, 177(2), 213–232.

Cai, M., Del Negro, M., Herbst, E., Matlin, E., Sarfati, R., and Schorfheide, F. (2019), "Online Estimation of DSGE Models," Federal Reserve Bank of New York Staff Report No. 893.

Carpenter, J., Clifford, P., and Fearnhead, P. (1999), "An Improved Particle Filter for Non-linear Prolems," *IEE Proceedings—Radar, Sonar and Navigation*, 146(1), 2–7.

Chopin, N. (2004), "Central Limit Theorem for Sequential Monte Carlo Methods and its Application to Bayesian Inference," *The Annals of Statistics*, 32(6), 2385–2411.

Clark, T. E. (2011), "Real-Time Density Forecasts From Bayesian Vector Autoregressions With Stochastic Volatility," *Journal of Business & Economic Statistics*, 29(3), 327–341.

Croushore, D. (2011), "Frontiers of Real-Time Data Analysis," *Journal of Economic Literature*, 49(1), 72–110.

Croushore, D. and Stark, T. (2001), "A Real-Time Data Set for Macroeconomists," *Journal of Econometrics*, 105(1), 111–130.

Dawid, A. P. (1984), "Statistical Theory: The Prequential Approach," *Journal of the Royal Statistical Society, Series A*, 147(2), 278–292.

Del Negro, M., Giannoni, M. P., and Schorfheide, F. (2015), "Inflation in the Great Recession and New Keynesian Models," *American Economic Journal: Macroeconomics*, 7(1), 168–196.

Del Negro, M., Hasegawa, R. B., and Schorfheide, F. (2016), "Dynamic Prediction Pools: An Investigation of Financial Frictions and Forecasting Performance," *Journal of Econometrics*,

192(2), 391–403.

Del Negro, M. and Schorfheide, F. (2013), "DSGE Model-Based Forecasting," in G. Elliott and A. Timmermann (Editors), *Handbook of Economic Forecasting*, volume 2, 57–140, North Holland, Amsterdam.

Diebold, F., Gunther, T. A., and Tay, A. S. (1998), "Evaluating Density Forecasts with Applications to Financial Risk Management," *International Economic Review*, 39(4), 863–883.

Diks, C., Panchenko, V., and van Dijk, D. (2011), "Likelihood-Based Scoring Rules for Comparing Density Forecasts in Tails," *Journal of Econometrics*, 163(2), 215–230.

Doan, T., Litterman, R., and Sims, C. A. (1984), "Forecasting and Conditional Projection Using Realistic Prior Distributions," *Econometric Reviews*, 3(1), 1–100.

Douc, R., Cappé, O., and Moulines, E. (2005), "Comparison of Resampling Schemes for Particle Filtering," in *Proceedings of the 4th International Symposium on Image and Signal Processing and Analysis, ISPA 2005*, IEEE, conference Location: Zagreb, Crotia.

Doucet, A., Briers, M., and Sénécal, S. (2006), "Efficient Block Sampling Strategies for Sequential Monte Carlo Methods," *Journal of Computational and Graphical Statistics*, 15(3), 693–711.

Doucet, A. and Johansen, A. M. (2011), "A Tutorial on Particle Filtering and Smoothing: Fifteen Years Later," in D. Crisan and B. Rozovskiĭ (Editors), *The Oxford Handbook of Nonlinear Filtering*, volume 12, 656–704, Oxford University Press, Oxford.

Durbin, J. and Koopman, S. J. (2012), *Time Series Analysis by State Space Methods*, Oxford University Press, Oxford, 2nd edition.

Eklund, J. and Karlsson, S. (2007), "Forecast Combinations and Model Averaging using Predictive Measures," *Econometric Reviews*, 26(2–4), 329–363.

Fagan, G., Henry, J., and Mestre, R. (2005), "An Area-Wide Model for the Euro Area," *Economic Modelling*, 22(1), 39–59.

Galí, J., Smets, F., and Wouters, R. (2012), "Unemployment in an Estimated New Keynesian Model," in D. Acemoglu and M. Woodford (Editors), *NBER Macroeconomics Annual 2011*, 329–360, University of Chicago Press.

Geweke, J. (2010), *Complete and Incomplete Econometrics Models*, Princeton University Press, Princeton.

Geweke, J. and Amisano, G. (2011), "Optimal Prediction Pools," *Journal of Econometrics*, 164(1), 130–141.

Geweke, J. and Amisano, G. (2012), "Prediction and Misspecified Models," *American Economic Review*, 102(3), 482–486.

Giannone, D., Henry, J., Lalik, M., and Modugno, M. (2012), "An Area-Wide Real-Time Database for the Euro Area," *The Review of Economics and Statistics*, 94(4), 1000–1013.

Giannone, D., Lenza, M., and Primiceri, G. E. (2015), "Prior Selection for Vector Autoregressions," *The Review of Economics and Statistics*, 97(2), 436–451.

Giannone, D., Lenza, M., and Primiceri, G. E. (2019), "Priors for the Long Run," *Journal of the American Statistical Association*, 114(526), 565–580.

Gilks, W. R. and Berzuini, C. (2001), "Following a Moving Target—Monte Carlo Inference for Dynamic Bayesian Models," *Journal of the Royal Statistical Society Series B*, 63(1), 127–146.

Gneiting, T. and Katzfuss, M. (2014), "Probabilistic Forecasting," *The Annual Review of Statistics and Its Applications*, 1, 125–151.

Gneiting, T. and Raftery, A. E. (2007), "Strictly Proper Scoring Rules, Prediction, and Estimation," *Journal of the American Statistical Association*, 102(477), 359–378.

Gordon, N. J., Salmond, D. J., and Smith, A. F. M. (1993), "Novel Approach to Nonlinear/non-Gaussian Bayesian State Estimation," *Radar and Signal Processing, IEE Proceedings-F*, 140(2), 107–113.

Hall, S. G. and Mitchell, J. (2007), "Combining Density Forecasts," *International Journal of Forecasting*, 23(1), 1–13.

Herbst, E. and Schorfheide, F. (2016), *Bayesian Estimation of DSGE Models*, Princeton University Press, Princeton.

Hoeting, J. A., Madigan, D., Raftery, A. E., and Volinsky, C. T. (1999), "Bayesian Model Averaging: A Tutorial," *Statistical Science*, 14(4), 382–417.

Hol, J. D., Schön, T. B., and Gustafsson, F. (2006), "On Resampling Algorithms for Particle Filters," *Proceedings of the IEEE Nonlinear Statistical Signal Processing Workshop*, Cambridge, U. K., Sept. 2006, 79–82.

Johansen, S. (1996), *Likelihood-Based Inference in Cointegrated Vector Autoregressive Models*, Oxford University Press, Oxford, 2nd edition.

Jore, A. S., Mitchell, J., and Vahey, S. P. (2010), "Combining Forecast Densities from VARs with Uncertain Instabilities," *Journal of Applied Econometrics*, 25(4), 621–634.

Kapetanios, G., Mitchell, J., Price, S., and Fawcett, N. (2015), "Generalised Density Forecast Combinations," *Journal of Econometrics*, 188(1), 150–165.

Kitagawa, G. (1996), "Monte Carlo Filter and Smoother for Non-Gaussian Nonlinear State Space Models," *Journal of Computational and Graphical Statistics*, 5(1), 1–25.

Kocherlakota, N. (2010), "Modern Macroeconomic Models as Tools for Economic Policy," *The Region*, May(1), 5–21, Federal Reserve Bank of Minneapolis.

Koop, G. and Korobilis, D. (2012), "Forecasting Inflation using Dynamic Model Averaging," *International Economic Review*, 53(3), 867–886.

Kullback, S. and Leibler, R. A. (1951), "On Information and Sufficiency," *The Annals of Mathematical Statistics*, 22(1), 79–86.

Li, T., Bolić, M., and Djurić, P. M. (2015), "Resampling Methods for Particle Filtering: Classification, Implementation, and Strategies," *IEEE Signal Processing Magazine*, 32(3), 70–86.

Liu, J. S. and Chen, R. (1998), "Sequential Monte Carlo Methods for Dynamic Systems," *Journal of the American Statistical Association*, 93(443), 1032–1044.

McAdam, P. and Warne, A. (2018), "Euro Area Real-Time Density Forecasting with Financial or Labor Market Frictions," ECB Working Paper Series No. 2140.

McAdam, P. and Warne, A. (2019), "Euro Area Real-Time Density Forecasting with Financial or Labor Market Frictions," *International Journal of Forecasting*, 35(2), 580–600.

McAlinn, K. and West, M. (2019), "Dynamic Bayesian Predictive Synthesis in Time Series Forecasting," *Journal of Econometrics*, 210(1), 155–169.

Newey, W. K. and West, K. D. (1987), "A Simple, Positive Semi-Definite, Heteroskedasticity and Autocorrelation Consistent Covariance Matrix," *Econometrica*, 55, 703–708.

Opschoor, A., van Dijk, D., and van der Wel, M. (2017), "Combining Density Forecasts using Focused Scoring Rules," *Journal of Applied Econometrics*, 32(7), 1298–1313.

Papadopoulos, G. (2017), "A Model Combination Approach to Developing Robust Models for Credit Risk Stress Testing: An Application to a Stressed Economy," *Journal of Risk Model Validation*, 11(1), 49–72.

Pauwels, L. L. and Vasnev, A. L. (2016), "A Note on the Estimation of Optimal Weights for Density Forecast Combinations," *International Journal of Forecasting*, 32(2), 391–397.

Raftery, A. E., Kárný, M., and Ettler, P. (2010), "Online Prediction Under Model Uncertainty via Dynamic Model Averaging: Application to a Cold Rolling Mill," *Technometrics*, 52(1), 52–66.

Sims, C. A. (1993), "A Nine-Variable Probabilistic Macroeconomic Forecasting Model," in J. H. Stock and M. W. Watson (Editors), *Business Cycles, Indicators and Forecasting*, 179–212, University of Chicago Press, Chicago.

Sims, C. A. (2000), "Using a Likelihood Perspective to Sharpen Econometric Discourse: Three Examples," *Journal of Econometrics*, 95(2), 443–462.

Sims, C. A. and Zha, T. (1998), "Bayesian Methods for Dynamic Multivariate Models," *International Economic Review*, 39(4), 949–968.

Smets, F., Warne, A., and Wouters, R. (2014), "Professional Forecasters and Real-Time Forecasting with a DSGE Model," *International Journal of Forecasting*, 30(4), 981–995.

Smets, F. and Wouters, R. (2007), "Shocks and Frictions in US Business Cycles: A Bayesian DSGE Approach," *American Economic Review*, 97(3), 586–606.

Waggoner, D. F. and Zha, T. (2012), "Confronting Model Misspecification in Macroeconomics," *Journal of Econometrics*, 171(2), 167–184.

Wallis, K. F. (1986), "Forecasting with an Econometric Model: The Ragged Edge Problem," *Journal of Forecasting*, 5(1), 1–13.

Warne, A. (2019), "YADA Manual — Computational Details," Manuscript, European Central Bank. Available with the YADA distribution.

Warne, A., Coenen, G., and Christoffel, K. (2017), "Marginalized Predictive Likelihood Comparisons of Linear Gaussian State-Space Models with Applications to DSGE, DSGE-VAR and VAR Models," *Journal of Applied Econometrics*, 32(1), 103–119.

Peter McAdam
European Central Bank, Frankfurt am Main, Germany; email: peter.mcadam@ecb.europa.eu

Anders Warne
European Central Bank, Frankfurt am Main, Germany; email: anders.warne@ecb.europa.eu